



Università degli Studi di Ferrara

DOTTORATO DI RICERCA IN
BIOCHIMICA, BIOLOGIA MOLECOLARE E BIOTECNOLOGIE

CICLO XXIII

COORDINATORE Prof. BERNARDI FRANCESCO

Lab-on-a-chip and integrated strategies in tumor immunotherapy

Settore Scientifico Disciplinare BIO/10

Dottoranda

Dott. DESTRO FEDERICA

Tutore

Prof. GAMBARI ROBERTO

CoTutore

Prof. GAVIOLI RICCARDO

Anni 2008/2010

CONTENTS

PRELIMINARY REMARK.....	1
--------------------------------	----------

PART I

1 INTRODUCTION.....	3
1.1 BIOSENSOR DESIGN AND TEST.....	5
1.1.1 Biosensor architecture	6
1.1.1.1 Fluid carrier	8
1.1.1.2 Electrical interface.....	9
1.1.2 System architecture	9
1.2 CELL DELIVERY AND RECOVERY IN MICROWELLS	11
1.2.1 CellJet microdispenser	12
1.2.2 Commercial piezoelectric jetting device	12
1.2.3 Cell handling with a machined micropipette	13
1.3 BIOSENSOR TECHNOLOGY AND MANUFACTURING	15
1.3.1 Materials selection	16
1.3.2 Lab-On-Substrate manufacturing process flow	16
1.3.2.1 Lamination.....	17
1.3.2.2 Microwell and via formation	18
1.3.2.3 Via metallization	18
1.3.2.4 Funnel	19
1.3.3 Hydrophobic / hydrophilic surface modifications	19
2 MATERIALS AND METHODS.....	21
2.1 MATERIALS	21
2.1.1 Tested materials for biosensor manufacturing	21
2.1.2 Cell lines and culture conditions	25
2.1.3 Compounds used to induce erythroid differentiation in K562.....	25
2.2 METHODS	26
2.2.1 Analysis of <i>in vitro</i> cell growth	26
2.2.2 Erythroid differentiation of K562 cells	26
2.2.3 CTL-mediated LCL lysis: chromium release assay	27
2.2.4 Cytokine profiles	27
2.2.5 RNA isolation	28
2.2.6 Real-time quantitative RT-PCR	28
3 AIMS	30
4 RESULTS	32
4.1 IDENTIFICATION OF BIOCOMPATIBLE MATERIALS FOR BIOSENSOR MANUFACTURING	32
4.1.1 Effects of materials on cell growth.....	35
4.1.2 Effects of materials on erythroid differentiation	39
4.1.3 Effects of materials on cytokines release by IB3-1 cells	40
4.1.4 Effects of materials on CTL-mediated lysis of LCL cells	41
4.2 BIOSENSOR CHARACTERIZATION	42
4.2.1 Beads, cells and cells group levitation and trapping	42
4.2.2 Analysis of cell to cell interaction.....	43
4.2.2.1 Evaluation of CTL mediated lysis	45
4.2.2.2 Evaluation of NK mediated lysis	47

4.3	BIOTECHNOLOGICAL SENSOR VALIDATION	48
4.3.1	Isolation and <i>in vivo</i> expansion of single cells	48
4.3.2	Biological characterization of isolated clone	49
4.3.3	Analysis of gene expression after single cell manipulation	51
4.3.4	Comparison between biosensor platform and BioStation	52
5	DISCUSSION	55

PART II

1	INTRODUCTION	60
1.1	IMMUNE SYSTEM	60
1.1.1	T lymphocytes	61
1.1.2	Proteasome and antigen processing	62
1.1.3	MHC class I molecules	64
1.1.4	Viral and tumor escape mechanisms	66
1.2	EPSTEIN BARR VIRUS	67
1.2.1	EBV infection	68
1.2.1.1	Latent infection	69
1.2.1.2	Lytic infection	69
1.2.2	EBNA1 protein	71
1.3	EBV ASSOCIATED MALIGNANCIES	73
1.3.1	Burkitt's lymphoma	74
1.3.2	Hodgkin's lymphoma and nasopharyngeal carcinoma	75
2	MATERIALS AND METHODS	76
2.1	MATERIALS	76
2.1.1	Cell lines	76
2.1.2	Synthetic peptides	76
2.2	METHODS	77
2.2.1	Proteasomes purification	77
2.2.2	Enzymatic assays	77
2.2.3	Peptide degradation	78
2.2.4	Western blot assay	78
2.2.5	Preparation of antigen-presenting cells	78
2.2.6	Generation of memory CTL cultures	78
2.2.7	Cytotoxicity assay	79
2.2.8	IFN- γ ELISPOT	79
2.2.9	Immunofluorescence detection of HLA-ABC molecules	80
3	AIMS	81
4	RESULTS	82
4.1	IMMUNE RECOGNITION AND EBNA1 DERIVED EPITOPE PRESENTATION IN LCL AND BL CELLS	82
4.1.1	Identification of a new EBNA1 epitope	82
4.1.2	Induction of EBNA1-specific memory CTL responses directed to the HLA-B35 and -B53-presented HPV CTL epitope	85
4.1.3	Recognition of LCL and BL by HPV-specific CTL cultures	87

4.2 DIFFERENCE IN ANTIGEN PROCESSING MACHINERY BETWEEN LCLs AND BLs	89
4.2.1 Expression of HLA class I and TAP molecules	89
4.2.2 Expression and activity of proteasomes in LCL and BL	91
4.3 MODULATION AND INDUCTION OF BLs RECOGNITION BY HPV-SPECIFIC CTL	94
4.3.1 Evaluation of the effect of the Gly-Ala repeat domain on HPV-mediated lysis in BL ..	94
4.3.2 Modulation of antigen processing affects HPV epitope presentation in BL cells	95
4.3.3 <i>In vitro</i> generation of HPV epitope by proteasomes isolated from BLs	96
5 DISCUSSION.....	98
REFERENCES.....	102
ABBREVIATIONS.....	109
PUBLICATIONS	111
ACKNOWLEDGEMENTS.....	126

PRELIMINARY REMARK

While conventional chemotherapy and radiation therapy have improved the survival of many cancer patients, there are still major disadvantages associated with these treatments such as high toxicity and drug-resistance. The possibility to manipulate the immune system to recognize and kill tumor cells is very attractive despite numerous obstacles remaining to be overcome, such as tolerance and tumor escape. In particular, the ability of the immune system to seek out and destroy disseminated micro-metastases in a specific way makes immunotherapy an attractive alternative or complement to conventional therapies. Nevertheless today other unconventional technologies have reached many progresses, in particular the analysis and monitoring of single cell-to-cell interactions and the capability of individually controlling single cells have become of interest in different areas of life sciences, ranging from immunotherapy and cancer research to rare cell identification and isolation. These new technologies in combination with progresses reached in anti-tumor vaccines could be useful to identify, understand and improve immune T cell responses against tumor antigen and the sensitization of tumors to T cell effector mechanisms for a more efficient immunotherapy.

In particular, this thesis focuses on two tumor immunotherapy issues:

- 1) design, realization and validation of innovative Lab-on-a-chip devices for immune system study, that allow single tumor cell and effector cells interaction, detection and isolation;
- 2) identification of molecular mechanisms that prevent Burkitt's lymphoma recognition by T cells and study of their potential correction by specific treatments.

The main goal of this study remains indeed the evaluation of integrated strategies for immunotherapy development enhancing for malignancies treatment.

Part I

1 INTRODUCTION

A Lab-on-a-chip (LOC) is a device that integrates one or several laboratory functions on a single chip of only millimeters to a few square centimeters in size. LOCs deal with the handling of extremely small fluid volumes down to less than pico liters. These devices are a subset of MicroElectroMechanical systems devices (MEMS) and often indicated by "Micro Total Analysis Systems" (μ TAS) as well. In particular often LOC integrates microfluidics and electronics on the same platform. Microfluidics is a broader term that describes also mechanical flow control devices like pumps and valves or sensors like flowmeters and viscometers. However, strictly regarded "Lab-on-a-Chip" indicates generally the scaling of single or multiple lab processes down to chip-format, whereas " μ TAS" is dedicated to the integration of the total sequence of lab processes to perform chemical analysis. The term "Lab-on-a-Chip" was introduced later on when it turned out that μ TAS technologies were more widely applicable than only for analysis purposes. Although the application of LOCs is still novel and modest, a growing interest of companies and applied research groups is observed in different fields such as analysis (e.g. chemical analysis, environmental monitoring and medical diagnostics) but also in synthetic chemistry (e.g. rapid screening and microreactors for pharmaceuticals).

Besides further application developments, research in LOC systems is expected to extend towards downscaling of fluid handling structures as well, by using nanotechnology. Sub-micrometre and nano-sized channels, single cell detection and analysis, and nano-sensors, might become feasible, allowing new ways of interaction with biological species and molecules. The development of Lab-on-a-chip devices for biomedical applications, including manipulation of single cells, is

an exciting new research field requiring strict collaboration between electronic engineers and biologists¹⁻¹⁰. In the past few years, printed circuit board (PCB) technology, that can be used for Lab-on-a-chip devices producing, has reached a resolution of tens of micrometers, which is enough for many microfluidics applications¹¹⁻¹⁴. The main limitation of this approach in biomedical applications remains constituent materials biocompatibility. Recently the range of materials for PCB technologies has been extended. Most of them have already been developed for flex circuits and have rapidly become an industrial standard. Cost-effective technologies have also been proposed by introducing additional preparatory steps¹⁵⁻¹⁶ or by testing corrosion-resistant materials (like aluminum) in standard PCB processes¹⁷. The use of these “board technologies” is particularly relevant to the development of microtiter plates with sensing and actuating features that allow fast, parallel manipulation and analysis of biological samples¹⁸⁻²⁰. The adaptation of standard PCB processes, which ensure low production costs and large-scale development, may here boost progress in the design of many disposable applications. Lab-on-a-chip technology may soon become an important part of efforts to improve global health particularly through the development of point-of-care testing devices²¹. Despite the first LOC analysis system was developed in 1975 by S.C. Terry, Stanford University (it was a gas chromatograph), only at the end of the 1980s, and beginning of the 1990s, the LOC research started to seriously grow as a consequence of few research groups in Europe developing micropumps, flowsensors and concepts for integrated fluid treatments for analysis systems. A big boost in research and commercial interest came in the mid 1990's, when μ TAS technologies turned out to provide interesting tooling for genomics applications, like capillary electrophoresis and DNA microarrays.

1.1 BIOSENSOR DESIGN AND TEST

The idea of this project is to implement a microwell array using printed circuit board (PCB) technologies for the construction of the biosensor. Each microwell integrates actuation and sensing features by electrodes realized as structured conductor lines. The envisioned structure that is used for determining the cell-cell interaction by means of impedance change maintains the cells in equilibrium and traps them through dielectrophoresis forces (DEP). Figure 1 shows the sensor principle, but for the final device additional features will be added to the structure. Cells medium solution will flow from the bottom side into the microwells. Furthermore, a hydrophobic coating on PCB top will ease cell positioning into the microwells. Ultimately, the platform developed within the project, as shown in Figure 2, consists of an orderly matrix of up to thousands of microwells where living cells can be deposited and where microfluidics and electronics are integrated in a high-density circuit board.

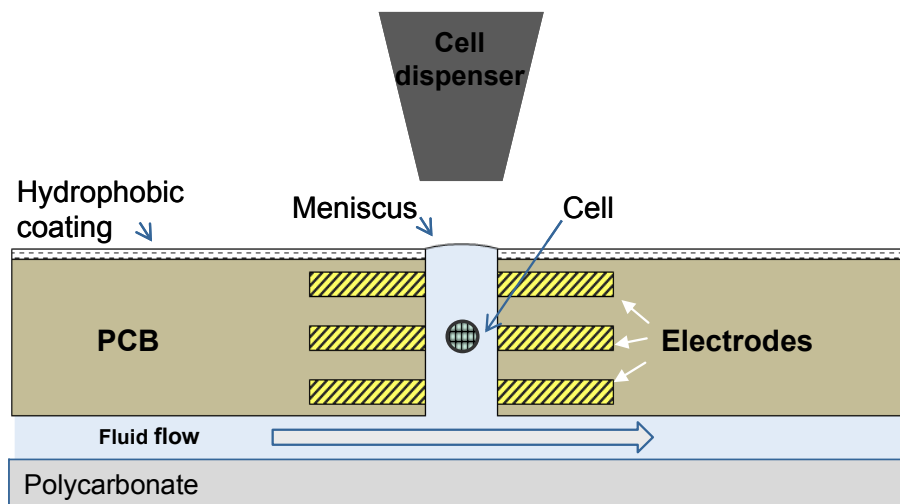


Figure 1. Biosensor principle, schematic cross section. This biosensor represents a novel concept of active microwells based on cylindrical wells able to vertically trap and control single particles by means of negative dielectrophoresis. The device is fabricated by drilling through holes on a solid substrate with metals layers, forming three annular electrodes within the well. A channel under the device provides a fluid flow filling the microwell by capillarity and cells or particles are delivered from the top by a microdispenser.

The microwells are monitored by an external microscope, the electronics allow to control the biosensor electrodes, necessary to DEP forces induction, and to perform impedance measurements. The key point of this technology is that each microwell can force contact between individual cells, and detect consequences of these interactions.

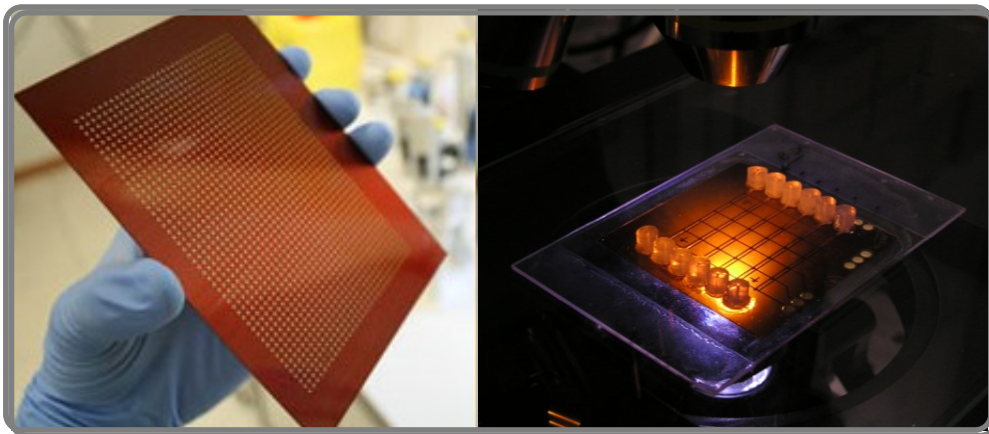


Figure 2. Example of matrix with up to thousands of microwells and a small assembled biosensor prototype with microfluidics and electronics integrated.

1.1.1 Biosensor architecture

Each microwell contains, as previously mentioned and as shown detail in Figure 3D, three annular electrodes at the top, middle and bottom levels (TOP, MID and BOT electrodes); by applying them a sinusoidal signals at frequencies ranging from 100 kHz to 1.5MHz and amplitudes between 2V and 7V the microwell levitates the cells keeping them in the center of the structure. All possible configurations are obtained by applying the same sinusoidal signal on two electrodes and a counter-phase signal to the third one (Figure 3). The trap configuration is achieved by phase-shifting the MID electrode, thus creating an almost spherical cage at the level of the MID electrode and in the horizontal center

of the microwell. To guarantee this shape, the distance between TOP/MID and MID/BOT electrodes must be equal to the microwell diameter. Figure 3B shows a contour plot of the mean square electric field for a 2D structure representing a vertical cross section along one of the diameters of the hole. The reference particle for these simulations is a polystyrene bead. As it can be noticed in Figure 3B, the trap mode also creates a semi-spherical cage on the top side of the microwell, thus preventing a particle dispensed from the top from entering the well. A different electrode polarization scheme is then used to create a load configuration by applying the counter-phase signal on BOT electrode (Figure 3A), thus creating an electric field minimum, in the region above MID electrode.

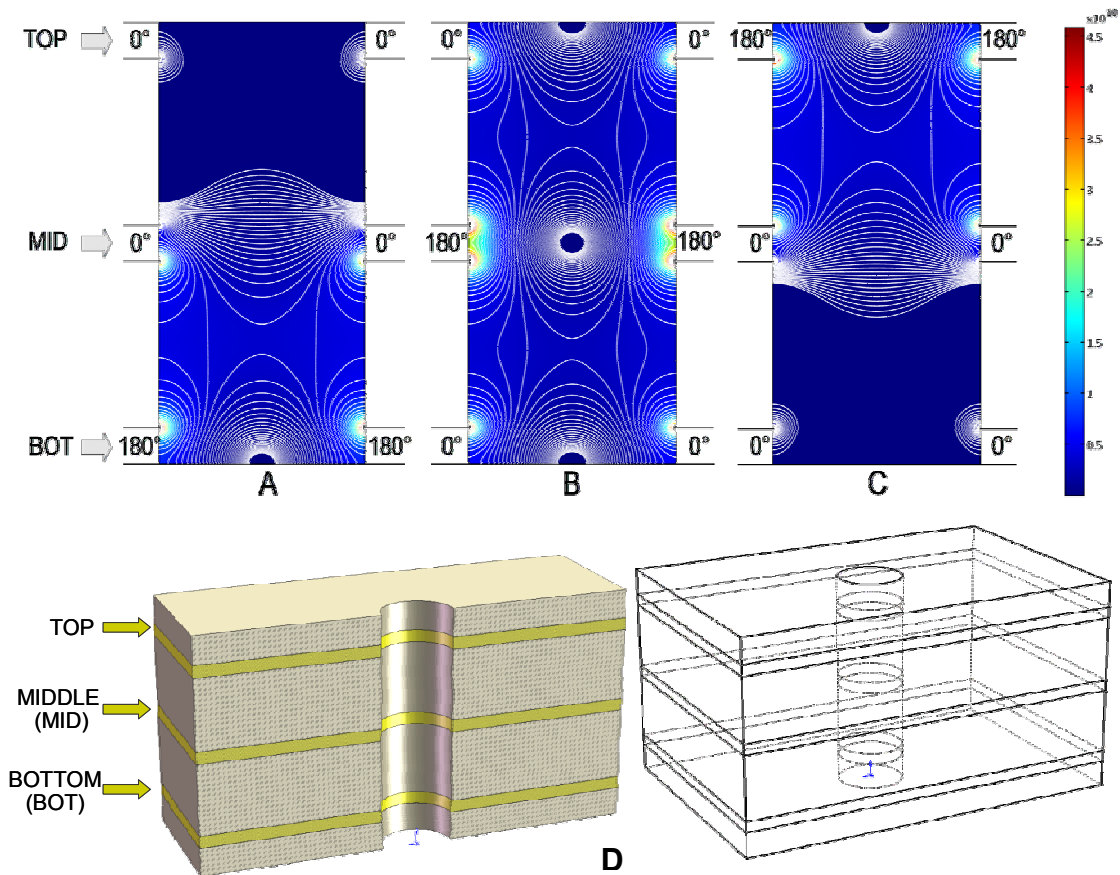


Figure 3. 2D contour plot of mean square electric field on the vertical plane of a microwell. Load configuration (A) trap configuration (B) and eject configuration (C) are obtained by applying a 180° phase-shifted signal on Bottom (BOT), middle (MID) and TOP electrodes respectively and a 0° phase-shifted signal on the two remaining electrodes. (D) 3D views of the microwell; each microwell consists of a hole drilled on a flexible PCB substrate containing three annular electrodes (Top, Middle, Bottom).

Finally, the eject configuration (Figure 3C) opens the cage from the bottom, allowing particles to be removed from the microwell. When implementing microwell arrays, independent addressing of single microwells is possible by changing the phases of the applied signals. An important consideration for cells controllability is related to the electrodes thickness, with particular reference to the middle electrode. As shown in Figure 3B, the region close to middle electrode has two electric fields maxima corresponding to the electrode edges, while in the middle region the electric field becomes null. As a consequence, the effect of the middle electrode to repel a particle towards the central region in negative dielectrophoresis (nDEP) conditions is reduced for particles with a small size compared to the electrode thickness. These particles, in fact, will find a region corresponding to the level at the center of the middle electrode where the horizontal DEP force becomes null or small.

1.1.1.1 Fluid carrier

Regarding the biosensor microfluidic, to provide a fluid flow to fill microwells and change the supernatant, a fluid carrier was created by structuring polycarbonate sheets and sealing them with silicone gaskets (Figure 4A). The carrier includes a chamber with height of 2mm, a volume of 4ml and a fluid inlet and outlet on two sides, providing fluids to microwells. Spring-loaded connectors were integrated to provide the signals to microwells (Figure 4B).

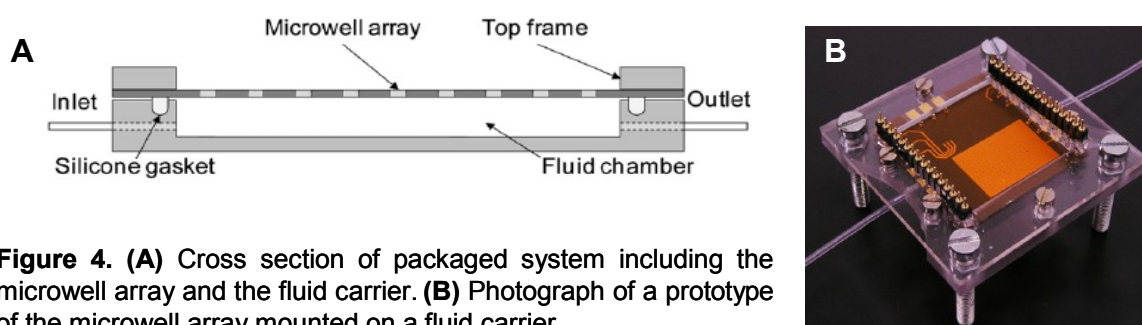


Figure 4. (A) Cross section of packaged system including the microwell array and the fluid carrier. (B) Photograph of a prototype of the microwell array mounted on a fluid carrier.

1.1.1.2 Electrical interface

In order to send electrical signals to the biosensor, a PCB board (named “PCB Host”) was realized (Figure 5A). The board is equipped with different connectors arrays and when the fluid carrier is positioned on the board the electrical contact are allowed (Figure 5B). In particular electrical signals for electrode polarization were generated by a multifunction synthesizer (Hewlett-Packard 8904A, Palo Alto, CA). The two sinusoidal signals have a frequency of 600 kHz, an amplitude between 0.2V and 0.7V, a programmable phase shift and were amplified by 10 times on a custom circuit, thus providing a final amplitude between 2V and 7V.

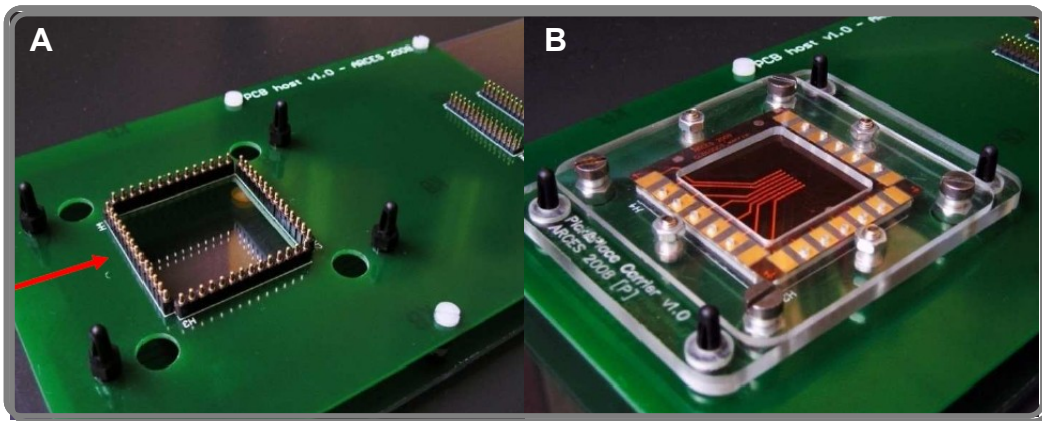


Figure 5. (A) Picture of “PCB Host” board, a red arrow indicates where fluid carrier will be positioned on the board (B) Picture of fluid carrier assembled on the “PCB Host” board.

1.1.2 System architecture

At the end, the biosensor considered in this thesis, is a fully automated system that integrates optical observation of microwells, alignment of target microwells beneath the microdispenser, automated motion, microfluidic handling and image/video capturing. Optical observation from the top of the microwell was performed by a fluorescence microscope (Nikon Eclipse 80i, Tokyo, Japan)

equipped with a Nikon DXM1200 digital camera. Precise positioning within the micron-range of the biosensor under the microscope or under the microdispenser was made with an XYZ motorized microscope stage (Märzhäuser Wetzlar, Steindorf-Wetzlar, Germany). A fluid flow in the channel beneath the microwells was provided by a KDS-210 syringe pump (KD Scientific, Holliston, MA). All system parts were controlled by a set of modules implemented in LabView software (National Instruments, Austin, TX) to achieve complete automation of experimental procedures. The complete system architecture and its electrical and fluidic interfaces were specifically designed to maintain an easy way to disassemble the package, to remove the biosensor when necessary, replacing it with a new one and to perform the required cleaning procedures. A complete system scheme is reported in Figure 6, while Figure 7 shows its corresponding 3D view.

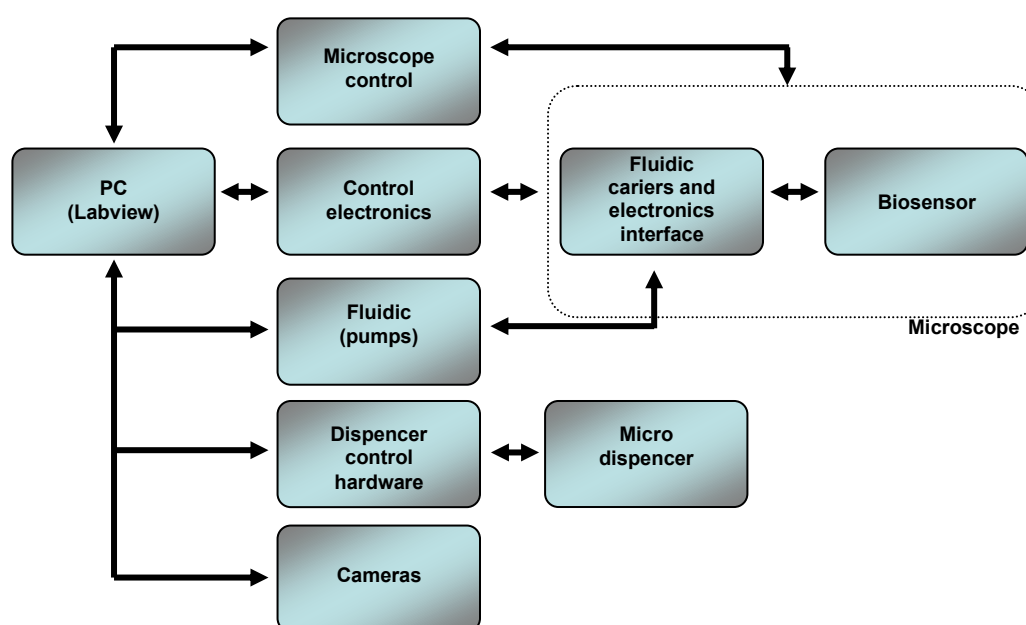


Figure 6. System diagram.

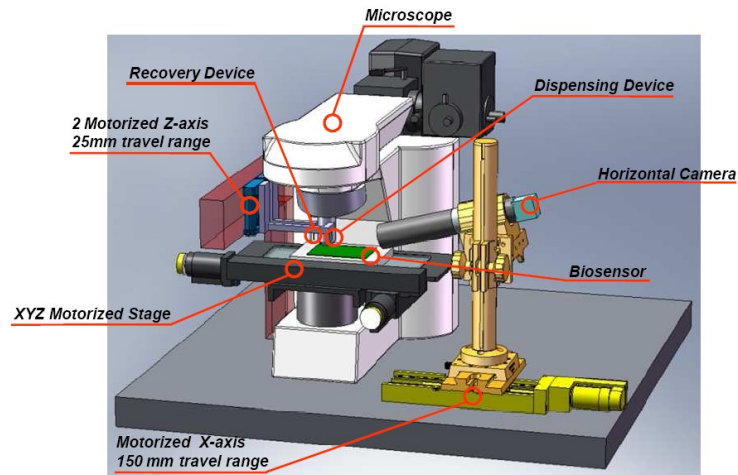


Figure 7. 3D view of the system.

1.2 CELL DELIVERY AND RECOVERY IN MICROWELLS

Equipments and procedures for depositing cells into biosensor microwells, as well as for recovering specific cells from selected microwells, were also developed inside this project. In particular to identify the best and most suitable dispensing technique three different dispenser system were investigated:

- 1.2.1) CellJet microdispenser. developed at Biochips Laboratory in CEA;
- 1.2.2) a commercial piezoelectric jetting device;
- 1.2.3) cell handling with a machined ceramic micropipette.

The instrumentation for cell handling includes some mechanical supporting structures, such as, motorized stages, pressure control, optical devices, software, and development of operational loading methods (Figure 8).

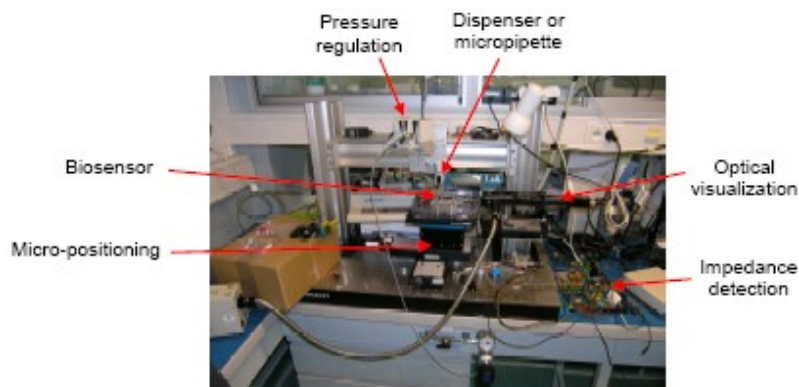


Figure 8. Integrated modules for cells dispensing and recovery towards microwells.

1.2.1 CellJet microdispenser

In CellJet microdispenser, the cells are introduced into a microfluidic chip, transported and lined up along a microchannel, and detected by microelectrodes. For achieving cell dispense, some $\sim 1 \mu\text{L}$ droplets are generated by a miniaturized solenoid valve so that the cells are brought out through the orifice of the microchannels. The cell-containing droplets are finally collected and absorbed by the microwell of the biosensor placed underneath (Figure 9). Deposited cells were proved to enter and pass through the microwells within few minutes. A software program for the cell microdispenser was developed, it automatically drives the CellJet microdispenser. Moreover, electrical profiles of cells flowing through the microfluidic chips were investigated to parameterize cell dispense.

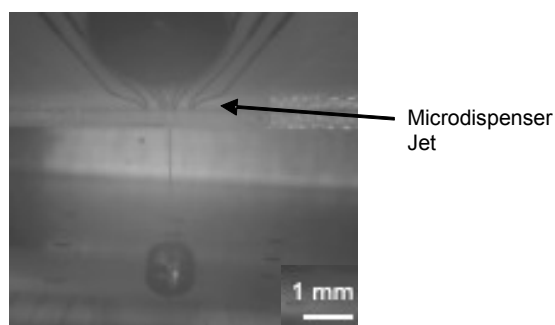


Figure 9. Spot dispensed onto a microwell by the CellJet microdispenser. The jet is narrow and very straight, allowing the spot to be located in the near vicinity of the microwell. The spot is absorbed by the microwell within seconds or minutes according to the fluidic resistance of the underneath microwell.

1.2.2 Commercial piezoelectric jetting device

In second analysis a commercial piezoelectric dispenser was also employed for cells depositing. As the diameter of human cells is about $20 \mu\text{m}$, a dispenser with an orifice of $60 \mu\text{m}$ was chosen. The formed droplet has generally a diameter slightly larger than the orifice diameter, e.g. $65 \mu\text{m}$ in diameter which results in an

individual ejected volume of ~140 pL. A droplet generation requiring no pressure controller was implemented, and drivers using LabView software were programmed for controlling the electronic triggering of droplet jetting. Two modes of dispense were developed: a 'stop-on-spot' mode where the biosensor is moved and stopped under the microdispenser for dispense; and a 'in-fly ejection' mode where dispense is very rapid so that the ejected droplets can reach the underneath microwell while the biosensor is still moving at a constant velocity. Heterogeneity of the number of deposited cells were generally observed, which is likely due to sedimentation of cells upstream of the dispenser orifice. A classical limit dilution strategy, in which a low concentration of cells is introduced so that the total volume of cells statistically contains one single cell, was successfully investigated to resolve this heterogeneity.

1.2.3 Cell handling with a machined micropipette

Finally, a micropipette was machined from a capillary made in alumina (Al_2O_3) and toughened by zirconia (ZrO_2), as shown in Figure 10. This material is very resistant to mechanical shocks and thus is tolerant to abrupt contacts with the microwell walls. Moreover, the micropipette extremity was micromachined for providing inner and outer diameters of 56 μm and 150 μm respectively. As a result, the pipette can handle T, B lymphocytes and NK cells of ~8 μm in diameter, and tumor cells of epithelial origin and melanomas of ~16 μm in diameter, as well as penetrate into the conical entrance of the microwell (300-400 μm in diameter) and collect the upper fraction of the microwell liquid. The microwell is supplied with liquid from the bottom fluidic chamber, and thus a prolonged aspiration of liquid by the micropipette is possible by continuous replacement of liquid during pipetting. Eventually, the meniscus height in the

microwell can be increased beyond the microwell border by controlling the pressure inside the fluidic chamber. Meniscus upward movements can form a droplet above the microwell which facilitates the contact between the pipette and the liquid and this aids the aspiration process. The ultrathin micropipette can be used both for depositing cells and for aspirating cells from microwells. By reversing the flow direction in the micropipette, the volume of liquid previously aspirated by the pipette can then be deposited into another microwell.

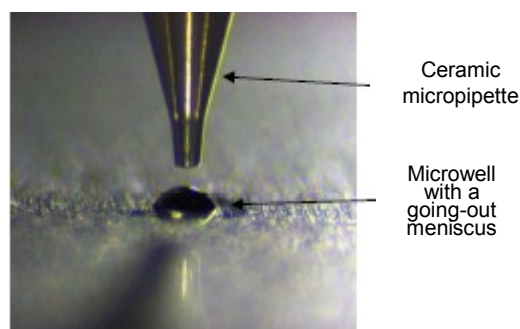


Figure 10. Handling of cell-containing liquid with a micromachined ceramic micropipette. The micropipette inner channel can be seen by transparency. A meniscus is formed above the microwell by enhancing pressure inside the fluidic biosensor chamber.

1.3 BIOSENSOR TECHNOLOGY AND MANUFACTURING

A key point in this innovative device is the fabrication technology of the microwell array. Several technologies for microfluidic device fabrication and packaging have been proposed to integrate sensing capabilities and electrical interfaces into a single device. All these approaches require complex steps or expensive facilities, and mostly are useful for prototyping only. In opposition to existing technologies, the biosensor developed within this project needs to be low cost and disposable to be applicable for the intended purpose. Due to these requirements, standard printed circuit board (PCB) manufacturing processes were selected as base technology. In addition to be a low cost mass production tool, it allows the realization of fine structures and vias with feature widths below 100 μm . Drawback of this technology is the default use, as conductive substrate, of non-biocompatible materials as e.g. copper (Cu). Therefore, the first task was to identify a list of materials which could be processed with standard PCB technologies as substitutes of non-biocompatible materials. As a consequence with the hypothetic use of new materials and new material combinations also processes as lamination, conductor line structuring, microwell drilling, via formation and via metallization need to be developed or at least adapted. Additionally surface modifications have to be developed for the sensor manufacturing. The bottom side of the microwell sensor should have a hydrophilic surface for a bubble free wetting and flow of medium solution for the cells. On the other hand the top side of the sensor should have a hydrophobic surface for easier cell positioning into the microwell.

1.3.1 Materials selection

In standard PCB manufacturing process typically Resin Coated Copper (RCC) and glass fiber filled epoxy films are used. These materials are not applicable for the microwell array realization due to copper incompatibility and the poor processability of fiber filled epoxies by laser structuring. Standard copper technology in combination with biocompatible metallization on top does not work due to the proposed manufacturing technology of the device (smearing of Cu particles during via drilling is contaminating also dielectric surfaces) and the metallization growth of an additional layer. Thus, no safe biocompatible device could be achieved using such a process combination. Therefore, new dielectric materials have to be evaluated in combination with biocompatible metal layers. As possible metals for conductive layer formation palladium, aluminum and gold were taken into account. Pyralux (Py), a B-staged modified acrylic adhesive, in combination with Polyimide, printable epoxies and epoxy films with aramid fibers have been discussed as dielectric layers. For the realization of the final Lab-on-Substrate device also a hydrophobic / hydrophilic surface modification is needed, therefore, different coatings and modifications have to be evaluated.

1.3.2 Lab-On-Substrate manufacturing process flow

The starting process for PCB production, that will constitute biosensor heart/ physical support, is the lamination of the inner Aluminum–Pyralux–Polyimide layer. In sequential steps aluminum (Al) structuring is done by wet chemical etching followed by lamination of the next dielectric and metal layer. Final layer on top and bottom side is a Polyimide (PI) passivation. Microwells, through vias and blind vias are realized by laser drilling. The last process step would be the electroless metal

deposition for via metallization. Briefly, the general process sequence for Lab-On-Substrate manufacturing with standard technologies is shown in Figure 11.

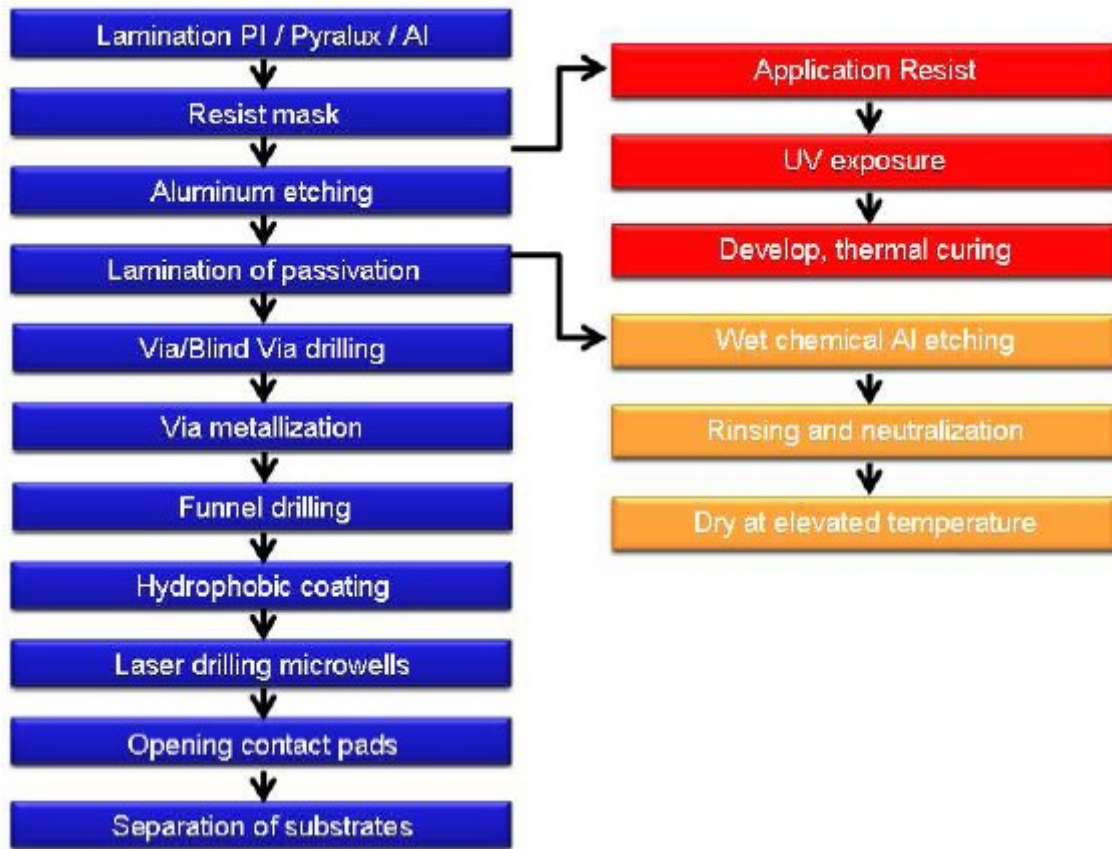


Figure 11. PCB manufacturing process flow.

1.3.2.1 Lamination

A Lauffer vacuum laminating press was used for all lamination processes described. This press allows the lamination under vacuum with defined parameters as pressure, temperature and time. The lamination process starts with a drying step at 50 °C under vacuum without pressure. The following lamination steps under force, heating and vacuum are used to achieve homogeneous layer thicknesses and good adhesion between the different layers. In particular Figure 14 shows a cross section of a final laminated Al-Py-PI stack.

1.3.2.2 Microwell and via formation

Once obtaining laminated Al-Py-PI stack it is necessary to create via and microwell inside the support for the final device ideation (Figure 12A). In particular for this purpose an UV laser system is used and the drilling process is milling the material through the laser beam. A 60 μm via in a Al-Py-PI stack of 210 μm overall thickness is shown in Figure 12B as an example. Due to the different material properties of Pyralux and the PI layer, the resulting via diameter of these materials is often different. Vias in Pyralux are larger, possibly due to a combination of higher ablation rate and larger thermal shrinkage with this material. Another important and crucial aspect of this process is the protection of the substrate surface, since the material removed during the laser drilling process can be re-deposited and consequently contaminate the substrate surface.

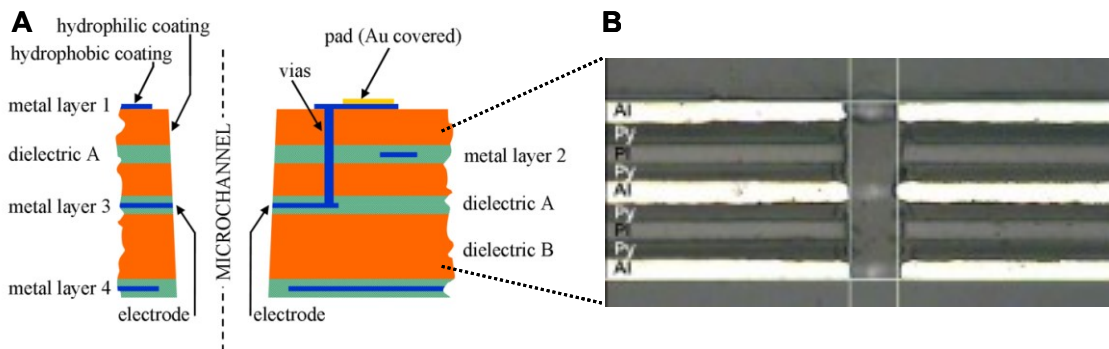


Figure 12. (A) Schematic cross section of device where microwell, different material layer and vias are shown (B) Picture of 60 μm via in Aluminum/Pyralux/Polyimide stack (Al/Py/PI).

1.3.2.3 Via metallization

An electroless Ni/Au process has been used to realize electrical connections between inner aluminum layers and solder able pads on top of the device. The basic process chain is a sequential treatment of the Al with different chemicals,

which are needed to apply the desired pretreatment to the pads, followed by the electroless Ni and immersion Au deposition.

1.3.2.4 Funnel

To get cell spotting into the microwells easier, a funnel has been projected above each microwell, therefore on top of the final metal layer two thick polyimide layers will be laminated. The polyimide will act as passivation on the metal structures and as a base for funnels. Funnels are mechanically drilled before the microwells are drilled by laser. An example of a microwell with funnel structure is shown in Figure 13.

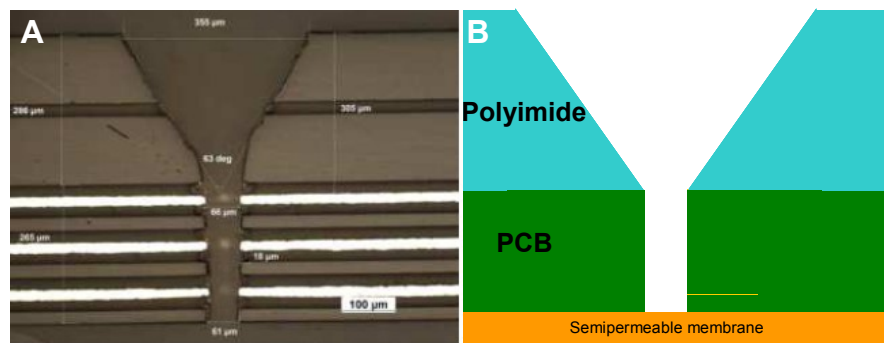


Figure 13. (A) Picture of funnel realized by mechanical drilling in the final Polyimide top layer; (B) Schematic microwell cross section where funnel is realized, different material layer assembled in final device are indicated in different colours.

1.3.3 Hydrophobic / hydrophilic surface modifications

Different hydrophobic/hydrophilic coatings on device have been investigated, for example, to ease cell positioning into the microwells or to ease flow inside biosensor microchannel. For these purposes, all materials used for device realization were characterized and classified according to their surface energy; in particular, contact angle measurement of different candidate materials were determined with test liquids bromonaphthalene (nonpolar), glycerol (slightly polar)

and water (highly polar). It was found that the surfaces of both Polyimide and Aluminum must be treated to allow a designing of a hydrophilic/hydrophobic microfluidic network required for a successful operation of sensor devices. Other different surface modifications were considered e.g. fluoralkyl polymer, hydrocarbon polymer, octadecane thiol and SF₆-plasma to increase hydrophobicity; and organic acids, O₂-plasma and several polar silanes to increase hydrophilicity.

2 MATERIALS AND METHODS

2.1 MATERIALS

2.1.1 Tested materials for biosensor manufacturing

The materials under-test (Table 1) were embedded in standard multiwell plates for cell culture (Costar-Corning, USA) in which the biological experiments for biocompatibility were carried out.

Group	Name	Abbreviation
Metals	Copper	Cu
	Aluminum	Al
	Palladium	Pd
	Gold over Nickel	Au over Ni
	Gold over Palladium	Au over Pd
Dielectrics-adhesives	Polyimide	PI
	Pyralux uncured	Py uncured
	Pyralux cured	Py cured
	Poly(dimethylsiloxane)	PDMS
	Polyurethane foil before lamination	PF before lam
	Polyurethane foil after lamination	PF after lam
	Polyurethane Powder	PP
	Epoxy cured	Epoxy cured
	Die Attach Film	DAF
	Aramid fiber cured	Aramid fiber cured
	Aramid fiber uncured	Aramid fiber uncured
	Tesa 4983	Tesa 4983
	Tesa 4985	Tesa 4985
CMC 15581	CMC 15581	
Surface treatments	Copper + Octadecanethiol	Cu + ODT
	Palladium + Octadecanethiol	Pd + ODT
	Gold over Nickel + Octadecanethiol	Au over Ni + ODT
	Gold over Palladium + Octadecanethiol	Au over Pd + ODT
	Certonal FC-732	Certonal FC-732
	Certonal FC-732 Tempered	Certonal FC-732T
	Chemlease 41-90	Chemlease

Table 1. Complete list and abbreviation of tested materials.

The materials, mostly foil, were cut by laser machining in round samples of 5.7 mm diameter for 96-well plates and 15 mm for 24-well plates. Blue film was used to cover the sample during the cutting preventing its surface contamination due to the melting materials produced by the laser process. The sample has been embedded in the well with a droplet of PDMS. It was dispensed in each well by an air pressured dispenser (EFD, USA) with a 0,020' tip (internal diameter; EFD Precision Tips, USA) applying a pressure of 1.5 bar for 2.3 s for a 96 well plates and 13.8 s for a 24 well plates. The dispensing parameters were defined by tuning dispensing time, fixed pressure and tip diameter. The covering of the sample edges was optically measured by a Wild H3Z microscope (Heerbrugg, Switzerland) equipped with a MFK II measuring system (Kappa, Germany) at different dispensing time for a 96-well. PDMS was partially dried for 5 minutes at 45°C after the dispensing. The round samples were deposited by a vacuum tip (EFD, USA) applying a light pressure. The protocol including dispensing, heating and sample deposition was repeat for each row of the multiwell plate. Finally PDMS was fully cured at 45°C for 24 h.

Aluminum (18 μm thickness, Al), Copper (136 μm thickness, Cu), Polyimide (100 μm thickness) were bought in foils and tested without any further process. In particular in this study materials will be referred as uncured (the material as delivered), b-stage (intermediate stage of the curing process) and cured (after complete processing).

In order to understand the possible effect of a non-complete curing of internal layers during lamination process, Pyralux LF0300 adhesive (DuPont, USA) and aramid fiber filled epoxy F161 (HEXCEL, California) were tested both as uncured and cured materials (Pyralux uncured or cured and aramid fiber uncured or cured). Similarly, Polyurethane films (TPU-4201, Epurex Films, Bayer MaterialScience, Germany) were tested either before and after the lamination process (PF before

lam and PF after lam), while a second type of Polyurethane (94AU925, Merkel Freudenberg Fluidtechnic, Hamburg, Germany) provided as powder (PP) was tested after lamination.

Aramid fiber filled epoxy was laminated following the curing cycle reported in its datasheet (Hexel, California).

Patternable Epoxy (SEMICOAT513E, Shin-Etsu Chemical Co. LTD., Japan) requires up to 150°C to be cured [60min, 100°C + 90 min, 150°C] (Epoxy cured). This temperature is not compatible with the multiwell plate made with Polystyrene, which glass transition temperature is 95°C. To overcome this limitation a film of epoxy, 100µm-thick, has been patterned on a support covered with cured Doubling silicone for dental copy (SUPERIUM Dubliersilikon, Weber Dental - Germany), cured, peeled out as a foil and cut by laser. The hydrophobicity of the Doubling silicone avoids the sticking of the epoxy film.

The Die Attach Film (DAF) is a polymer film (thickness 120 µm) consisting of a thermosetting and UV curable resin. This commercially available film could also be used for large-area lamination of different layers, as is needed in the case of a multilayer PCB.

Poly(dimethylsiloxane) (PDMS, Sylgard 184, DowCorning) was prepared mixing the two components of Sylgard 184 with a ratio of 1:10 for 5 minutes and degassed for 30 minutes at 0.1 bar (4 min were required to reach 0.1 bar), prepared according to previous study²², and cured in the well at 45°C overnight.

Palladium (Pd) and Gold (Au) have been chemically deposited on copper substrates by electroless process. For Pd deposition, first Nickel (Ni) was deposited as adhesion layer (15 min, 90°C) followed by Pd activation (1 min, 55°C) and Pd deposition (30 min, 60°C). For Au deposition on Ni (Au over Ni), Ni was deposited as adhesion layer (15 min, 90°C) followed by Pd activation (1 min, 55°C) and Au deposition (30 min, 50°C). For Au deposition on Pd (Au over Pd), Ni

was deposited as adhesion layer (15 min, 90°C) followed by Pd activation (1 min, 55°C), Pd deposition (30 min, 60°C) and Au deposition (30 min, 50°C). The Cu substrates were cleaned in HCl 0.5% for 30 sec before the deposition, rinsing with DI-water and drying with nitrogen.

The acrylic adhesive transfer films Tesa 4985 and 4983 (Tesa tape, USA), with a thermal stability up to 200°C, and CMC 15581 (CMC technical tapes, Germany), with a thermal stability up to 130°C, have been prepared in multiwell plates. The tapes, protected on both sides by cover papers, have been cut in samples by laser. All the tapes are transparent and provide a permanent adhesion. The transfer tapes were stuck in the well and PDMS was manually dispensed to cover their edges and cured as for the other multiwell plates.

Certonal FC-732 was deposited filling the well for half of its volume for 5 min, rinsing with water and drying with a nitrogen flux at RT. Certonal was also deposited on an aluminum foil and tempered for 20 min at 150°C on a hotplate (Certonal FC-732T), after which it was cut by laser. A thin layer of Chemlease 41-90 (Chemlease) has been applied on an aluminum foil, tempered for 20 min at 150°C on hotplate and cut in samples.

The Au, Pd and Cu surfaces have been functionalized with 1-octadecanethiol (ODT) (Sigma-Aldrich) making it hydrophobic. Ethanol was deoxygenated with bubbling nitrogen for 1 h before using it as a solvent for thiols, but not purified further²³. The metal substrates, embedded in multiwell, have been cleaned with isopropanol for 2 h, rinsing with DI-water and ethanol before the thiol monolayer deposition (24 h at RT). ODT 1 mM has been prepared in ethanol. Any significant variation in the contact angle was recorded using piranha solution²⁴ or plasma etching²³ for the cleaning of the substrates. After the deposition, the samples were rinsed with ethanol and dried with a jet of high purity nitrogen.

Since all the surface treatments (Certonal, Chemlease and ODT) produce an hydrophobic behavior of the treated surface, the presence of these coatings was verified by measuring contact angle of the processed surfaces²⁵. All materials were UV-light sterilized before testing.

2.1.2 Cell lines and culture conditions

Lymphoblastoid cell lines (LCL) have been obtained after infection of human B-lymphocytes with B95.8 strain of Epstein-Barr Virus (EBV)²⁶. LCL and the human erythroleukemia K562 cells²⁷ were maintained in RPMI 1640 medium (Sigma-Aldrich, Milwaukee, Wisc., USA) at 37°C in a humidified 5% CO₂ atmosphere, supplemented with 10% fetal bovine serum (FBS; CELBIO, Milano, Italy), 100 units/ml penicillin and 100 µg/ml streptomycin (Sigma-Aldrich, St.Louis, MO, USA). IB3-1 were cultured in LHC-8 (Gibco; Invitrogen, San Diego, CA) supplemented with 5% FBS. The other cell lines employed in this work such as 221 and 221-G1 lymphoblastoid cells, NKL and YTS natural killer-like cell line were provided by Regina Elena Cancer Institute, Rome.

2.1.3 Compounds used to induce erythroid differentiation in K562

Mithramycin (Sigma-Aldrich, St.Louis, MO, USA), cytosine arabinoside (AraC) (Sigma-Aldrich, St.Louis, MO, USA), and a C(5) modified uracil derivate³⁰ (referred as AA55) kindly provided by Prof. R. Corradini (Department of Organic and Industrial Chemistry, University of Parma).

2.2 METHODS

2.2.1 Analysis of *in vitro* cell growth

For studying the effects on *in vitro* cell growth, with continuous incubation or after pulse incubation (60 minutes) with the materials, cells were seeded at the initial cell concentration of 30,000 cells/ml (K562 cells) or 50,000 cells/ml (LCL and IB3-1 cells), cultured in RPMI supplemented with 10% FBS (or LHC-8 supplemented with 5% FBS for IB3-1) and the cell number/ml was determined using a model ZBI Coulter Counter (Coulter Electronics, Hialeah, FL, USA) after different days of cell culture.

2.2.2 Erythroid differentiation of K562 cells

The experimental protocols for analysis of the effects of the biomaterials on the erythroid differentiation were the following: (a) K562 cells were cultured to within biomaterial-treated 24-well plates for different days and treated with 25 nM mithramycin a powerful inducer of erythroid differentiation²⁸ (continuous exposure); (b) K562 cells were exposed to the different biomaterials for 1 hour, then washed, sub-cultured in standard medium conditions and treated with 25 nM mithramycin for the following days (short exposure). The proportion of benzidine-positive cells was determined after 5 and 6 days of cell culture using a solution containing 0.2% benzidine in 5 M glacial acetic acid (10% H₂O₂)²⁹.

2.2.3 CTL-mediated LCL lysis: chromium release assay

Monocyte-depleted PBLs from HLA-A2 positive blood donor were plated at $3,5 \times 10^6$ cells per well in 24-well plates in RPMI 1640 containing 10% fetal bovine serum (FBS Hyclone; CELBIO, Milano, Italy) and stimulated with EBV nuclear antigen 3 (EBNA-3) SVR peptide (10 μ M). Cultures were restimulated after 7 and 14 days, and the medium was supplemented from day 8 with 10 U/ml rIL-2 (Chiron). On days 14 and 21, T cell cultures were tested for CTL activity using cytotoxicity assay. SVR-specific CTL cultures efficiently lysed SVR-pulsed human leukocyte antigen A2 (HLA-A2) positive LCLs, but did not lyse SVR-pulsed HLA-A2 negative LCLs (data not shown). Cytotoxic activity was tested by a standard 5h ^{51}Cr -release assay³¹. Briefly, target cells were labeled with 0.1 $\mu\text{Ci}/10^6$ cells of $\text{Na}_2^{51}\text{CrO}_4$ for 90 minutes at 37°C and pulsed for 45 minutes with 10^{-5} M of peptide at 37°C. Cells were then washed and used as targets at different effector : target (E:T) ratios. Percentage specific lysis was calculated as $100 \times (\text{cpm sample} - \text{cpm medium}) / (\text{cpm Triton X-100} - \text{cpm medium})$, where cpm is counts per minute.

2.2.4 Cytokine profiles

Cytokines in tissue culture supernatants released from IB3-1 under analysis, were measured by Bio-Plex cytokine assay (Bio-Rad Laboratories, Hercules, CA)^{32,33} as described by the manufacturer. The Bio-Plex cytokine assay is designed for the multiplexed quantitative measurement of multiple cytokines in a single well using as little as 50 μl of sample. In our experiments, we used the premixed multiplex beads of the Bio-Plex human cytokine 11-Plex Panel, which included eleven cytokines (IL-1 α , IL-2 α , IL-3, IL-12, CTACK, GRO- α , ICAM-1, LIF, M-CSF, SDF-1 α , TRAIL). Briefly, 50 μl of cytokine standards or samples (supernatants from treated cells) were incubated with 50 μl of anti-cytokine

conjugated beads in 96-well filter plates for 30 min at RT with shaking. Plates were then washed by vacuum filtration three times with 100 μ l of Bio-Plex wash buffer, 25 μ l of diluted detection antibody were added, and plates were incubated for 30 min at room temperature with shaking. After three filter washes, 50 μ l of streptavidin-phycoerythrin was added, and the plates were incubated for 10 min at room temperature with shaking. Finally, plates were washed by vacuum filtration three times, beads were suspended in Bio-Plex assay buffer, and samples were analyzed on a Bio-Rad 96-well plate reader using the Bio-Plex Suspension Array System and Bio-Plex Manager software (Bio-Rad Laboratories, Hercules, CA).

2.2.5 RNA isolation

Total RNA was phenol–chloroform-extracted from cytoplasm of treated and untreated K562 cells²⁸. All solutions were made in diethylpyrocarbonate (DEPC)-treated water. The extracted RNA was precipitated in two volumes of absolute ethanol and stored at -80 °C, washed once with cold 75% ethanol, dried and dissolved in DEPC-treated water before use.

2.2.6 Real-time quantitative RT-PCR

Quantitative real-time PCR assay of α -, β -, γ -, δ -, ϵ -, ζ -globin mRNA and α -, β -, γ -, δ -, ϵ -, ζ -globin transcripts have been carried out using gene-specific double fluorescently labelled probes in an ABI Prism 7700 Sequence Detection System version 1.7.3 (Applied Biosystems, Monza, Italy). The following primer and probe sequences were used: α -globin forward primer: 5'-CAC GCG CAC AAG CTT CG-3', α -globin reverse primer: 5'-AGG GTC ACC AGC AGG CAG T-3', α -globin probe: 5'-FAM-TGG ACC CGG TCA ACT TCA AGC TCC T-TAMRA-3'; β -globin

forward primer: 5'-CAA GAA AGT GCT CGG TGC CT-3', β -globin reverse primer: 5'-GCA AAG GTG CCC TTG AGG T-3', β -globin probe: 5'-FAM- TAG TGA TGG CCT GGC TCA CCT GGA C-TAMRA-3'; γ -globin forward primer: 5'-TGG CAA GAA GGT GCT GAC TTC-3', γ -globin reverse primer: 5'-TCA CTC AGC TGG GCA AAG G -3', γ -globin probe: 5'-FAM- TGG GAG ATG CCA TAA AGC ACC TGG-TAMRA-3'; δ -globin (Applied Biosystems, Hs00426283_m1); ϵ -globin (Applied Biosystems, Hs00362216_m1) and ζ -globin (Applied Biosystems, Hs00923579_m1). For real-time PCR, the reference gene was 18S; this probe was fluorescent-labeled with VIC (Applied Biosystems, Monza, Italy)³⁴.

3 AIMS

The Cell-On-CHIp biosensor (COCHISE) for detection of cell-to-cell interactions is a specific targeted research project which addresses integrated systems for point-of-care diagnosis, monitoring, and drug delivery. This project is the first step of an activity aimed at the development of enabling micro-technologies to monitor physiological cellular interactions at single cell level with a high throughput. One of the primary applications of this technology is the immunological monitoring of anti-tumor vaccinations, singling out the rare effector cells (in the order of 1 cell among 1000 cells) that are actually active against tumor cells.

The first aim within the project was to develop an appropriate platform that combines microfluidics and electronics together and that consists in an orderly matrix of up to thousand microwells where living cells can be deposited. Secondly the aim of this thesis was to identify a correct protocol for biocompatibility analysis of materials that should be subsequently chosen for biosensor manufacturing. After biosensor assembling, with the most biocompatible materials, it has been necessary to test the platform from a functional point of view, in particular the third intention was the development of experimental cellular systems useful to validate the COCHISE platform. For this purpose several proofs were performed to trap before beads, cluster cells and single cells from different cell lines. After demonstrating that the biosensor was functional and allowed to trap and recover single cells we have set ourselves the objective to understand whether single cells manipulation was a not toxic procedure, determine if the manipulated cells maintained their biological activity and finally if gene expression remained unaltered. Since the main purpose of this research is the definition of new

therapeutic and diagnostic protocols for tumor immunotherapy, our next step was to apply our technology to the analysis of anti-tumor lytic effector cells.

In particular our aim was to demonstrate that this platform is suitable for detection and isolation of specific immune cells, that have shown, into the biosensor, ability to recognize and lyse tumor cells. On the other hand our purpose was also to identify and recover tumor cells that resist to CTL or NK lysis for further more detailed analysis and characterization from a biomolecular point of view, or to isolate rare stem cells. Ultimately the final goal was to develop a specific tool able to improve immune system response analysis in order to advance tumor immunotherapy.

4 RESULTS

4.1 IDENTIFICATION OF BIOCOMPATIBLE MATERIALS FOR BIOSENSOR MANUFACTURING

The first aim of this study was to determine the biocompatibility of materials employed for the COCHISE platforms fabrication. This objective is related to the concept that the manipulation of single cells requires that the employed materials are non-toxic and defined as biocompatible. For this purpose the foils of materials under testing were cut in round samples (see Figure 1A) by laser: 5.7mm of diameter for 96-well plate and 15mm for 24-well plate. A blue-foil were used to cover the material during the cutting, in order to prevent surface contamination caused by melted material particles. Then the sample were embedded in well bottom of a standard multiwell culture plate with a droplet of PDMS as reported in Figure 1B. The PDMS was dispensed in each well by an air pressured dispenser (EFD, USA) with a 0,020' tip applying a pressure of 1.5 bar for 2.3 sec for a 96-well plate and 13.8 sec for a 24-well plate.

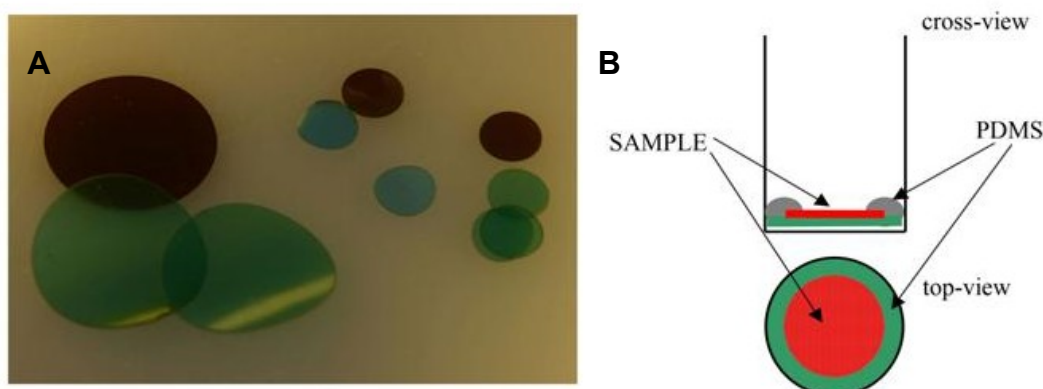
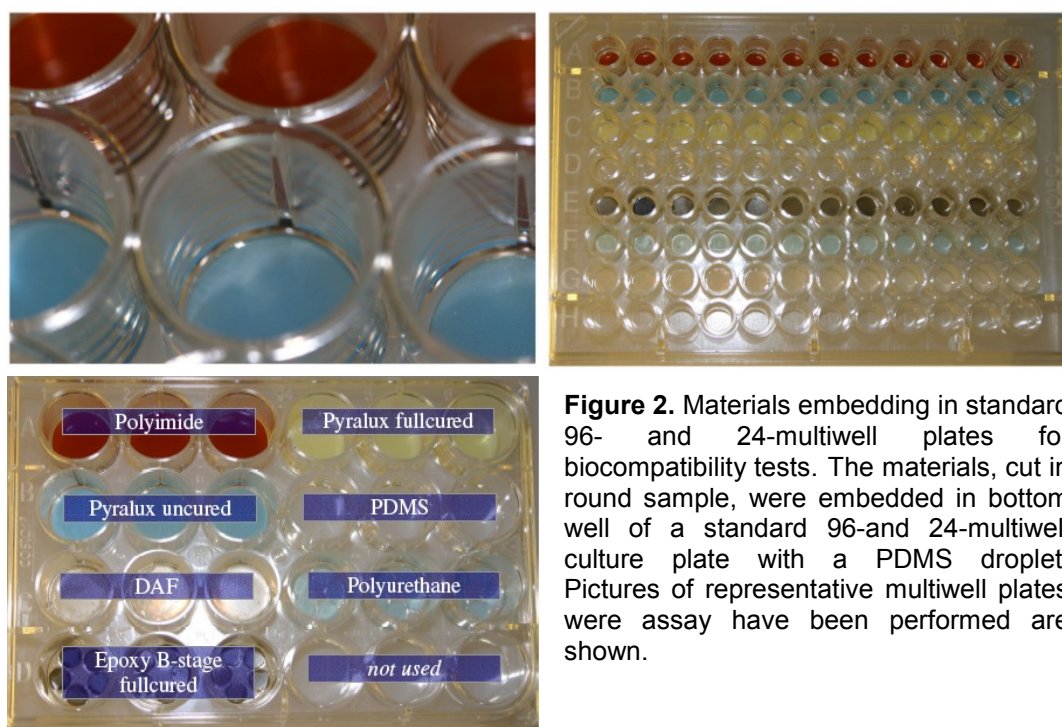


Figure 1. Materials embedding in standard multiwell plate for biocompatibility tests. **(A)** Materials are cut by laser in round samples and then **(B)** embedded with a PDMS droplet; PDMS was also used for covering the cut edges to prevent any contamination coming from the support material.

The dispensing parameters were defined tuning the dispensing time keeping fixed pressure and tip diameter. Subsequently, after the dispensing and the round samples deposition by a vacuum tip and applying a light pressure, PDMS was partially dried for 5 min at 45°C. Finally the PDMS was fully cured at 45°C for 24h. An example of a 96-well plate and 24-well plate with embedded materials are shown in Figure 2. After obtaining the appropriate plates, biocompatibility tests were performed to identify suitable materials for biosensor construction. In particular we studied a significant number of materials, commonly used for the implementation of Lab-on-a-chip platforms, all materials tested are shown in Table 1. Biological tests were performed on several cell lines (e.g. as model of cells growing in suspension were chosen LCLs and K562 cells, while as model of attached cell cultures were chosen IB3-1 and rat hippocampal primary cells) and on different biological functions (e.g. cell growth, erythroid differentiation of K562 cells, CTL-mediated cell lysis and cytokine release by IB3-1 cells).



Group	Materials	Comments and possible drawbacks	Ref.
METALS	Copper (Cu)	Standard metal in a PCB; due to high chemical instability in wet environment is not used in bio-devices.	12
	Palladium (Pd), Nickel (Ni), Gold (Au)	Applied with an electroless process to a copper substrate.	17 35
	Aluminum (Al)	Widely and cheaply available as a foil; potential substitute of copper in PCB process flows; few nanometers of its oxide self-passivate the aluminum surface making it stable in wet environments. This thin protective layer can be overcome in electrical measurements by increasing the signal frequency.	19 25 35
DIELECTRICS	Polyimide	Used in the electronics industry for flexible PCBs or as a high-temperature adhesive; used as a substitute of the FR4 substrate material, typically used for rigid PCB devices.	12 25 35
	Pyrulux	A B-stage acrylic adhesive, where B-stage means an intermediate stage in the cure reaction of a thermosetting resins. Used as an adhesive to create stacks of multiple dielectric and metal layers. Available in a wide range of thicknesses and in different forms: adhesive sheet itself, or coupled with polyimide.	25 35
	Polyurethane	Widely used as flexible and rigid foams, durable elastomers and high performance adhesives and sealants. Available either as powder and as films which can be applied during the lamination process.	36
	Epoxy films filled with aramid fibers	Applied as an alternative to standard glass filled epoxies used for rigid substrates as hole and microwell drilling by laser ablation is not possible for glass fiber filled materials. Patternable epoxy resins are liquid polymers used as adhesives or encapsulant in microelectronics. They can be applied by screen or stencil printing over large areas and can be also used during the lamination process.	37
	Die Attach Film (DAF)	Polymer film consisting of a thermosetting and UV curable resin. This commercially available film could also be used to spaciouly laminate different layers together.	38
ADHESIVE FOILS	Tesa 4985, Tesa 4983, CMC 15581	Transfer double-sided tapes used for cold bonding. Available with several thicknesses and adhesives.	41
SURFACE TREATMENTS	Octadecanethiol (ODT)	It is a well known self-assembled monolayer (SAM) allowing to tune the hydrophobicity of Au, Pt and Cu. Moreover it passivates the metal with a protective mono-atomic layer which, in most of the cases, is thin enough for not requiring an increase of the electrical signal frequency. Hydrophilic coating with SAM are also available, but here not tested. The ODT SAM presents a good thermal stability up to 50°C.	22 23 25
	Certonal FC-732	Molding release agent and hydrophobic coating for metals and dielectrics. High performance anti-corrosion surface modifier; used also as an anti-migration barrier or anti-wetting mask. Its low surface energy repels liquids and oils. Widely used in electronics for protection of circuit boards from airborne contamination and humidity, which can lead to corrosion. The dried film is approximately 1micron thick and thermal stable at 175°C.	25 35
	Chemlease 41-90 (Chemlease)	Semi-permanent, multiple release system and is also used for molded applications where high chemical aggression is common, providing a chemical stable layer and a hydrophobic coating.	25 35

TABLE 1. Complete list of tested materials.

4.1.1 Effects of materials on cell growth

The experimental protocol for analysis of biomaterials effects on cell growth was the following: (a) cells (K562 or LCL) were cultured within biomaterial-treated 24 well plates for different days (continuous exposure); (b) cells were exposed to the different biomaterials for 1 hour, then washed and sub-cultured in standard medium conditions for different days (short-term exposure). The 1 hour short-term exposure was chosen, since this length of time is compatible with most of the protocols available in literature for cellular manipulations using Lab-on-a-chip platforms^{20,34,35,42-46}.

In both continuous and short-term exposures, cell concentrations (cell number/ml) were determined after 3, 4, 5 and 6 days of cell growth for K562 and LCL cell lines. In Figures 3 and 4 the value determined after three days was reported; at this time, indeed, both control K562 and LCL cells are in the log-phase of cell growth, allowing the best comparison to detect cell growth inhibition in experiments aimed at studying possible inhibitors of cellular proliferation⁴⁷. However similar results were obtained also at day 4, 5 and 6 (data not shown). The effects of the employed materials were considered as inhibitory effects in the case of 75% inhibition of cell proliferation, in consideration of the fact that inhibition around 50% of cell growth might be associated in K562 cells, instead to cytotoxic effects, to activation of terminal erythroid differentiation²⁷. Results of these experiments are shown in Figures 3 and 4. In particular, in Figure 3, the data obtained, allow to conclude that continuous exposure to materials is not compatible with efficient cell growth, for the following materials: Cu, Au over Ni, Au over Pd (metals), Cu + ODT, Au over Pd + ODT (surface treatments), Pyralux uncured, DAF, aramid fiber uncured, Tesa 4985 (dielectrics/adhesives). In fact these materials inhibited cell growth of both K562 and LCL cells. Epoxy cured,

instead, was inhibitory only on LCL cell growth. Therefore, very consistent effects were obtained on these two cellular systems when continuous exposure to the tested materials was undertaken.

When exposure was limited to 1 hour (Figure 4), most of the materials displayed no inhibitory activity, with the exception of aramid fiber uncured (which maintained the inhibitory activity on both cell lines) and DAF, Cu and Cu+ODT (which maintained the inhibitory activity only on LCL cells). Interestingly, Pyralux cured renders Pyralux compatible with cell growth (see Figures 3 and 4B). In addition, aramid fiber cured was found to be not active in inhibiting cells growth with the exception of long-time treated LCL cells. These data indicate that caution should be taken when using uncured Pyralux and aramid fibers for the construction of Lab-on-a-chip platforms.

Similar results, as shown in Figure 5, were obtained in another cell line: IB3-1. Ultimately the achieved results firmly demonstrate that some materials exhibited strong inhibitory effects on most of the cell lines and biological functions assessed. When long-term exposure was carried out uncured Pyralux, printable epoxy fully-cured, Au over Ni, Au over Pd, Au over Pd+ODT, Cu and Cu+ODT inhibited biological functions. Aluminum and palladium were found to be not cytotoxic in most of the assays employed. Preparation of the materials appears to be a critical point. In this sense, both uncured preparation of Pyralux and aramid displayed inhibitory activities in several assays, while cured Pyralux and cured epoxy films with aramid fibers did not. Ultimately with these assays has been demonstrated that most of the selected materials can be used for a short exposure of the cells, with the exception of Cu, Cu+ODT and aramid uncured.

A complete list of the tested materials and their effects on cell growth are summarized in detail in Table 2.

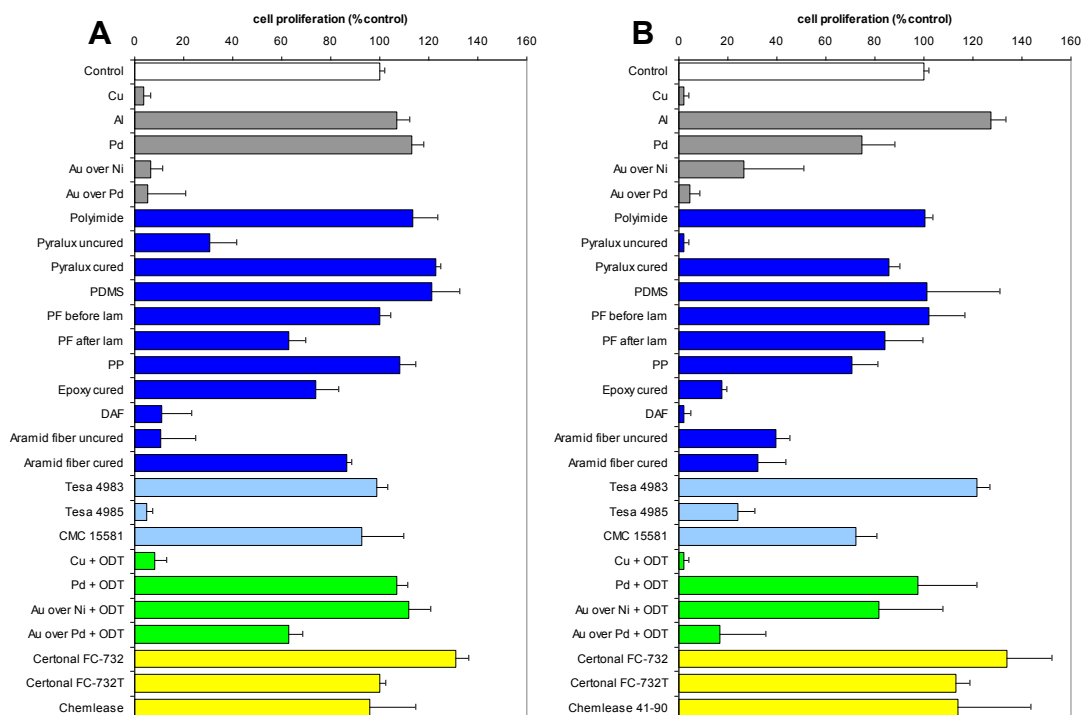


Figure 3. Effects of the materials on cell proliferation of K562 and LCL cells after **continuous exposure**. **K562 cells (A)** or **LCL cells (B)** were cultured in RPMI, 10% FBS for different days in 24 well plates containing the indicated materials. The cell number/ml was determined and compared with control untreated cells cultured in standard conditions. The data reported in the Figure represent cell proliferation in respect to control cells (average \pm SD from three different experiments). The cell number/ml was evaluated after 3 days, when both K562 and LCL cells are in the logarithmic phase of cell growth.

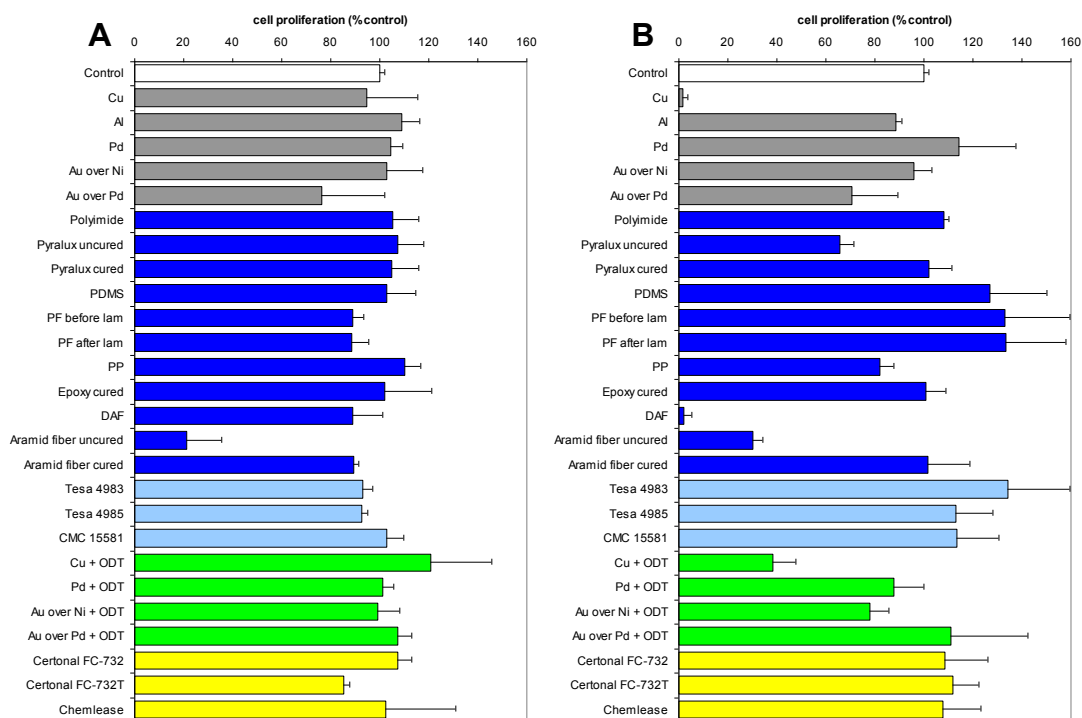


Figure 4. Effects of the materials on cell proliferation of K562 and LCL cells after **short-term (1 hour)** exposure. **K562 cells (A)** or **LCL cells (B)** were exposed in RPMI 10% FBS for 1 hour in 24 well plates containing the materials. After two washing steps with RPMI, cells were sub-cultured in standard conditions. The cell number/ml was determined and compared with control cells after three days of cell culture. The data represent the average \pm SD from three different experiments.

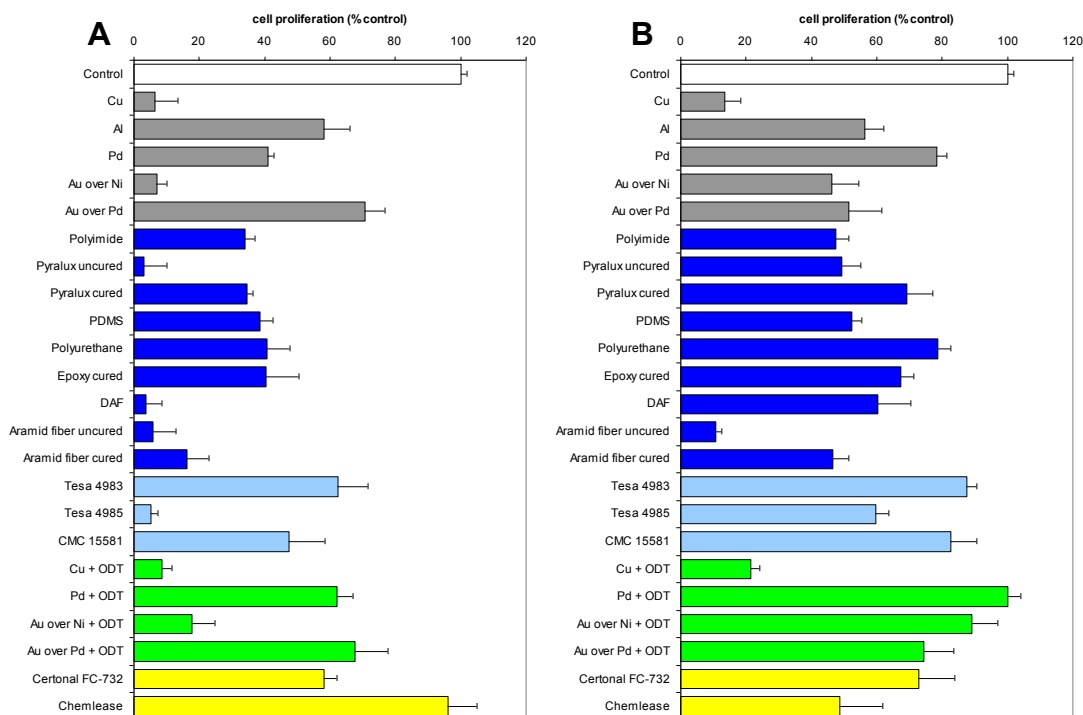


Figure 5. Effects of the materials on cell proliferation of IB3-1 cells. **(A) continuous exposure; (B) short-term exposure.** The cell number/ml was determined and compared with control cells after three days of cell culture. The data represent the average \pm SD from three different experiments.

	Continuous exposure			Short exposure		
	LCL	K562	IB3-1	LCL	K562	IB3-1
Metals	Cu	X	X	X	-	X
	Al	-	-	-	-	-
	Pd	-	-	X	-	-
	Au over Ni	X	X	X	-	-
	Au over Pd	X	X	-	-	-
Dielectrics-adhesives	PI	-	-	X	-	-
	Py uncured	X	X	X	-	-
	Py cured	-	-	X	-	-
	PDMS	-	-	X	-	-
	PF before lam	-	-	X	-	-
	PF after lam	-	X	X	-	-
	PP	-	-	X	-	-
	Epoxy cured	X	-	X	-	-
	DAF	X	X	X	X	-
	Aramid fiber cured	-	-	X	-	-
	Aramid fiber uncured	-	X	X	-	X
Tesa 4983	-	-	-	-	-	
Tesa 4985	-	X	X	-	-	
CMC 15581	-	-	-	-	-	
Surface treatments	Cu + ODT	X	X	X	X	X
	Pd + ODT	-	-	-	-	-
	Au over Ni + ODT	-	-	X	-	-
	Au over Pd + ODT	X	X	-	-	-
	Certonal FC-732	-	-	-	-	-
	Certonal FC-732T	-	-	-	-	-
	Chemlease	-	-	-	-	-

Table 2. Tested materials and their effects on *in vitro* cell growth. (- =no effects; X = inhibition)

4.1.2 Effects of materials on erythroid differentiation

The analysis of the effects of the materials on differentiated functions of K562 cells was performed by determining the proportion of benzidine-positive (hemoglobin containing) K562 cells treated with mithramycin, a powerful inducer of erythroid differentiation. The results obtained, both for continuous and short-term exposures, are shown in Figure 6, and clearly indicate a full suppression of percentage increase of benzidine-positive cells with respect to control erythroid induced cells (K562 cells treated with 25 nM mithramycin) after a continuous incubation (long exposure) with the following materials: Cu, Au over Pd, Au over Ni (metals), Cu+ODT, Au over PD+ODT (surface treatments), Pyralux uncured, DAF, aramid fiber uncured, Tesa 4985 (dielectrics-adhesives).

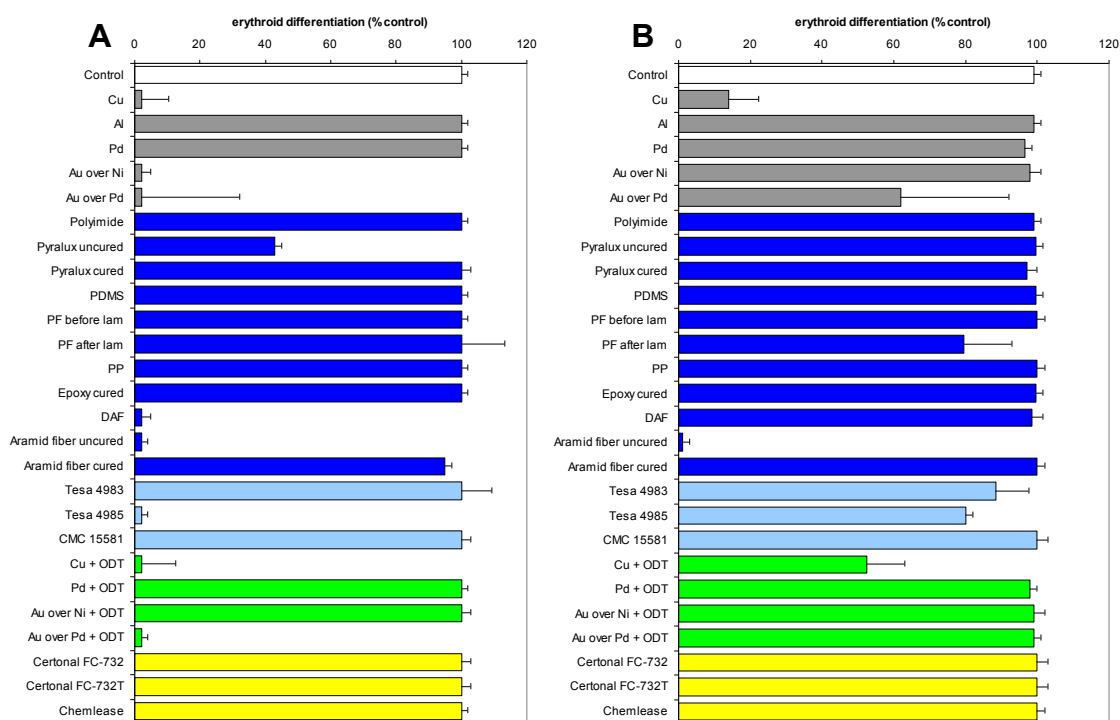


Figure 6. Effects of the materials on **erythroid differentiation** of mithramycin-induced K562 cells during **(A) continuous exposure** or **(B) after short-term (1 hour) exposure** with the different materials under investigation. The proportion of benzidine-positive cells was determined after 6 days of cell culture. In our experiments, uninduced cells displayed $0.5\% \pm 2$ of benzidine-positive cells. Control mithramycin-treated cells exhibited always very high values of benzidine-positive cells ($92\% \pm 5.5$). The results are presented as % of differentiated cells in respect to control mithramycin-treated cells (considered as 100%). The data represent the average \pm SD from three different experiments.

In the case of a short exposure (1 hour), Cu and aramid fiber uncured induced a strong reduction of the percentage of benzidine-positive cells; also Au over Pd and Cu + ODT exhibited inhibitory activity, although to a lesser extent.

These data are fully in agreement with the results obtained in the cytotoxic and antiproliferative tests (Figures 3A and 4A).

4.1.3 Effects of materials on cytokines release by IB3-1 cells

The cystic fibrosis IB3-1 cell line was chosen, unlike the other lines previously analyzed, as a representative example of adherent growing cells. Furthermore IB3-1 cells were employed as a model system releasing several cytokines and chemokines as indicators of their differentiated state. As a consequence the analysis of the effects of materials on IB3-1 biological function were evaluated measuring the amount of cytokines released by cells after continuous or short incubation with different materials. Results obtained were in line with data showed for erythroid differentiation. In particular some cytokines profile (e.g. IL-1 α , M-CSF, GRO- α , ICAM-1) were changed by Cu, Au over Ni, Cu+ODT, Au over PD+ODT, DAF, aramid fiber uncured, and Tesa 4985 after continuous incubation. However when exposure was limited to 1 hour only Cu, Cu+ODT and aramid fiber uncured induced a significant variation in cytokine release profile, while slightly changing were noticed for all the other materials (data not shown).

4.1.4 Effects of materials on CTL-mediated lysis of LCL cells

The analysis of the effects of the biomaterials on CTL-mediated lysis is shown in Figure 7, in particular it indicates that CTL-mediated lysis is detectable using all the biomaterials analyzed, with the exception of Tesa 4985. The values of the percentage of lysis, in fact, were in all cases very similar to those of the control, represented by untreated cells (Figure 7A). However some tested materials caused increase background levels (spontaneous release) of LCL lysis, including Cu, Cu+ODT, Tesa 4985 and aramid fiber uncured (Figure 7B). Interestingly, Cu, Cu+ODT, Tesa 4985 and uncured epoxy filled with aramid fiber are materials exhibiting antiproliferative activity on LCL cells, as reported in detail in Figures 3B and 4B.

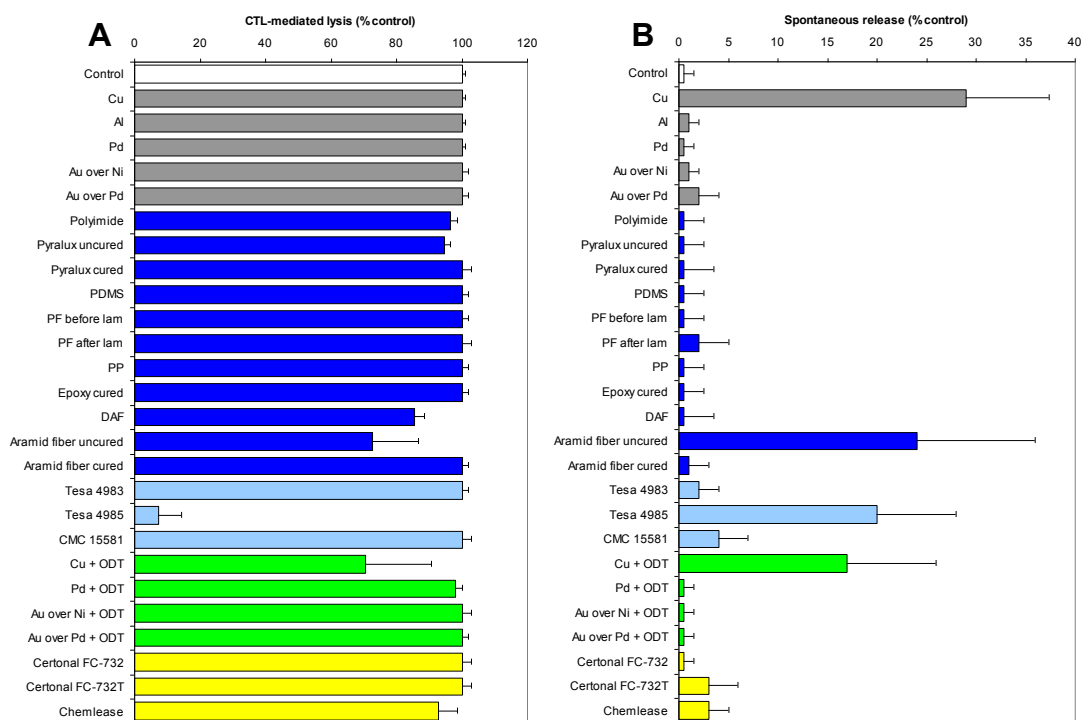


Figure 7. Effects of biomaterials on **CTL-mediated lysis**. ^{51}Cr -labelled LCL cells were incubated for 5 hours with CTL in a CTL:LCL ratios of 10:1 in 96 well plate with different materials. Incubation for 5 hour was performed in order to compare the effects of the employed materials with optimal CTL-mediated lysis of LCL. **(A)** % lysis ratio CTL:LCL 10:1. **(B)** % spontaneous release (sample - control).

4.2 BIOSENSOR CHARACTERIZATION

One of the purposes of this thesis was the development of experimental cellular systems useful to validate the biosensor functionality. In particular our focus was the manipulation of single cells using the available COCHISE platform, performed with the following specific aims: (a) determine whether this procedure is feasible initially with beads and after with cells, (b) verify if COCHISE platform is suitable to allow interaction between cluster cells e.g. target and effector cells, (c) find out if biosensor could be used for identification of active immune system cells like CTLs or NKs.

4.2.1 Beads, cells and cells group levitation and trapping

Initially the first evidence of trapping was carried out using polystyrene beads. This trapping was possible both in physiological medium and in DI water at frequencies ranging from 100KHz to 2MHz. 90 μ m polystyrene beads were trapped in an up-scaled device with a 300 μ m well filled with DI water with a signal amplitude of 18V. When loading beads in the microwell from the top with load configuration active, the electric field minimum is represented by a circular region along the well boundary at the level of MID electrode and particles are levitated by nDEP in random positions within this region (Figure 8A). After switching to trap configuration, beads move to the central spherical cage (Figure 8B). Reducing the microwell diameter to 125 μ m, smaller beads with a diameter of 25 μ m were successfully controlled in the microwell. Successively other trapping and levitation tests were conducted with K562 cell line. Initially K562 were too small in diameter (15-20 μ m) so there were some trouble in trapping them inside the well thus we decided to treat K562 cells with 1 μ M cytosine arabinoside (AraC). This treatment

induces an increase in cell diameter, so we were able to trap the cells (Figure 8C). Other experiments were conducted in order to identify ideal parameters that allowed manipulation of small size cells, in particular modifying well diameter and frequency range also K562 wt were successfully trapped inside the biosensor. Cells delivery was performed either manually or by use of a microdispenser, by spotting them into the well from top and with the load configuration active. Single cells or small clusters were successfully kept levitating in the microwell in load mode at the level of central electrode in random positions along the well boundary. After switching to trap mode, cells were moved towards the center of the well and maintained in this position until the application of the eject mode.

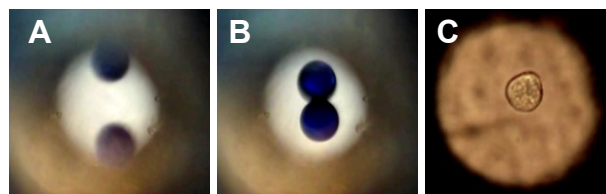


Figure 8. (A) Two polystyrene beads are first levitated in load mode (B) and then made interact by setting the microwell in trap mode. Hole diameter: 300 μ m, Bead diameter: 90 μ m, Voltage amplitude: 18V; (C) a single K562 cell, previously treated with 1 μ M cytosine arabinoside (AraC), trapped in the center of a microwell filled with physiological medium. Hole diameter: 125 μ m.

4.2.2 Analysis of cell to cell interaction

The manipulation of single cells and particles, and the analysis and monitoring of cell-to-cell interactions, is of great interest in various areas of the life sciences ranging from immunotherapy and cancer research, to rare cell identification and isolation. The main requirements for a biotechnological platform supporting these features are:

- Cell delivery in predefined locations as to force cell-to-cell interactions
- Single cell trapping and manipulation
- Recovery of selected cells

- High throughput allowing multiple interactions to be activated in parallel
- Support for automated fluid handling

All these requirements are accomplished, in our biosensor, by electrically active microwells, based on microwells open at both top and bottom, where single cells can be trapped by means of negative dielectrophoresis (nDEP). Comparing to Lab-on-a-chip solutions based on single fluidic chambers or channels, the main advantage of this approach is the isolation of cells in separate sites with a support for flexible supernatant substitution and easier single-cell recovery procedures, guaranteeing mechanical compatibility with standard high-density microtiter plates. Since one of our goal is to employed the biosensor for immune system studying, and whereas it is composed of different cells in size, we demonstrated first that cells with different diameters could be trapped inside the same microwell, and then that they could be force to interact together. In particular some representative data of cells-trapping and cell to cell interaction are shown in Figure 9.

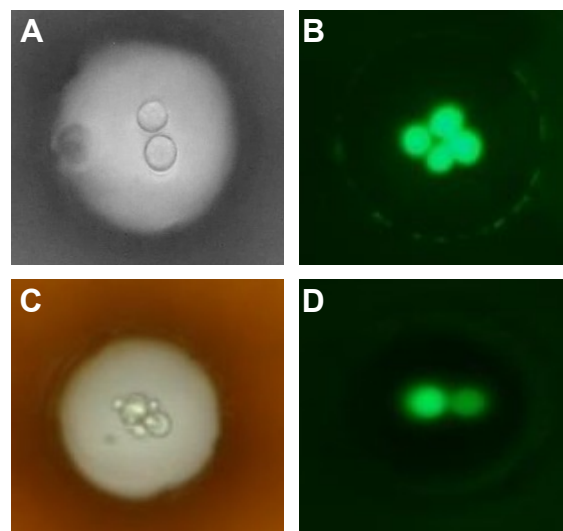


Figure 9. Trapped cells inside the same microwell and cells induced to interact together. **(A)** Image of two K562 cells trapped in a 70um microwell by optical microscope; **(B)** Image of four calcein-labelled K562 cells trapped in a 70um microwell by fluorescence microscope; **(C)** Image by optical microscope of cluster cell with different diameters (LCLs calcein-labelled and CTLs) that levitate together in the same microwell; **(D)** Image by fluorescence microscope of cluster cells where only calcein-labelled LCLs are visible.

4.2.2.1 Evaluation of CTL mediated lysis

In order to validate the biosensor, generation of EBV-EBNA1-derived specific cytotoxic T-lymphocytes was performed. In particular HPV specific CTLs were obtained from monocyte-depleted PBLs from EBV-seropositive donors stimulated with synthetic peptide HPV (HPVGEADYFEY from EBNA1–EBV protein, aa 407–417). The specificity of CTL cultures was tested after three stimulations using standard ^{51}Cr release assays against autologous PHA-blasts, pulsed or not with the synthetic peptide. For analysis of CTL-mediate lysis, through biosensor, LCL cell line was employed as target cells. The first control experiment on LCL cells is depicted in Figure 10B and demonstrated the possibility to isolate single LCL in a microwell and to assess its viability. Calcein fluorescence of target LCL cells was tested inside the device for more than 45 minutes.

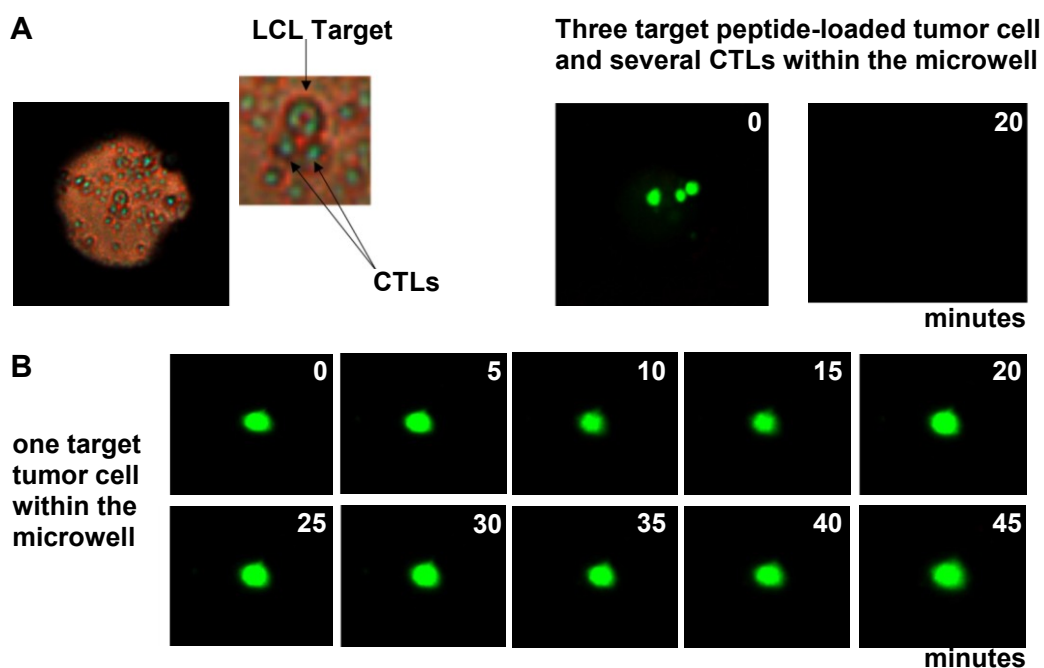


Figure 10. Biosensor validation. **(A)** Image of a microwell within LCLs and CTLs; in the next panel lysis of three peptide-loaded LCLs by CTLs is shown, the lysis of these cells, shown by calcein disappearance, happen in 20 minutes. **(B)** Viability of one single calcein-labelled LCL trapped into the biosensor microwell, calcein fluorescence of this cell is stable for more than 45 minutes. Pictures has been taken every 5 minutes.

These results have firmly demonstrated that calcein fluorescence of target cells was stable within the COCHISE device, rendering feasible the analysis of CTL mediated cell lysis leading to calcein loss from target cells.

In a typical experiment aimed at determining CTLs activity, CTLs were delivered in microwells when three LCL (Figure 10A) or single LCL (Figure 11A) cells have been previously deposited. In particular, in these figures, pictures show calcein disappearance in LCL pre-loaded with synthetic peptide and consequently demonstrate the lysis of these cells by the surrounding CTLs. Repeated experiments indicate that the lysis happen between 10 and 15 minutes. Also LCL not loaded with synthetic peptide has been considered as control, in this case CTLs did not lyse these target cell and as shown in Figure 11B calcein fluorescence of target cells was stable.

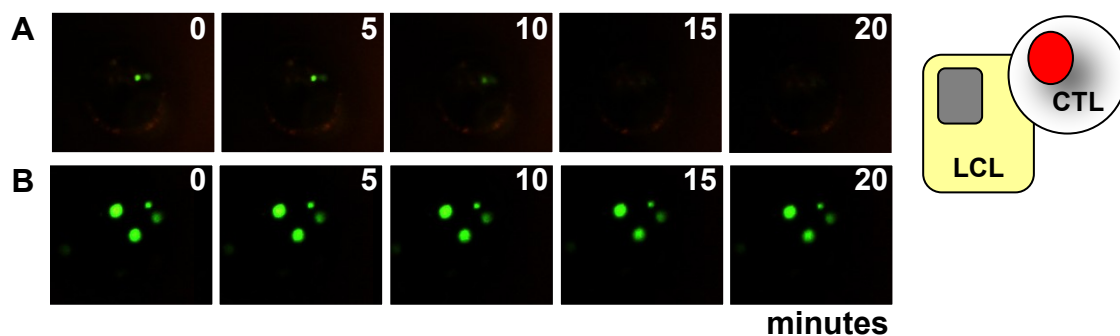


Figure 11. Biosensor validation. **(A)** One LCL pre-loaded with synthetic peptide surrounding by CTLs, the lysis of this cell shown by calcein disappearance happen in 20 minutes. **(B)** LCLs not loaded with synthetic peptide has been considered as control, in this case CTLs did not lyse these target cell in fact calcein fluorescence of target cells was stable more then 20 minutes. Pictures has been taken within biosensor microwells at different time point as indicated.

4.2.2.2 Evaluation of NK mediated lysis

In addition, to analyze cell to cell interaction, NKL cells were employed exhibiting (a) differential lytic properties and (b) possibility to be identified by antibody-antigen interactions. For NK-mediated lysis, two tumor cell lines were utilized: the 221 and 221-G1 lymphoblastoid cells. NKL cells were able to lyse the 221 cells, but unable to efficiently lyse 221-G1 cells; NK-YTS (YTS) cells, instead, were able to lyse with high efficiency both 221 and 221-G1 cells. Control experiment were, obviously, conducted on calcein stability of trapped target cells 221 or 221-G1. Obtained data demonstrate that calcein was stable more than 1h, suggesting that the device is suitable for NK cytolytic assay. Figures 12A and 12B demonstrate that NK-mediated lysis is detectable into COCHISE biosensor using the 221 cell line as target and both NKL and YTS cells as effectors respectively. In particular these data firmly demonstrate that the biosensor is suitable for real-time detection of single target cells lysis by CTLs (Figure 11A) and NKs (Figure 12) cells.

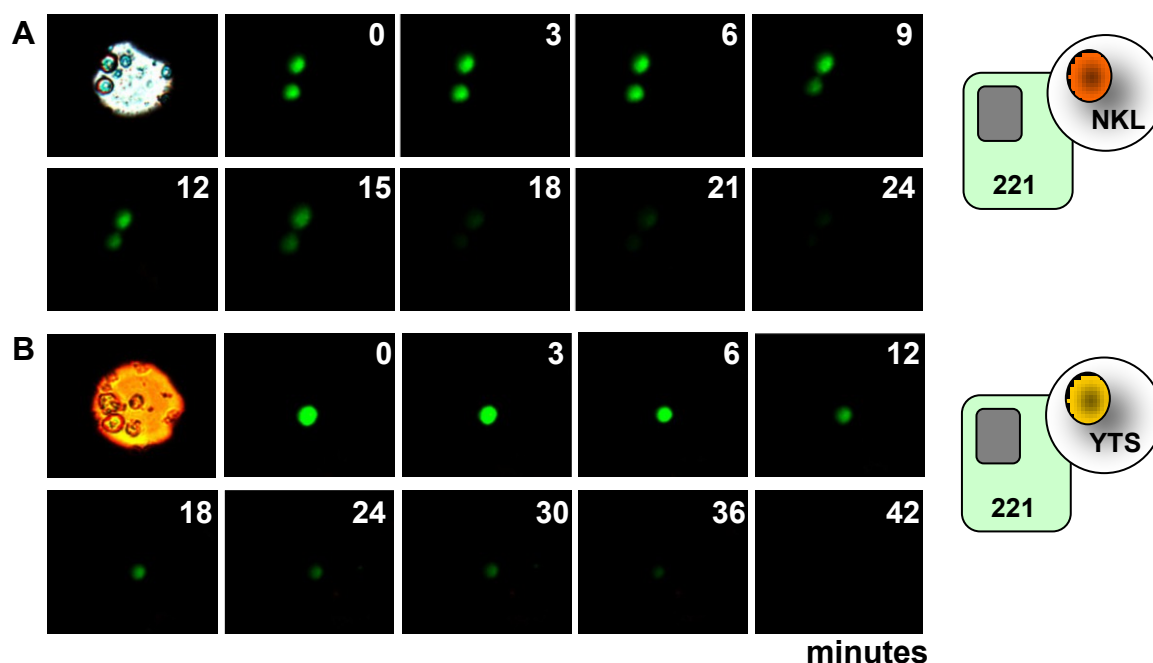


Figure 12. Biosensor validation. (A) NK-mediated lysis of calcein-labelled 221 cells (B) NK-YTS mediated lysis of calcein-labelled 221 cell. Pictures has been taken within biosensor microwells at different time point as indicated.

4.3 BIOTECHNOLOGICAL SENSOR VALIDATION

Other aims of this work were to determine if cell isolation procedure was not toxic, to find out if manipulated cells maintained their biological activity and finally to compare data obtained with the biosensor to other technologies.

4.3.1 Isolation and *in vivo* expansion of single cells

Our study was keeping on in order to determine biosensor functionality about isolation and single cells recovery. In particular K562 cells were used to perform several recovery experiments. For this purpose, cells were washed twice and resuspended in NaCl 0,9% sterile solution to a final concentration of 1 to 5×10^5 cells/ml. Using a peristaltic pump, at a speed of $8 \mu\text{l}/\text{min}$, cells were fluxed in the channel from a reservoir to the device inlet and, when the channel was full, the flux was stopped to permit cells to fall down inside the holes. Concentration of 1×10^5 cells/ml allows to achieve 1 cell/hole. Subsequently cells reservoir was replaced with a new one with NaCl 0,9% sterile solution, and finally the device were rinsed for at least 20min to remove every cell inside the channel before the recovery procedure. Cells recovery were performed using an electrovalve connected to the device from inlet and outlet with pulse of 5msec on a 96well microtiter aligned with the device and filled with RPMI+10% FCS. As shown in Figure 13, clonal expansion of recovered single cells were subsequently conducted in 96well plate until a sufficient cells number was available to perform other biological assays.

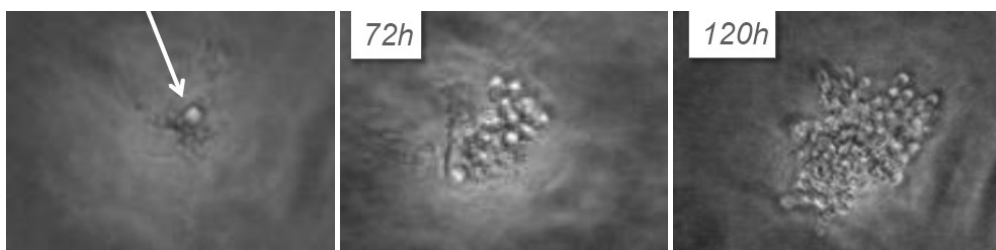


Figure 13. A single K562 recovered from biosensor into a 96well plate. First picture shows a single K562 (signed by white arrow) inside 96well plate, other photos show clonal expansion of recovered cell after 72h and 120h.

4.3.2 Biological characterization of isolated clone

The analysis of the effects on K562 manipulation in the biosensor was performed analyzing cells growth (proliferation) and erythroid differentiation, after recovered cells clonal expansion. The results of cell proliferation in K562 and in K562 manipulated in Lab-on-a-chip (LOC K562) are summarized in Figure 14 and displayed an analogue pattern of growth both in treating with mithramycin²⁸ and AraC, two inducers of erythroid differentiation, and in standard condition without treating. For mithramycin has been chosen different treating concentration (20nM, 40nM, 80nM) while for AraC has been selected a single treatment at concentration that induce the best erythroid differentiation (500nM).

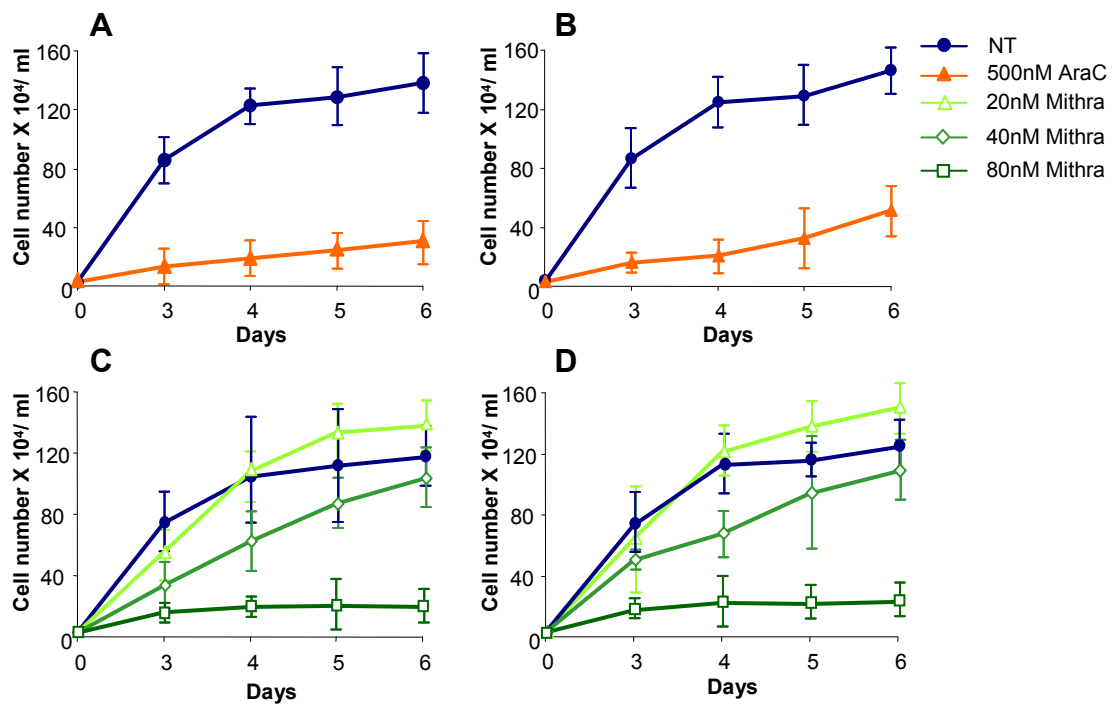


Figure 14. Analysis of the effects of cell manipulation on K562 cells growth. Cell growth (proliferation) was studied by determining the cell number/ml after 3, 4, 5 and 6 days of cell culture. The experiment was performed by treating the cells with 500nM AraC or without treating (NT), upper panel; or treating cells with 20nM, 40nM or 80nM mithramycin (Mithra) lower panel. **(A-C)** data obtained in K562; **(B-D)** data obtained in LOC K562. The data represent the average \pm SD from three different experiments.

The analysis of the effects on erythroid differentiation of K562 cells was performed by treating control and recovered cells with mithramycin (20nM, 40nM, 80nM) and with 500nM AraC. After 3 to 6 days culturing with this two differentiation inducer, the proportion of benzidine positive (erythroid hemoglobin-containing) cells was analyzed using the benzidine-test. The results reported in Figure 15 have shown the same percentage of benzidine-positive in LOC K562 cells respect to control (K562 cells not manipulated) both with mithramycin, at the different concentrations, and with 500nM AraC. These results demonstrate that cell manipulation in the biosensor do not interfere in K562 biological functions, so this validation shows that biosensor could be used for cells recovery and isolation for a subsequent cell culture.

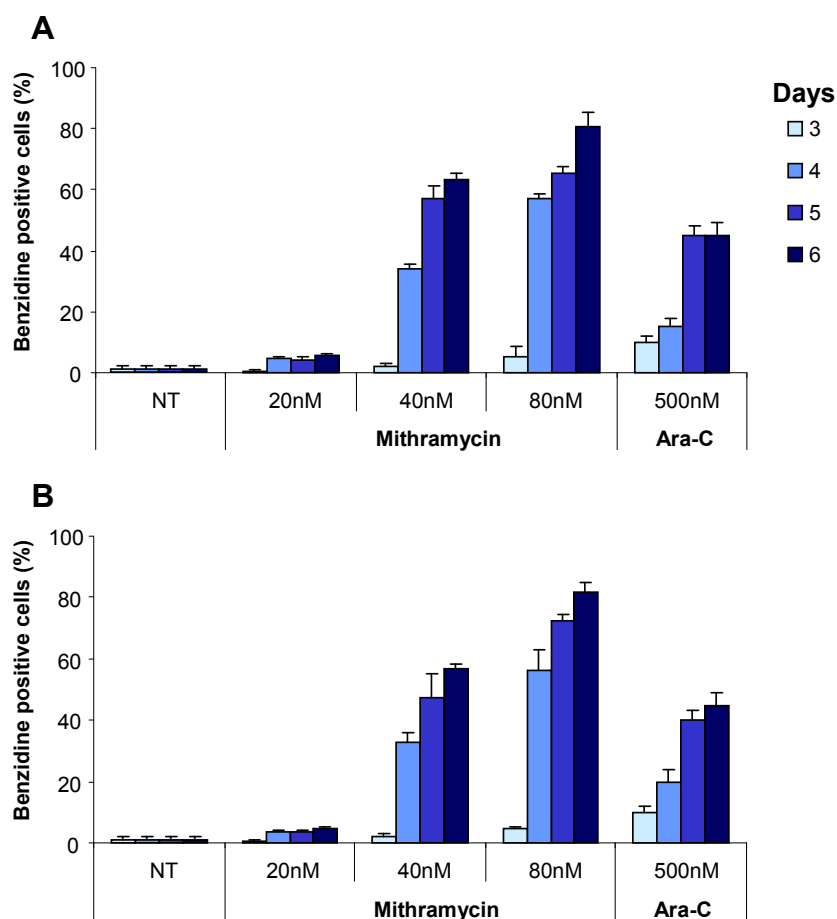


Figure 15. Effects of cells manipulation on erythroid differentiation in K562 cells. The experiment was performed by treating **(A)** K562 and **(B)** LOC K562, or not (NT) with 20nM, 40nM or 80nM mithramycin and with 500nM AraC. The proportion of benzidine positive (erythroid hemoglobin-containing cells) was analyzed using the benzidine-test after 3 to 6 days culturing. The data represent the average \pm SD from three different experiments.

4.3.3 Analysis of gene expression after single cell manipulation

Afterwards our attention has been focused on the analysis of gene expression in recovered cells. In particular globin genes expression were assayed in K562 not manipulated and LOC K562 after treatment with a strong differentiation inducer, referred as AA55. For this purpose cells were treated for 5 days with 50 μ M AA55; at this time both K562 and LOC K562 reached a 98% of erythroid differentiation analyzing with benzidine-test (Figure 16). Subsequently cells were pelleted and total RNA was phenol–chloroform-extracted from cytoplasm.

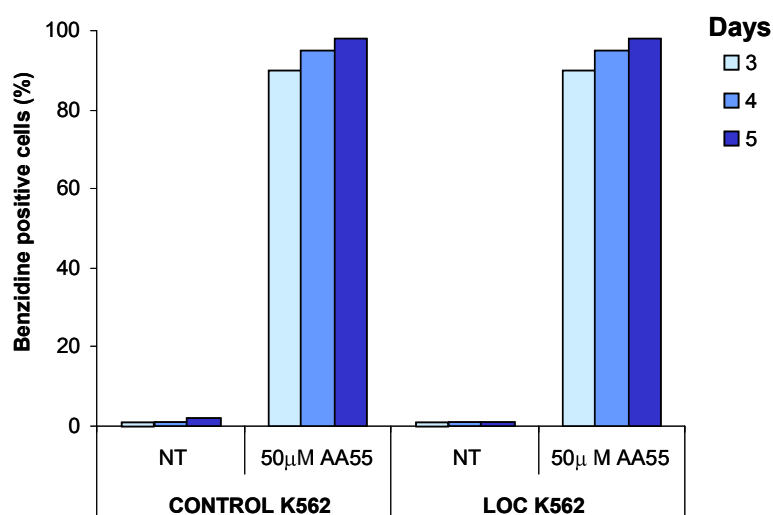


Figure 16. Erythroid differentiation of K562 and LOC K562 treated with 50 μ M AA55. The proportion of benzidine positive (erythroid hemoglobin-containing) cells was analyzed using the benzidine-test after 3 to 5 days culturing.

Successively, to identify any differences in globin genes expression, a quantitative real-time PCR assay of α -, β -, γ -, δ -, ϵ -, ζ -globin transcripts were carried out using gene-specific double fluorescently labelled probes. Q-RT-PCR amplifications were performed on RNA from untreated or treated cells using primers amplifying 18S ribosomal RNA as reference gene. These data demonstrate no significant differences in globin mRNAs content in K562 and in LOC K562 cells (Figure 17),

so we could affirm that cell manipulation into biosensor do not interfere in globin genes expression. These are preliminary data but other extensive experiments about different genes expression will be performed.

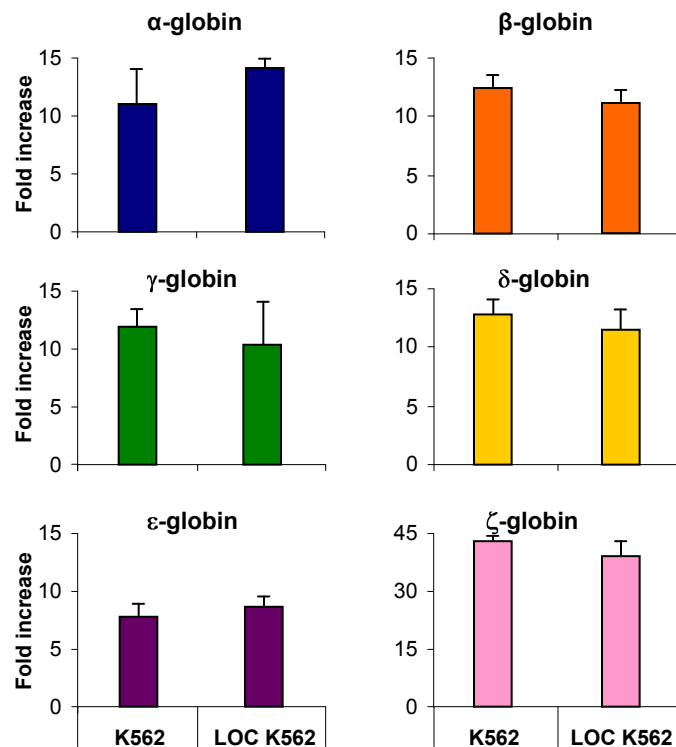


Figure 17. Quantitative real-time PCR assay on α -, β -, γ -, δ -, ϵ -, ζ -globin genes expression in K562 and LOC K562. After recovery, LOC K562 and control cells were treated with 50 μ M AA55 for 5 days, total RNA was phenol–chloroform–extracted from cytoplasm and Q-RT-PCR were performed for all globin genes; fold increased were evaluated respect to untreated cells. The data represent the average \pm SD.

4.3.4 Comparison between biosensor platform and BioStation

In this part of the study we wanted to compare lysis data achieved by biosensor technology and data obtained with BioStation IM instrument (Figure 18A). In particular this last technology is a compact system that consist in a cell incubation and monitoring system that allows sophisticated time-lapse imaging with a highly

integrated microscope and cooled CCD camera. The BioStation IM moreover facilitates a broad array of long term time-lapse experiments, including studies of cell growth, morphology, and protein expression, by providing consistent environmental control of temperature, humidity and gas concentration in combination with phase and fluorescence imaging.

For the comparison between the two platform, the same cellular systems, previously exploited, were chosen. In particular NKL (NK) and NK-YTS were utilized as effector cells while LCL 221 and LCL 221-G1 were calcein marked and used as target cells. All effector : target combinations and their respective controls were seeded in specialized Hi-Q4 culture dish (Figure 18B). These plates are divided into four segments in order to permit multi-sample observation. Afterwards long time-lapse phase and fluorescence imaging were taken for each sample to analyze specific lyses and controls.

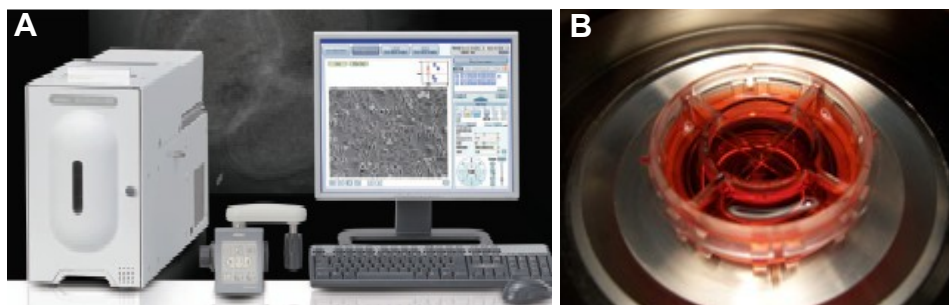


Figure 18. (A) BioStation IM (B) Specialized Hi-Q4 culture dish.

Some representative effector : target lysis assays performed into BioStation are shown in Figure 19. In particular in Figure 19A and 19B are depicted the 221 lysed by NK-YTS while in Figure 19C and 19D are reported 221 cells lysed by NK. These assays have specifically shown that target cells lysed by NK-YTS or NK cell lines assessed in BioStation IM system were essentially such as that shown in dielectrophoretic platform (Figure 12), suggesting that the biosensor is suitable to

study cell to cell interactions. The advantage of COCHISE platform is the ability to analyze single cells lysis and, if necessary, a subsequent recovery of particularly active effector cells could be done; unlike with BioStation we can monitor single cells lysis too, but in presence of other cells inside the plate. To work on single cells would be necessary to plate target and effector using limiting dilution, but the problem then would be the difficulty to reach correct cell to cell interaction. However the major limitation for BioStation technology remains recovery that cannot be performed.

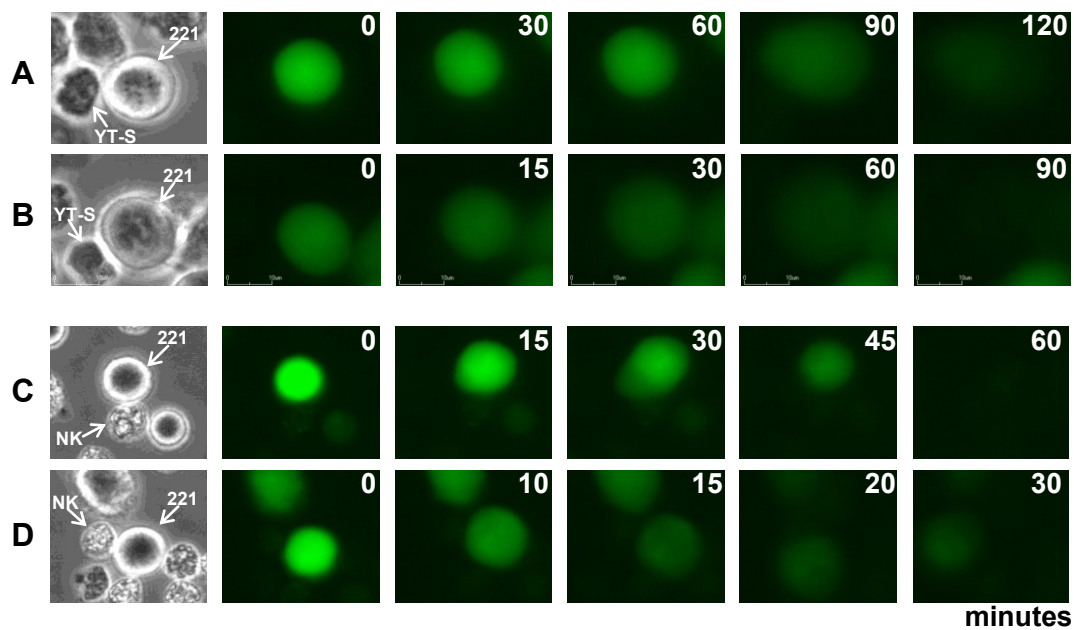


Figure 19. (A-B) 221 target cells lysed by NK-YTS and (C-D) 221 target cells lysed NK cell lines, assessed into BioStation.

5 DISCUSSION

Lab-on-a-chip (LOC) platforms are integrated semiconductor devices that serve as a laboratory for the testing and analysis of very small chemical and clinical samples. Normally, these instruments and analytical devices consist of a network of channels that are built on a semiconductor die for use as a micro or nano lab. In this thesis a specific Lab-on-a-chip platform for analysis of cell to cell interaction has been considered from its design, construction and validation. The platform developed within the project consists of an orderly matrix of up to 1536 microwells where living cells can be deposited. The platform is created in a biocompatible substrate that also serves as a high-density circuit board. The microwells are monitored by an external microscope, the electronics allow to control the biosensor electrodes, necessary to DEP forces induction, and to perform impedance measurements. The key point is that each microwell can force contact between individual cells, and detect consequences of these interactions.

The accurate analysis of the biological effects of materials used for construction of LOC platforms for cells manipulation is an essential pre-requisite in order to develop devices for biomedical and biotechnological applications. Therefore, as first purpose, the analysis of biomaterials effects on biological functions have been analysed on: (a) K562 cells induced to erythroid differentiation and production of haemoglobin by mithramycin; (b) CTL mediated LCL-lysis; (c) human IB3-1 tracheal cells producing a variety of interleukins and cytokines; and (d) rat hippocampal cells differentiating in neurons and astrocytes (in collaboration with the Department of Clinical and Experimental Medicine, Section of Pharmacology and Neuroscience Center, University of Ferrara). We have conclusively and reproducibly analysed all the selected materials, for biosensor manufacturing,

using long-term exposures, supporting the conclusion that among the 26 tested materials (7 employed in surface treatments, 14 dielectrics/adhesives, and 5 metals) some display strong inhibitory effects on biological functions. When the results obtained on cell growth parameters and biological functions are considered together it can be concluded that all materials can be used for a short exposure to cells, with the exception of aramid fiber uncured, Cu, Cu+ODT and, to a lower extent, Au over Pd and DAF. Therefore, the use of these materials should be avoided, even if the device under construction is designed for short-term cell exposure, for instance in the case the Lab-on-a-chip platform is simply dedicated to cell manipulation, isolation and sub-culturing. Of great importance for this project are the biocompatibility results obtained using CTLs as experimental model system. The results achieved support the concept that all materials are compatible with this biological activity for a short exposure, except aramid fiber filled epoxy uncured, Cu and, to a lower extent, Cu+ODT, Au over Pd and Tesa 4985. Therefore, since the most part of the tested materials did not negatively affect the considered biological functions, it has been demonstrated that PCB technology, with some limitations, is suitable for the realization of LOC devices well compatible at least for analytical purposes.

Once identify the most biocompatible materials in each analyzed group, the engineers (from ARCES-University of Bologna, in collaboration with the other project partners) developed some LOC prototypes that consecutively have been validated in our laboratories. First beads have been trapped inside the biosensor by DEP and, after modifying some parameter like well diameter and signal amplitude, also cluster or single cells have successfully been trapped and levitated into the platform. Viability of deposited and retrieved cells by this platform was successively demonstrated, showing biosensor functionality.

An important side of this research is, in particular, the definition of new therapeutic and diagnostic protocols for cancer immunotherapy. As a first step, we applied our technology to the analysis of anti-tumor lytic effector cells, for a precise detection of lytic events which happen into the device at certain locations and timings. A major advantage of the biosensor is that the cells trapped are kept alive and can be retrieved individually for further analysis, such as gene expression profiling or simply for cell amplification.

In particular it has been demonstrated that LOC platform, designed in this project, is suitable for single cell lysis monitoring (e.g. tumor cell lysis by CTL or NK effector cells) and, what is most important, that we could identify the precise well in which specific tumor cell lysis is achieved and recover active CTLs or NK cells for further analysis. Comparison between data obtained with COCHISE platform and BioStation has shown that target cells lysis by different immune effector cells assessed with these two monitoring systems were essentially similar, suggesting that this new device is suitable to study cell to cell interactions. Furthermore the great advantage of the biosensor is the capability to analyze single cells lysis and, if required, a subsequent cell recovery could be achieved, unlike with BioStation where these actions could not be performed.

The results obtained, during this project, represent a significant step in the development and implementation of an innovative tool that will allow important future progresses in cancer diagnosis and therapy. The possibility to manipulate the immune system to recognize and kill tumor cells is very attractive despite numerous obstacles remaining to be overcome, such as tolerance and tumor escape. In particular, the ability of the immune system to seek out and destroy disseminated micro-metastases in a specific way makes immunotherapy an attractive alternative or complement to conventional therapies. Today patients are treated with biological substances such as interferon, interleukin-2 or other factors

to stimulate and activate an immune response against tumor cells. These drug, however, are not always well tolerated and may cause adverse effects leading to discontinuous treatments. An alternative approach is to identify specific tumor-lytic CTLs that recognize and lyse cancer cells, their amplification *in vitro*, in presence of specific growth factors, and finally their re-injection into the patient. One of the main problems related to this approach is the identification and isolation of the very small number of cells that are selectively able to kill tumor cell. Nevertheless the platform designed in this project, although with some limitations, can be used for this purpose.

In conclusion this study is aimed at developing a new class of biosensors, produced with biocompatible materials, and able to detect interactions between single immune effector cells and tumor cells, for identification of tumor-specific CTLs. The development of these biosensors is designed to improve the possibility to find out effective cancer treatment. Many promising technologies for tumor immunotherapy, currently, have different limitation in their use for the difficulty of isolating and acquiring information on biologically active immune cells and tumor cell resistant to CTL-mediated lysis. This technology, instead, with some improvements, should permit to reach such information at a reasonable cost, quickly and without any complex laboratory equipment.

Part II

1 INTRODUCTION

1.1 IMMUNE SYSTEM

Viruses are obligate intracellular organisms that replicate inside cells, exploiting host biosynthetic pathways. The viruses infect a wide range of cellular targets using as receptors molecules that are normally expressed on cell surface. After their entry into the host cell, they can cause tissue damage and disease through several mechanisms. In particular viral replication can interfere with normal cellular functions, such as protein synthesis, leading to damage and ultimately to cell death (lytic infection). Some viruses also have the ability to induce latent infection, during this phase they remain inside the host cell producing proteins that can, in some cases, altering cell functions. To control viral infections and eliminate infected cells, the immune system responds through innate and cell-mediated immunity. The main mechanisms of innate immunity are the block of infection by production of type I interferon (IFN) and lysis of infected cells by natural killer lymphocytes (NK). The latter mechanism represents an important defence during the early stages of infection before intervening specific responses. Specific immunity, instead, is mediated by antibodies and cytotoxic T lymphocyte (CTL). Specifically, antibodies prevent virus interaction with target cells and its penetration inside host cells, while T lymphocytes eliminate infection reservoir by killing infected cells.

1.1.1 T lymphocytes

Cytotoxic T lymphocytes are immune system cells with a key role in recognition and elimination of tumor cells or virus infected cells. They are able, through their surface T cell receptor (TCR), to recognize antigens presented on specialized antigen presenting cells (APCs) surface, in association with molecules of the Major Histocompatibility Complex (MHC)⁴⁸ (Figure 1A and 1B). Each T cell expresses a TCR with a single antigen specificity. This receptor consists of two polypeptide chains, called α and β chains linked by a disulfide bond in the peptide portion anchored to the membrane. CTLs recognize antigens (small peptide of about 8-10 amino acids in length) derived from viral or tumor protein degradation by cytosolic enzymes and in particular by proteasomes (see 1.1.2 paragraph). For a successful recognition these antigens are successively transported into the endoplasmic reticulum by TAP transporters, loaded on MHC class I molecules and expressed on cell surface where they are definitively presented to CTLs.

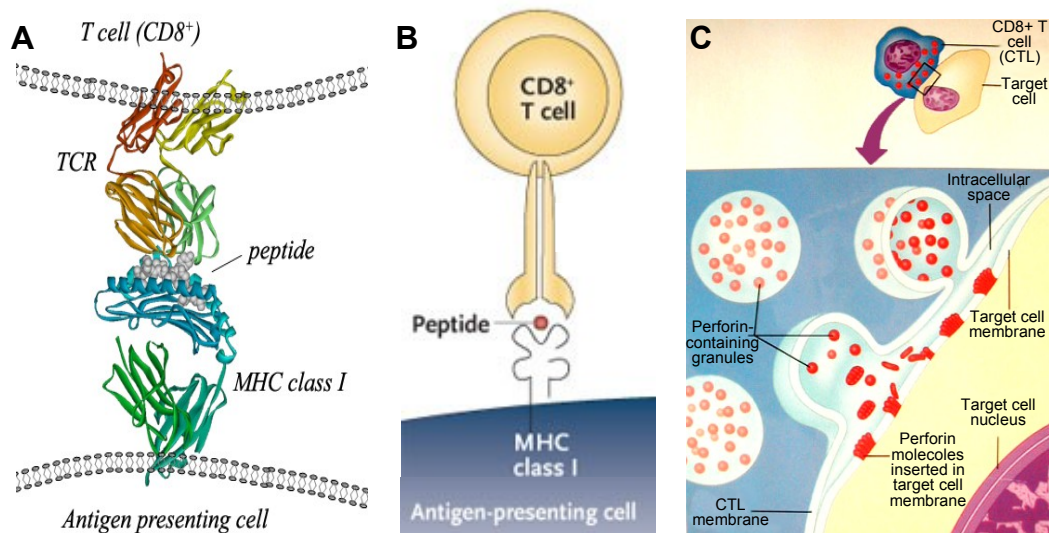


Figure 1. (A-B) Recognition of antigenic peptide mediated by interaction between MHC-I/peptide complex, exposed in antigen presenting cell (APC), and T cell receptor (TCR) of T CD8+ cell. (C) Killing of infected target cells by cytotoxic T lymphocyte through exocytosis of perforins-containing granules.

The interaction between MHC-I/peptide complex and TCR receptor, together with interaction of other costimulatory molecules expressed on APC surface and accessory molecules in T cell surface, activates CTL mediated lysis (Figure 1C).

In particular, CTLs kill their cellular target mainly via three mechanisms⁴⁸:

- 1) exocytosis of granules containing perforin, a pore forming protein, that polymerize on the target cell membrane causing osmotic cell lysis;
- 2) entry through open pores, generated by perforin, of serine proteases (granzymes) that induce apoptosis in target cells;
- 3) expression of Fas ligand (FasL) that interacts with Fas molecules present on target cell, leading to activation of apoptotic pathway.

1.1.2 Proteasome and antigen processing

The proteasome is a big, barrel-shaped, multi-subunit protease complex consisting of a 19S regulatory particle (or cap) and a 20S core particle⁴⁹. The 20S core consists of 28 subunits, two α -heptamers forming the outer rings, and two β -heptamers forming the inner rings of core particle (Figure 2). The α -subunits create a channel that allows the polypeptide chains entry into the proteolytic chamber^{50,51}.

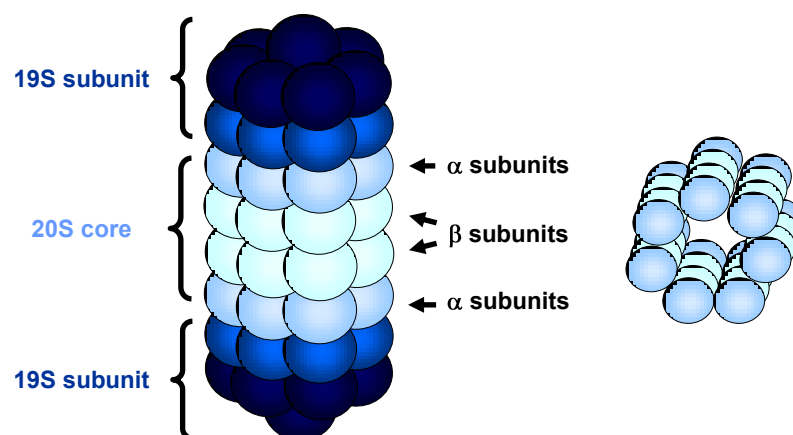


Figure 2. Proteasome structure.

This access route for proteins assumes open- or closed-conformation depending on its association with regulatory subunits and ATP presence. Hole diameter allows the entry of denatured proteins only. The proteasome proteolytic activities reside in the β -heptamers subunits; in particular $\beta 1$, $\beta 2$, $\beta 5$ subunits display different cleavage specificities referred to as chymotrypsin-like ($\beta 5$), trypsin-like ($\beta 2$) and caspase-like ($\beta 1$)^{50,51}. Upon complete assembly of the core 20S, the N-terminal extensions of the three β -subunits are automatically removed to allow N-terminal threonine exposure as active-site nucleophile.

In higher eukaryotes under interferon- γ stimuli the three catalytically active β subunits $\beta 1$, $\beta 5$, and $\beta 2$ are replaced with LMP2, LMP7 and MECL1 immunosubunits respectively; moreover the 19S cap is replaced by PA28 (11S) particle⁵¹ (Figure 3). This proteasome, called immunoproteasome, displays an increased peptide production efficiency and has a key role in the generation of antigenic peptides that are associated with MHC class I molecules and presented to cytotoxic T lymphocyte^{50,51}. Therefore the proteasome beyond to consent damaged proteins and regulatory proteins degradation, has a crucial role in the generation of antigenic peptides, playing an important part in the antigen processing. However other several cytosolic proteases have been implicated in the generation of antigenic peptides for MHC class I, such as leucine aminopeptidase⁵², hydrolases and tripeptidyl-peptidase II (TPPII)⁵³.

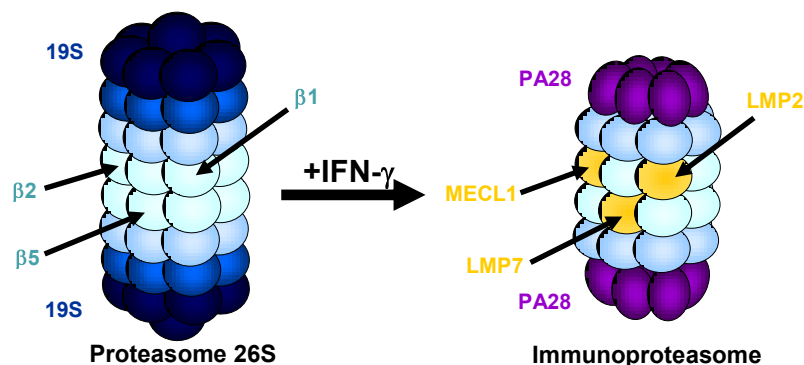


Figure 3. The switch from proteasome to immunoproteasome under IFN- γ treatment.

For protein degradation by the proteasome, firstly is required protein conjugation with a poly-ubiquitin chain. Ubiquitin is a small globular protein highly conserved of 8 kDa and consisting of 76 aa^{50,51}.

Furthermore the proteins have to present signals that activate ubiquitin pathway. In particular these signals are:

- 1) the presence of specific N-terminal amino acid (N-end rule): protein with N-terminal amino acid charged or with voluminous residues (e.g. Phe, Leu, Tyr, Trp, Lys and Arg) are rapidly ubiquitinated and then degraded, proteins with amino acid containing small residue in N-terminal are quite stable;
- 2) phosphorylation of the substrate to be degraded;
- 3) substrate denaturation with consequent exposure of hydrophobic surfaces;
- 4) association with an ancillary protein.

1.1.3 MHC class I molecules

The Major Histocompatibility Complex (MHC) in humans, also known as Human Leukocyte Antigen (HLA), is controlled by genes located on chromosome 6. It encodes cell surface molecules specialized to present antigenic peptides to T cells. MHC molecules are divided into two main classes: class I and II. MHC class I are cell surface glycoproteins present on all nucleated cells. They are heterodimers of a heavy chain, a 45kDa type I integral membrane glycoprotein, and β_2 -microglobulin (β_2m), a 15 kDa soluble protein (Figure 4). The heavy chain is encoded by genes at the HLA-A, HLA-B, and HLA-C loci. The extra cellular region of the heavy chain folds into three domains, ($\alpha 1$, $\alpha 2$ and $\alpha 3$), with β_2m contributing of a fourth domain. The $\alpha 1$ and $\alpha 2$ domains form the peptide-binding site: this is a groove on the upper surface of the MHC class I molecule, which binds antigenic peptides of 8-10 amino acids in length^{51,54-56} that bear specific

anchor residues in position 2 and at the C-terminus (Figure 4). For these residues, that occupied the groove (designated B and F) in the antigen binding site of class I molecules^{57,58}, it has been demonstrated that a polymorphic mutation influences the repertoire of peptides bound by a particular MHC type^{59,60}.

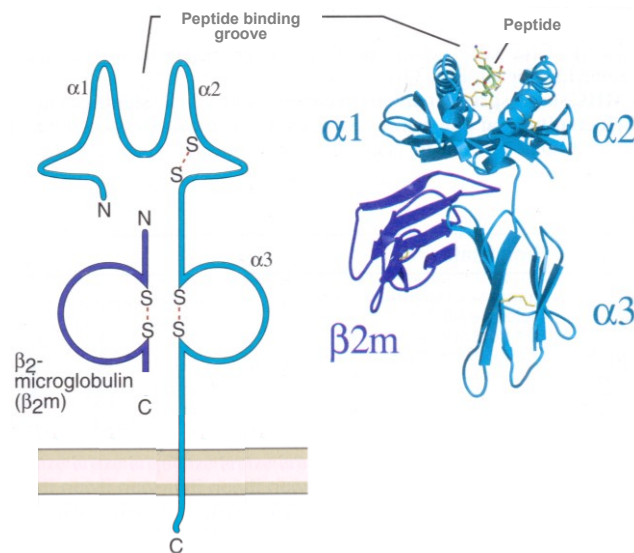


Figure 4. MHC class I molecule structure.

For the final peptide loading onto MHC, the first step in the trafficking process, after proteasome epitope generation, is the transport of peptides from the cytosol to the endoplasmic reticulum (ER) lumen. This is achieved by the transporter associated with antigen processing complex (TAPs) consisting of two multiple membrane-spanning subunits, TAP1 and TAP2⁶¹. TAPs preferentially bind peptides of 8–16 residues with a hydrophobic or basic C-terminal residue. After peptide-binding, TAPs undergo a conformational change, which facilitates the ATP-dependent transport of peptides into the ER lumen. Newly synthesized MHC class I molecules can then non-covalently bind peptide constituting the peptide-loading complex. After peptide-binding, folding of the MHC class I molecule is complete, allowing the complex to exit the ER, travel through the Golgi and reach

the cell surface (Figure 5). There, the peptide/MHC complex is subject to surveillance by CD8+ T cells.

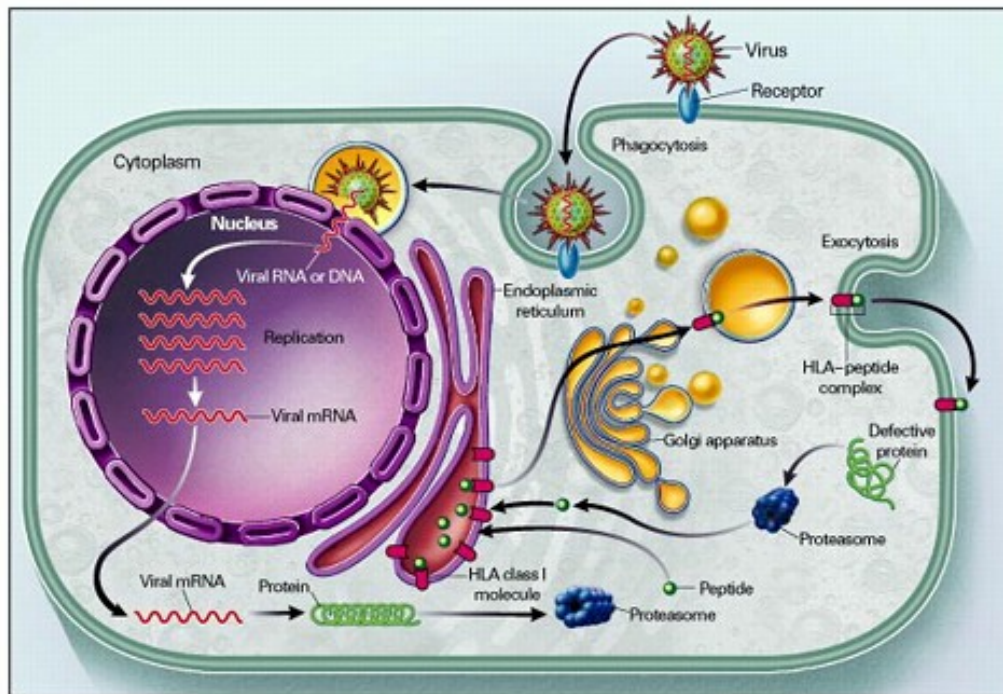


Figure 5. The endogenous pathway of antigen presentation. In the virus-infected cell, viral protein translated in the cytosol are degraded by proteasomes into peptides containing antigenic determinants. The antigenic peptides are transferred into the ER by TAP proteins and loaded onto antigenic groove of newly synthesized MHC class I molecules. Then the peptide/MHC-I complex traverses the Golgi apparatus and is presented on the plasma membrane. Here the peptide/MHC-I complex may be recognized by the cognate T-cell antigen receptor of a CD8+ cytotoxic T lymphocyte.

1.1.4 Viral and tumor escape mechanisms

Presumably, because of the selective pressure exerted by the immune system, many viruses have evolved proteins that interfere with antigen presentation by major histocompatibility complex class I molecules. These viruses utilize a whole variety of ingenious strategies to inhibit the MHC class I pathway⁶². Viral proteins often exploit bottlenecks in the MHC class I pathway down-regulating TAP expression and as a consequence reducing the peptide translocation into ER⁶³.

Alternatively, viral protein can cause the degradation or mislocalization of MHC I molecules⁶²⁻⁶⁴. This is often achieved by subversion of the host cell's own protein degradation and trafficking pathway. However MHC class I total loss is frequently associated also with mutations in the β_2 -microglobulin gene that result in loss of functional β_2 -microglobulin expression⁶⁵. Another strategy employed to evade the immune system surveillance is to interfere with the proteolysis processes, for example modifying proteasome or other peptidases activity in order to prevent antigenic peptides generation^{66,67}. In particular all these listed mechanisms, evolved in immune escape, are often common both in viruses and in tumors.

1.2 EPSTEIN BARR VIRUS

Epstein Barr virus (EBV) is a member of the herpesvirus family. It belongs to gammaherpesvirus subfamily and is an enveloped virus that contains a DNA core surrounded by an icosahedral nucleocapsid and a tegument. Its double-stranded DNA genome is 184Kpb long and encodes for more than 85 genes. EBV is widespread in all human populations in fact infects >90% of the world's people. It is the etiological agent of infectious mononucleosis (IM) but often gives asymptomatic infection if contracted in childhood. Upon primary infection, the individual remains a lifelong carrier of the virus and EBV can be transmitted by salivary contact. During acute infection, EBV primarily infects and replicates in the stratified squamous epithelium of the oropharynx. This is followed by a latent infection of the B lymphocytes. EBV infection of B lymphocytes is thought to occur in the oropharyngeal lymphoid organs, and in normal carriers, the virus persists in circulating memory B cells in episomal form. The B-lymphotropic nature of EBV is evidenced by the ability of the virus to immortalize normal resting B lymphocytes *in*

vitro, converting them into permanently growing lymphoblastoid cell lines (LCL). They carry multiple extrachromosomal copies of the viral episome (Figure 6) and constitutively express a limited set of viral gene products, the so-called latent proteins, which comprise six EBV nuclear antigens (EBNA1-6, also called EBNA 1, 2, 3A, 3B, 3C and -LP) and three latent membrane proteins (LMP 1, 2A and 2B)⁶⁸.

EBV is one of the most widely studied herpesvirus members because of its clinical and oncogenic importance, in fact recently it has been implicated in the pathogenesis of an increasing number of human malignancies such as Burkitt's lymphoma, Hodgkin's disease and nasopharyngeal carcinoma.

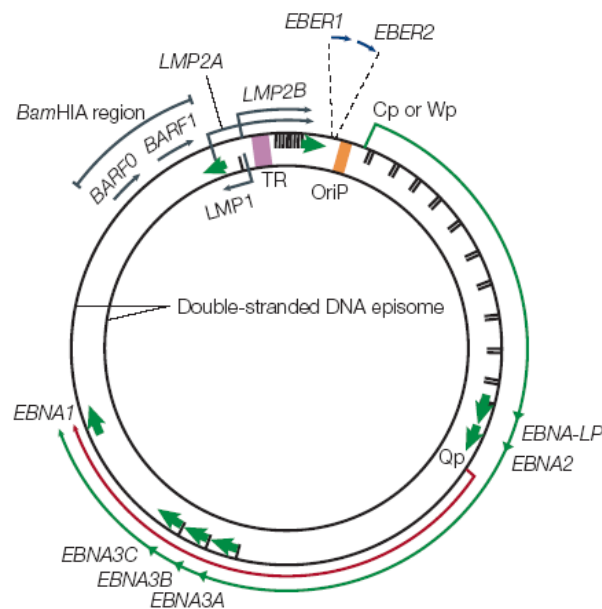


Figure 6. EBV genome: latent genes.

1.2.1 EBV infection

There are two distinct stages of the EBV life cycle. In latent infection, the genome is maintained at a constant copy number and a limited number of regions of the genome are expressed. In the other stage of infection (lytic cycle), viral DNA is amplified and a variety of viral antigens (lytic antigens) are produced prior to virion maturation.

1.2.1.1 Latent infection

The entry of EBV into B cells is initiated by an interaction between the major viral envelope glycoprotein gp350 and the B-lineage-associated C3d complement receptor CR2 (designated CD21). Infection of B lymphocytes with EBV results in persistent latent infection and immortalization of the cells to perpetual proliferation (Figure 7A). Specifically, EBV infection induces RNA and DNA synthesis, immunoglobulin (Ig) secretion, expression of B-cell activation markers, and cell division⁶⁹. Most of the details of latent infection in B lymphocytes have been drawn from studying EBV gene expression in LCLs. These cells express at least 11 EBV genes: two small polyadenylated RNAs (EBER-1 and EBER-2), EBNA1 through EBNA6, and the integral membrane proteins LMP1, LMP2A, and LMP2B. The proliferation of EBV-infected cells, normally, is monitored *in vivo* by T lymphocytes that specifically recognize viral antigens as peptides derived from the processing of endogenously expressed viral proteins presented on the surface of the target cell as a complex with MHC class I molecules⁷⁰. In particular, EBNA3, EBNA4 and EBNA6 contain immunodominant epitopes for CTL responses over a wide range of HLA backgrounds^{71,72}. In contrast, EBNA2, EBNA5, LMP1 and LMP2 are subdominant targets that are presented in the context of a limited number of HLA restrictions^{72,73,74}.

1.2.1.2 Lytic infection

In contrast to the latent phase of infection, when only a limited number of proteins are expressed, activation of the EBV lytic cycle is characterized by the appearance of as many as 80 virus-specific RNA species. On the basis of their time of appearance postinduction, these transcripts are designated early (immediate early

and delayed early) or late. Early genes are expressed independently of new protein synthesis, after switching the virus from latency into replication mediated by an early protein (BZLF1). Afterwards, for a successful packaging of the viral DNA and virion formation, are translated the components of the EBV late-antigen complex, which are mostly structural viral proteins. These new generated virions will definitively induce other infective cycles. Although considerable information has been generated recently on T-cell responses to viral antigens expressed during the latent cycle, much less is known about the contribution of cellular immunity against antigens synthesized during the viral replication cycle.

This is mainly because there is no known *in vitro* grown cell that can serve as the target for a fully permissive EBV infection. However it is well known that T cells play an important role in controlling the replicative EBV infection. In fact significantly increased shedding of virus has been found in the oropharynx of immunosuppressed or immunodeficient individuals.

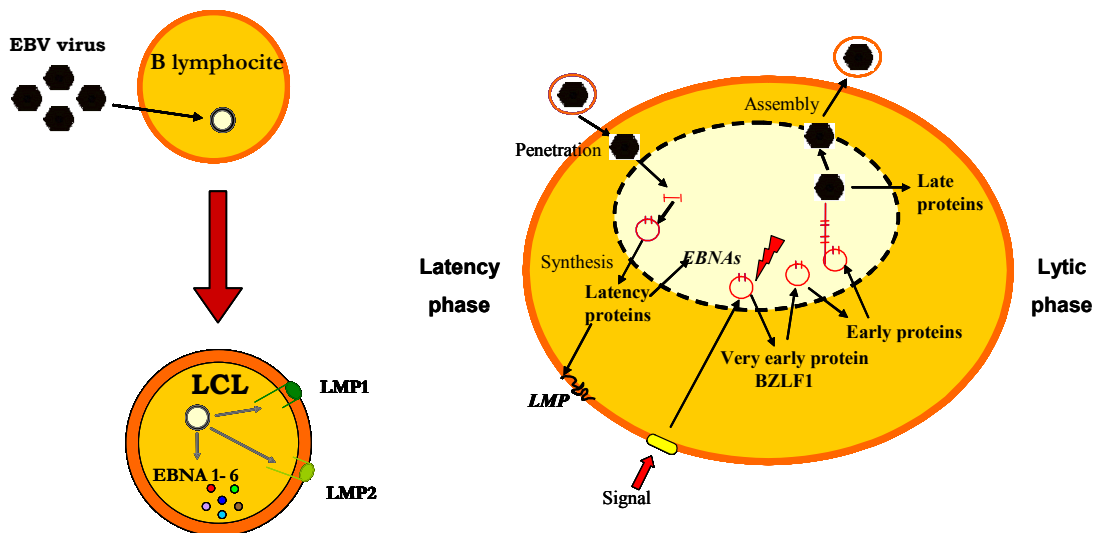


Figure 7. (A) *In vitro* EBV infection of a B lymphocyte and its transformation into permanently growing lymphoblastoid cell line (LCL). **(B)** EBV infection: latency and lytic phases are shown respectively.

1.2.2 EBNA1 protein

EBNA1 is a sequence-specific DNA binding phosphoprotein that is required for the replication and maintenance of the EBV genome. It also has a central role in maintaining latent EBV infection. EBNA1 is a 641 amino acid protein with a large internal repeat of glycine-alanine (Gly-Ala repeat domain, GAr) which make up about one third of the entire protein, but varies in length with every viral strain. EBNA1 presents also a DNA-binding domain (DBD) that, together with the nuclear localization signal (NLS), enhance transfection of EBV plasmids by facilitating their nuclear transport (Figure 8). EBNA1, encoded by the BKRF1 open reading frame, is the only virus-encoded trans-acting factor required for initiation of latent viral DNA replication and episomal maintenance. It performs these functions binding the origin of plasmid replication (OriP) or interacting with the latent Q promotor (Qp) respectively. Although a subset of genes is responsible for the growth-transforming function of EBV, EBNA1 is the only viral gene that is regularly detected in all EBV-associated tumors and is required for the long-term persistence of EBV as well as the pathogenesis of EBV-associated cancers. Although in the past this protein has been considered undetected by the cell-mediated immune system, recent studies show that EBNA1 can be presented to both CD4+ and CD8+ T cells, making it a potential new target for immunotherapy of EBV related cancers.

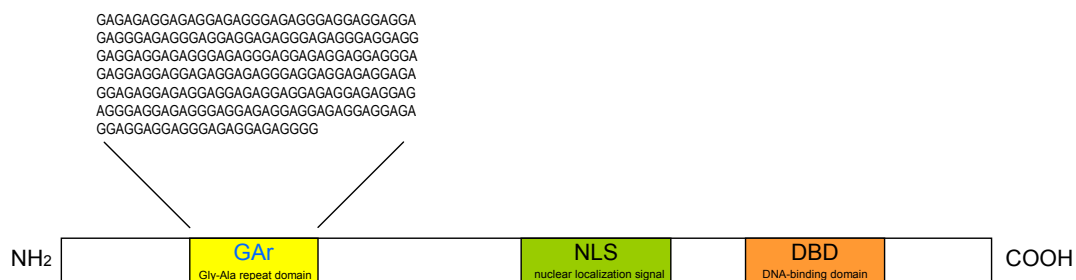


Figure 8. EBNA1 protein structure.

In fact, conflicting with previous observations^{71,74,75}, CTL responses against EBNA1 have been detected in healthy EBV-seropositive individuals⁷⁶⁻⁸⁰ but, thus far, the poor recognition and killing of target cells which naturally express EBNA1 by EBNA1-specific CTL cultures suggest a poor presentation of EBNA1-derived CTL epitopes (Figure 9). This has been attributed to the presence of Gar domainin, which prevents the presentation of EBNA1-derived antigenic peptides by MHC class I molecules. Furthermore, this GAR-mediated function has been linked to its capacity to prevent EBNA1 synthesis^{81,82} and block proteasomal degradation^{83,84}. Although the role of the GAR domain on the stability/turnover of EBNA1 has only partially been clarified, it is now evident that EBNA1 is immunogenic and capable of inducing CD8-mediated cells responses. As EBNA1 is the only antigen expressed in all EBV-associated tumors, and therefore represents an ideal tumour-rejection target for immunotherapy against EBV-associated malignancies, elucidation of the mechanisms by which EBNA1-specific CTLs recognize naturally EBNA1-expressing cells remains crucial^{85,86}.

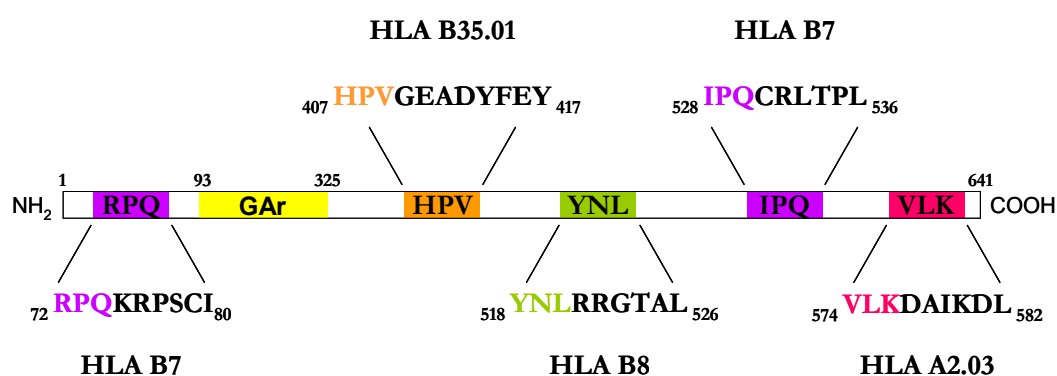


Figure 9. Known EBNA-1 epitopes presented by MHC-I molecules.

1.3 EBV ASSOCIATED MALIGNANCIES

EBV was the first virus to be identified as a cause of human cancers. Although it infects about 90% of the adult human population, it has been implicated as the causal agent of tumors only in a small percentage of EBV seropositive individuals. EBV-associated diseases include Burkitt's lymphoma, Hodgkin's lymphoma, nasopharyngeal carcinoma and immunoblastic lymphoma. All these EBV associated malignancies are characterized by a specific latency program which provides for the expression of specific viral antigens (Figure 10). EBNA1 is the only viral protein expressed in all tumors; this expression pattern is called latency I. Most other EBV-associated malignancies, like for example Hodgkin's lymphoma and nasopharyngeal carcinoma, express either the two latent membrane proteins LMP1 and LMP2 in addition to EBNA1; this is termed latency pattern II. Finally the expression of all EBV latent antigens, EBNA1 to 6, LMP1 and LMP2, common in lymphoproliferative disease, is the latency III expression pattern.

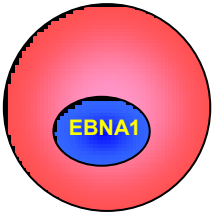
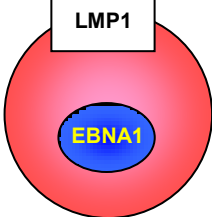
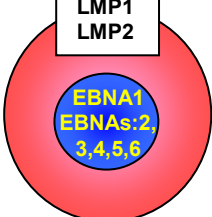
	Latency I	Latency II	Latency III
EBV Gene Expression Profile			
Lymphoma Type	Burkitt's Lymphoma	Hodgkin's Lymphoma	Lymphoproliferative Disease

Figure 10. EBV-associated malignancies and their specific latency program.

1.3.1 Burkitt's lymphoma

Burkitt's lymphoma (BL) is the most common childhood cancer in certain parts of equatorial Africa and Papua New Guinea. There are three recognized forms of this tumor: endemic, sporadic, and AIDS-associated BL. In spite of their clinical heterogeneity, all bear one of three reciprocal translocations between chromosome 8, near the site of the *c-myc* locus at 8q24, and either the Ig heavy-chain locus on chromosome 14 (the common translocation seen in up to 80% of tumors) or one of the light-chain loci on chromosome 2 or 22 (the variant translocations). Endemic BL accounts for approximately half of all childhood lymphomas occurring in equatorial Africa and Papua New Guinea and has an unusually high incidence of 8 to 10 cases per 100,000 people per year. EBV is present in tumor cells of more than 90% in African BLs, in the regions where malaria is hyperendemic. The association of BL with EBV is based on two observations: the demonstration of EBV genome in the majority of tumors from areas where the disease is endemic and the finding that BL patients have an unusually high titer of antibodies against EBV about 5 years before the clinical appearance of tumors. Endemic BL shows the strongest and most consistent association with EBV although the exact role which the virus plays in the etiology and pathogenesis of the tumor is still controversial. The virus might have an initiating role in which growth-transforming B-cell infections establish a pool of target cells that are at risk of a subsequent *c-myc* translocation, a process that has been successfully modelled *in vitro*⁸⁷. Alternatively, EBV might contribute to the Burkitt's lymphoma phenotype through the latency I-active genes themselves. EBNA1 is an obvious candidate, but its reported oncogenicity in mouse transgene assays remains controversial⁸⁸, and its contribution to virus-induced B-cell transformation *in vitro* seems to be limited to maintenance of the viral genome⁸⁹.

1.3.2 Hodgkin's lymphoma and nasopharyngeal carcinoma

Hodgkin's lymphoma is an EBV positive tumor in 90% of cases. This disease affects the lymph nodes and can easily spread through the lymphatic system to various organs and tissues. Hodgkin's disease (HD) displays a latency II program where EBNA1, LMP1, LMP2A and LMP2B proteins are expressed. In HD there is a high expression of activation antigens and MHC II antigens. In patients with nasopharyngeal carcinoma (NPC) has been found a significant depression of EBV-specific CTL responses. Nasopharyngeal cancer affects the epithelial cells on the nasopharynx surface and can be classified in three types: squamous cell, non-keratinized, or undifferentiated. It is one of the most common cancers in southern China and occurs less commonly in North African Arabs. The high incidence of NPC among southern Chinese suggests that, other than EBV, genetic or environmental factors may also contribute to the development of this carcinoma. NPC belongs to a latency II program, with EBNA1 and LMP1 protein expression. Several studies have demonstrated that proteasome/TAP pathway involved in antigen presentation remains unaltered in tumor cells both in Hodgkin's lymphoma and in nasopharyngeal carcinoma.

2 MATERIALS AND METHODS

2.1 MATERIALS

2.1.1 Cell lines

Lymphoblastoid cell lines (LCL) were obtained by infection of lymphocytes from HLA-typed donors with culture supernatants of a B95.8 virus-producing cell line, cultured in the presence of 0,1 $\mu\text{g/ml}$ of cyclosporine A (Sandoz International GmbH, Holzkirchen, Germany). LCL and Burkitt cell lines (BJAB B95.8 and Jijoye) were maintained in RPMI-1640 supplemented with 2 mM glutamine, 100 IU/ml penicillin, 100 $\mu\text{g/ml}$ streptomycin and 10% heat-inactivated fetal calf serum (HyClone; Thermo Fisher Scientific Inc., Waltham, MA). The BJAB (B-cell lymphoma) E1 and E1 Δ GA were kindly provided by Prof. MG Masucci (Department of Cell and Molecular Biology, Karolinska Institute, Stockholm); briefly were generated upon transfection using an amaxa V solution kit (Amaxa, Cologne, Germany) and were maintained in selection with 0,2 mg/ml G418 (Gibco; Invitrogen, San Diego, CA). PHA-activated blasts were obtained by stimulation of PBLs with 1 $\mu\text{g/ml}$ purified PHA (Wellcome Diagnostics, Dartford, England) for 3 days, and expanded in medium supplemented with human rIL-2 (Proleukin, Chiron Corporation, Emeryville, CA, USA)⁷².

2.1.2 Synthetic peptides

Peptides were synthesized by solid-phase method and purified to >98% purity by HPLC⁹¹. Structural verification was performed by elemental and amino acid

analysis and mass spectrometry. Peptide stocks were prepared in DMSO at 10^{-2} M concentration and maintained at -20°C .

2.2 METHODS

2.2.1 Proteasomes purification

Cells were washed in cold PBS and resuspended in buffer containing 50 mM TRIS-HCl (pH 7.5), 5 mM MgCl_2 , 1 mM DTT (Sigma), 2 mM ATP and 250 mM sucrose. Glass beads equivalent to the volume of the cell suspension were added, and the mixture was vortexed for 1 min at 4°C . Beads and cell debris were removed by 5 min centrifugation at 1,000g, followed by 20 min centrifugation at 10,000g. Lysates were cleared by ultracentrifugation for 1 hr at 100,000g, and supernatants were then ultracentrifuged for 5 hr at 100,000g⁶⁶. Proteasome-containing pellets were resuspended in 0.5 ml of homogenization buffer [50 mM TRIS-HCl (pH 7.5), 100 mM KCl, 15% glycerol]. Protein concentration was determined using the BCA protocol (Pierce, Rockford, IL).

2.2.2 Enzymatic assays

The chymotrypsin-like and trypsin-like activities of purified proteasomes were tested using the fluorogenic substrates Suc-LLVY-AMC and Boc-LRR-AMC, respectively⁶⁶. Fluorescence was determined by a fluorimeter (Spectrafluor plus; Tecan, Salzburg, Austria). Proteasome activity is expressed as arbitrary units of fluorescence (A.U.F).

2.2.3 Peptide degradation

In vitro degradation of HPVGEADYFEYHQEGG (HPV + 5) was performed using 150 µg of the peptide and 150 µg of purified proteasomes in 450 µl of activity buffer at 37°C. At different time points, 80 µl of samples were collected, and the reaction was stopped by adding 2 vol of ethanol at 0°C. Digestion mixtures were centrifuged, and 80 µl of supernatant was collected and analyzed by HPLC⁹⁰.

2.2.4 Western blot assay

Equal amounts of proteins or equal amounts of purified proteasomes were loaded onto a 12% SDS-PAGE and electroblotted onto Protran nitrocellulose membranes (Schleicher & Schuell Microscience, Keene, NH). Blots were probed with Abs specific for α, LMP2, LMP7, MECL1 subunits, PA28 α-β, 19S, TAP1 and TAP2, and developed by ECL (Amersham Biosciences, Uppsala, Sweden)⁹⁰.

2.2.5 Preparation of antigen-presenting cells

T2 and T2/A24 cells ($2 \cdot 10^6$) were cultured overnight at 26°C in 1 ml of serum-free AIM-V medium. Cells were then washed, treated with mitomycin C to avoid cell proliferation, and pulsed for 3 hr with 10^{-5} M of the different peptides in AIM-V medium at 37°C. After extensive washing, the cells were used as stimulators.

2.2.6 Generation of memory CTL cultures

Monocyte-depleted PBLs from HLA B35-restricted EBV-seropositive subjects were plated in RPMI-1640 containing 10% fetal calf serum (HyClone), at $3 \cdot 10^6$ cells per well in 24-well plates, and stimulated with either EBV encoded nuclear antigen 1

(EBNA1)-derived HPVGEADYFEY (HPV, aa 407–417) or EBV-encoded nuclear antigen 3 (EBNA3)-derived YPLHEQHGM (YPL, aa 464–473) peptide. For HLA-A2 EBV-seropositive subjects, PBLs were plated at the same above condition, but were stimulated with predicted peptide-pulsed T2 cells at a stimulator : responder ratio of 1 : 20. Cultures were restimulated after 7 and 14 days, and the medium was supplemented from day 8 with 10 U/ml rIL-2 (Chiron, Milan, Italy). On days 14 and 21, T-cell cultures were tested for CTL activity by cytotoxicity assay.

2.2.7 Cytotoxicity assay

Cytotoxic activity was tested by a standard 5 hr ^{51}Cr -release assay⁷³. Briefly, target cells were labelled with 0,1 $\mu\text{Ci}/10^6$ cells of $\text{Na}_2^{51}\text{CrO}_4$ for 90 min at 37 °C and, where indicated, were pulsed for 45 min with 10^{-6}M of the different peptides at 37°C. Cells were then washed, and $4 \cdot 10^3$ cells were used as targets of each CTL at different E:T ratios. The percent specific lysis was calculated as $100 \times [(c.p.m. \text{ sample}) - (c.p.m. \text{ medium}) / (c.p.m. \text{ Triton X-100}) - (c.p.m. \text{ medium})]$, where c.p.m. represents counts/min. Spontaneous release was always < 20% in all cases. None of the tested peptides affected spontaneous release.

2.2.8 IFN- γ ELISPOT

Enzyme-linked immunosorbent spot-forming cell assay [ELISPOT; for interferon- γ (IFN- γ)] was carried out using commercially available kits (Becton-Dickinson, Franklin Lakes, NJ) according to the manufacturer's instructions. In brief, 96-well nitrocellulose plates were coated with 5 $\mu\text{g}/\text{ml}$ of anti-IFN- γ , and maintained at 4°C overnight. The following day the plates were washed four times with phosphate-buffered saline and blocked for 2 hr with 10% fetal bovine serum-supplemented

RPMI-1640 at 37°C. CTLs were added to the wells (in triplicate) at a ratio of 10 : 1 and incubated with target cells at 37°C for 24 hr. Controls were represented by cells incubated with PHA (Sigma-Aldrich, St Louis, MO; 5 µg/ml) (positive control), or with the medium alone (negative control). Spots were read using an ELISPOT reader (A.EL.VIS GmbH, Hannover, Germany). Results are expressed as net number of spot-forming units (SFU)/10⁶ cells.

2.2.9 Immunofluorescence detection of HLA-ABC molecules

Surface expression of HLA-ABC molecules was detected by indirect immunofluorescence using anti-human HLA-ABC mouse monoclonal antibody (BD Pharmingen, San Diego, CA, USA). Mean logarithmic fluorescence intensity was determined by a fluorescence-activated cell sorter (FACS) analysis (Bryte HS, Bio-Rad, Milan, Italy).

3 AIMS

Cytotoxic T lymphocytes play a key role in immune system responses to identify and eliminate virus-infected cells or tumors. In particular, CTLs recognize antigens generated from peptide degradation by proteolytic systems and presented through HLA class I molecules on cellular membrane.

A characteristic of viruses is their ability to escape from immune control interfering for example with major processes of proteolysis by altering the activity of the proteasome and other peptidases involved in the generation of antigenic peptides. In this context is inserted the EBV latency protein EBNA1, whose several new epitopes have been recently identified, despite it was considered since long time a not immunogenic protein. EBNA1, being expressed in all EBV associated tumors, represents an optimal target for immune therapies aimed at enhancing the recognition of tumor cells by the immune system. The study of EBNA1-specific CTL responses and analysis of the processes involved in creating a specific epitope are therefore of considerable importance for the development of new therapeutic approaches against tumors associated with Epstein Barr virus.

The main purposes of the second part of this thesis are:

- 1) the identification of new epitope-specific T cell responses directed against EBNA1;
- 2) the evaluation of EBNA1-specific cytotoxic responses against an EBNA1 derived CTL epitope and its presentation in lymphoblastoid cell lines (LCL) and Burkitt's lymphoma cells (BL);
- 3) the identification of specific treatments to modulate antigen processing and to increase tumor immunogenicity.

4 RESULTS

4.1 IMMUNE RECOGNITION AND EBNA1 DERIVED EPITOPE PRESENTATION IN LCL AND BL CELLS

4.1.1 Identification of a new EBNA1 epitope

To identify new CTL epitopes within the EBNA1 latent antigen, the amino acid sequence of the protein was analysed by a web-based algorithm that predicts peptide binding to HLA-A2, and HLA-A24 (http://www-bimas.cit.nih.gov/cgi-bin/molbio/ken_parker_comboform). This analysis yielded a list of peptide sequences containing putative binding motifs and an estimation of the half-time dissociation of the HLA-peptide complex⁹². As the stability of MHC class I-peptide complexes is a crucial factor in determining CTL responsiveness^{73,93,94} only peptide sequences with the highest scores for HLA-A2 and HLA-A24 molecules, respectively, were selected for further analysis (Table 1). The PBLs obtained from healthy HLA class I-typed EBV-seropositive donors (20 donors: 14 HLA-A2, 10 HLA-A24 and four HLA-A2, HLA-A24), were stimulated with peptides or peptide-pulsed T2 or T2/A24 cells. The specificity of the CTL cultures was tested after three stimulations using standard ⁵¹Cr-release assays against autologous PHA-blasts, pulsed or not with the relevant synthetic peptide.

HLA	Sequence	Name	EBNA1 aa
A2	FLQTHIFAEV	FLQ	565-574
	SIVCYFMVFL	SIV	557-566
A24	VYGGSKTSL	VYG	509-517
	LYNLRRGTAL	LYN	517-526

Table 1. Predicted Epstein Barr virus nuclear antigen 1 (EBNA1)-derived epitopes selected and tested in this study.

Only cultures that showed specific lysis (peptide pulsed target – unpulsed target) above 20% were considered as epitope-specific. Based on this criterion, the HLA-A2-restricted 10-mer FLQ was deemed to induce peptide-specific responses in three of the 14 HLA-A2 donors tested (Figure 1A) while no specific responses were detected against other predicted EBNA1-derived epitopes SIV, LYN, VYG (data not shown). It is noteworthy that the frequency of FLQ responders (21%) was significantly lower compared with the frequency of responders to HLA-A2-restricted epitopes derived from EBNA3 (SVR) and LMP2 (CLG and LLW), which ranged between 42% and 93% of the donors; leading to the hypothesis that this is a weak epitope. To identify the minimal epitope sequence presented by HLA-A2, polyclonal CTL cultures derived from the three responders (Figure 1A) were cloned by limiting dilutions and four CD8⁺ FLQ-specific CTL derived from donor 19 were selected for further analysis. The PHA-blasts were pulsed with different concentrations of the FLQ peptide and used as a target of FLQ-specific CTL in cytotoxic assays. As shown in Figure 1B, half-maximal lysis was detected at high peptide concentrations (10^{-7} M), suggesting that, despite possessing the correct anchor residues for binding HLA-A2 molecules, FLQ 10-mer peptide may not represent the minimal epitope sequence. Two shorter peptides were therefore synthesized and tested for their ability to sensitize autologous PHA-blasts. As shown in Figure 1B, the 9-mer peptide EBNA1 565–573 (LQTHIFAEV) was able to sensitize target cells at 10^{-10} M concentrations, suggesting that it corresponds to the minimal epitope sequence. This was confirmed by the capacity of the LQT 9-mer to stimulate memory T-cell responses (data not shown).

Donor	HLA Type	Donor	HLA Type
1	A24, A32, B13, B35	11	A2, A24, B44, B39
2	A1, A24, B14, B35	12	A2, A28, B18, B75
3	A24, B35, B37, B35	13	A2, A24, B8, B60
4	A3, A24, B27, B35	14	A24, B7, B44
5	A2, B18, B35	15	A2, B44, B51
6	A24, B7, B35	16	A2, A36, B13
7	A2, A24, B35	16	A2, A26, B38, B57
8	A2, A10, B18, B35	18	A2, A24, B7, B18
9	A2, A11, B57, B35	19	A2, A26, B38, B63
10	A2, A26, B38, B39	20	A2, B18, B51

Table 1. List of healthy EBV-seropositive donors exploited and their relative HLA type.

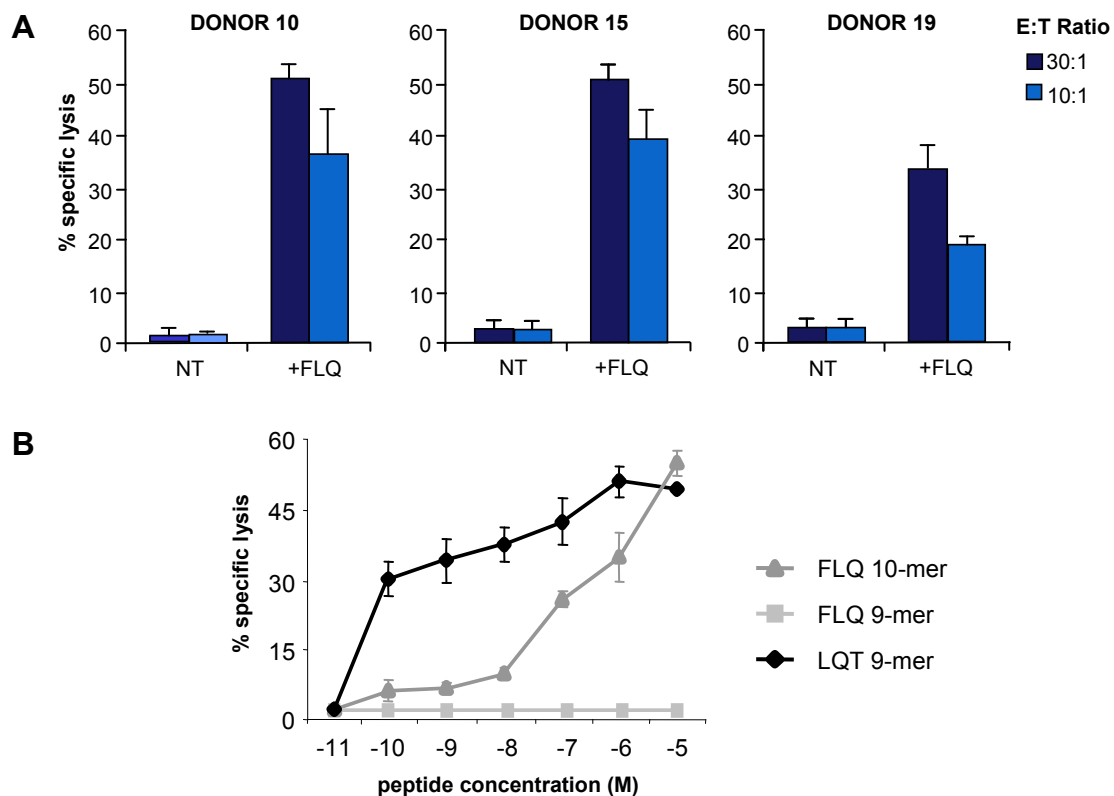


Figure 1. (A) FLQ-specific cytotoxic T lymphocyte (CTL) cultures obtained from three donors. CTL cultures were obtained after three consecutive stimulations and were then tested against untreated or FLQ-pulsed autologous phytohaemagglutinin (PHA)-blasts. Results are expressed as the per cent specific lysis obtained at the indicated effector : target ratio. One representative experiment out of three is shown. **(B)** Peptide titration. FLQ-specific CTL clones were tested against autologous PHA-blasts after pre incubation with the indicated concentration of synthetic peptides from EBNA1 region 565–574. The minimal epitope was defined as the 9-mer LQTHIFAEV (EBNA1 566–574). Results are expressed as the per cent specific lysis obtained at an effector : target ratio of 3 : 1. Means \pm SD of three independent experiments performed in triplicate are reported.

4.1.2 Induction of EBNA1-specific memory CTL responses directed to the HLA-B35 and -B53-presented HPV CTL epitope

It has been previously demonstrated that the HPVGEADYFEY (HPV) epitope, derived from the EBNA1 antigen (aa 407-417) and presented by HLA-B35 and B53 alleles of the B5 cross-reactive group, is one of the target of EBNA1-specific CTL responses in healthy EBV-seropositive individuals⁹⁵.

In order to identify specific responses to this epitope and to obtain HPV-specific CTL cultures for further evaluation, we investigated the presence of HPV-specific memory CTL responses in a panel of HLA-B35 healthy EBV-seropositive individuals. To this end, PBLs obtained from 9 healthy HLA-B35 positive, EBV-seropositive donors (Table 2) were stimulated with the HPV peptide⁷³. As control, parallel stimulations were performed using the HLA-B35-presented YPL epitope derived from the EBNA3 antigen⁷⁴. The specificity of CTL cultures was tested after three stimulations using standard ⁵¹Cr-release assays against autologous PHA-blasts, pulsed or not with the relevant synthetic peptide.

As shown in Figure 2, HPV-pulsed PHA-blasts were efficiently lysed by representative CTL cultures obtained from donors 5, 6, 7 and 8. Three of these donors also responded to the YPL epitope. Overall, these stimulations yielded HPV-specific CTL responses in 6 out of the 9 donors tested (Table 2). It should be noted that responses to the EBNA3-derived YPL epitope were detected in 4 out 8 donors tested (Table 2). Thus, these results suggest that the EBNA1-derived HPV epitope would appear to be a relevant target of EBV-specific CTL responses.

Donor	HLA Type	Specific CTL response Cytotoxic Activity	
		EBNA1 epitope HPVGEADYFEY	EBNA3 epitope YPLHEQHGM
1	A24, A32, B13, B35	-	-
2	A1, A24, B14, B35	-	+
3	A24, B35, B37, B35	+	-
4	A3, A24, B27, B35	-	-
5	A2, B18, B35	+	+
6	A24, B7, B35	+	-
7	A2, A24, B35	+	+
8	A2, A10, B18, B35	+	+
9	A2, A11, B57, B35	+	nd

(nd, not determined)

Table 2. List of healthy HLA-B35 EBV-seropositive donors and their responses against HPV and YPL epitopes.

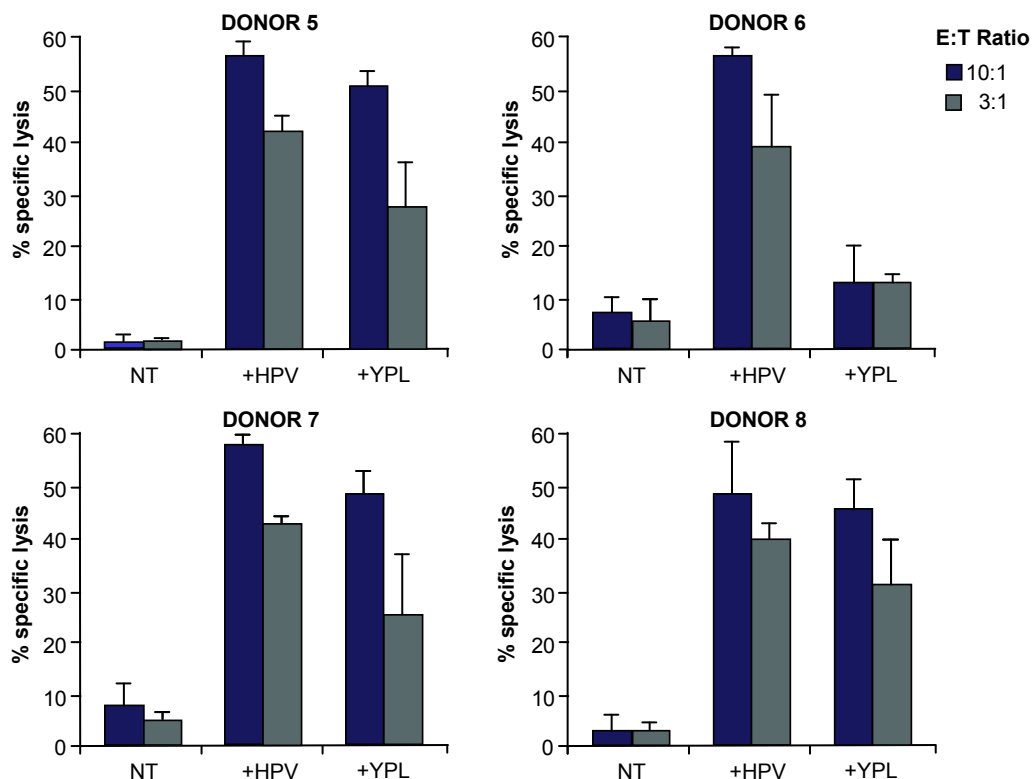


Figure 2. HPV-specific CTL cultures obtained from four different donors. As control, parallel stimulations were performed using the HLA-B35 presented YPL epitope derived from the EBNA3 antigen. CTL cultures were obtained after three consecutive stimulations, and were then tested in triplicate against untreated, HPV or YPL-pulsed autologous PHA-blasts. Results are expressed as the percentage of specific lysis obtained at the indicated effector : target ratio. Mean \pm SD of 3 independent experiments is shown.

4.1.3 Recognition of LCL and BL by HPV-specific CTL cultures

To investigate the presentation of the HPV CTL epitope in EBV-positive cells, HLA-B35 or -B53 positive LCLs and BLs were used as targets of HPV-specific CTL cultures obtained from donors 5 and 7. We found, in 5h ^{51}Cr -release assay, that unmanipulated HLA-B35- and HLA-B53-matched LCLs were lysed by HPV-specific CTL cultures (Figure 3A) while BLs were not recognized suggesting that the HPV epitope is poorly presented at the surface of BL cells (Figures 3B). To exclude poor sensitivity to lysis of BL lines, we evaluated the killing of BLs loaded with the synthetic HPV epitope by cytotoxic assay. We found that HPV-pulsed BL cells were recognized by HPV-specific CTLs indicating that BL cells are sensitive to lysis and able to present the HPV T-cell epitope when exogenously added (Figure 3B). IFN- γ production assays have been mainly used in studies documenting the presentation of EBNA1-derived MHC-I-presented CTL epitopes since it is considered a more sensitive indicator of target cell recognition^{77,79-80}. Therefore, we tested whether recognition of EBNA1-expressing BL cells could be revealed by monitoring IFN- γ release in ELISPOT assays. To this end, HPV-specific CTLs and matched LCLs and BLs were seeded at an effector : target ratio of 10:1, and the number of HPV-specific IFN- γ producing cells was evaluated after 24 hrs. As shown in Figure 3C, release of IFN- γ was specifically induced by HLA-B35-matched LCLs while HLA-B35- and -B53 matched BLs did not stimulate IFN- γ release, thereby confirming the poor presentation of this epitope in BL cell lines. As a whole, these results demonstrate that the EBNA1-derived HPV epitope is generated and presented in LCLs but not in BL cells.

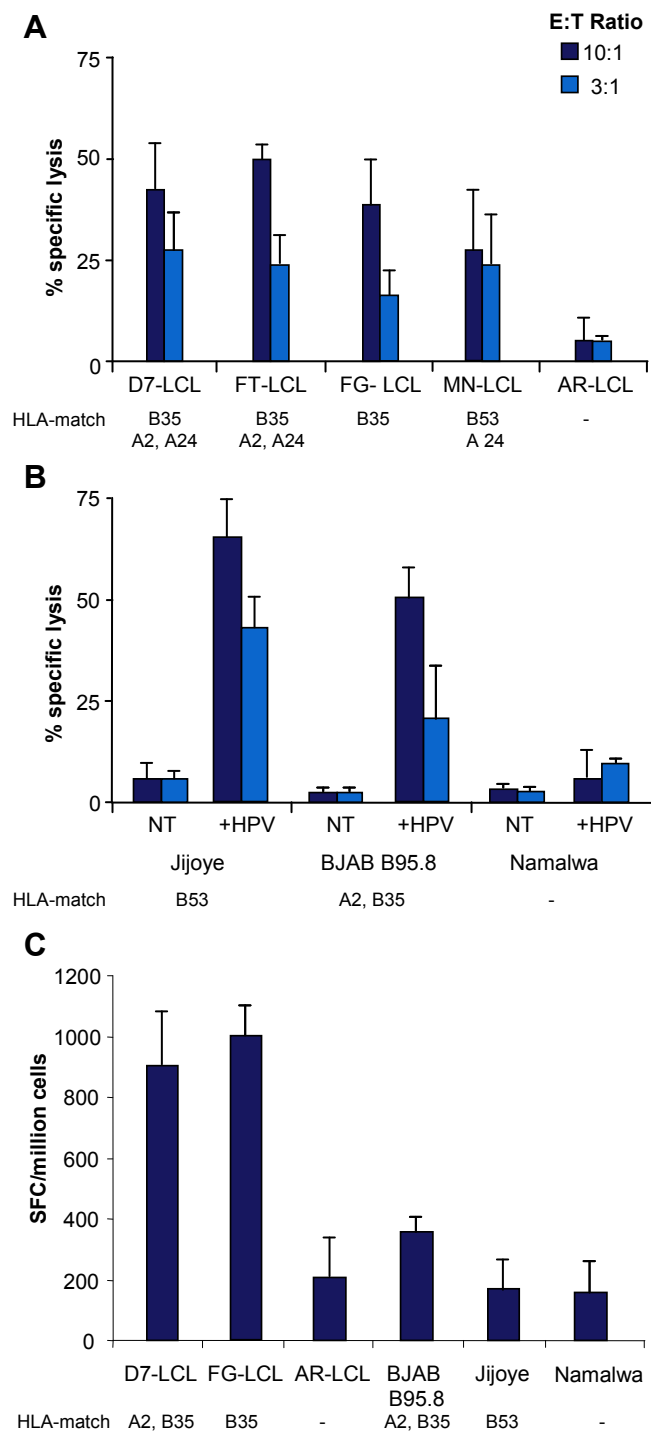


Figure 3. Recognition of LCLs and BLs by HPV-specific CTL cultures. **(A)** HLA-B35 or -B53 positive LCLs and **(B)** BLs were used in a 5h ^{51}Cr -release assay as targets of HPV-specific CTL cultures obtained from donor 7. Target cells were tested either after HPV-pulse (+HPV) or no treatment (NT). Results are expressed as the percentage of specific lysis obtained at the indicated effector : target ratio. Mean \pm SD of 3 independent experiments is shown. **(C)** Matched or mismatched LCLs and BLs were co-cultured for 24 hrs with HPV-specific CTL at an effector : target ratio of 10 : 1. Interferon- γ (IFN- γ) release was detected by ELISPOT. Results are expressed as net spot number/ 10^6 cells. Mean \pm SD of 3 independent experiments is shown.

4.2 DIFFERENCE IN ANTIGEN PROCESSING MACHINERY BETWEEN LCLs AND BLs

4.2.1 Expression of HLA class I and TAP molecules

Loss or down-regulation of HLA class I is one of the routes of immune escape in a variety of human tumors, including BL cell lines⁹⁶⁻⁹⁹. Therefore, the surface expression of class I molecules in BL lines (Jijoye and BJAB B95.8) and LCLs was tested by indirect immunofluorescence. As shown in Figure 4, Jijoye cells expressed lower amount of class I molecules while BJAB B95.8 cell lines showed similar levels of total HLA class I molecules, as compared to LCLs. However, significant levels of lysis were achieved by the addition of HPV peptide to BL cells, thereby suggesting that sufficient levels of class I molecules were expressed at the cell surface (Figure 3B). As the TAP1/TAP2 heterodimer is required for translocation of the majority of peptides from the cytosol into the lumen of the endoplasmic reticulum, lack of these proteins in the ER could also be a reason for limited presentation of MHC-I peptides⁹⁹. In order to investigate this theory, TAP expression was evaluated by probing Western blots of total cell extracts with TAP1- and TAP2-specific antibodies, as shown in Figure 4. The obtained results demonstrate that Jijoye and BJAB B95.8 cells expressed both TAP proteins, albeit to a lesser degree than LCLs, thereby suggesting that lack of presentation of the HPV peptide antigen is not due to loss of TAP1/TAP2 expression. These results suggest that the expression of class I molecules and TAP, although very relevant in the presentation of MHC-I/peptide complexes, may only partially affect the presentation of the EBNA1-derived HPV epitope. Indeed, treatment of cells with IFN- γ (Figure 8), which increases HLA class I molecules and TAP expression, does not sensitize target cells to lysis by HPV-specific CTLs. Furthermore, we

have demonstrated that BJAB cells are able to present the HPV epitope if they express a GAR-deleted form of EBNA1, suggesting that the lower expression of class I molecules and TAPs may only partially contribute to lack of the HPV epitope presentation⁷⁸.

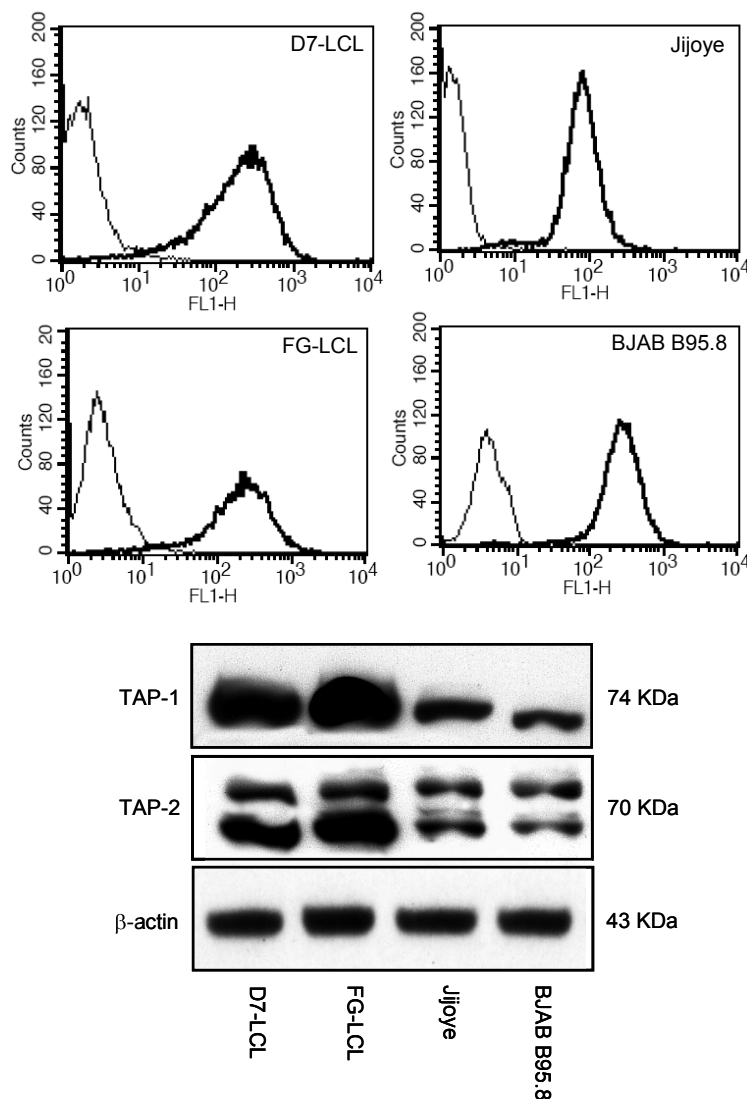


Figure 4. HLA class I and TAP heterodimer expression in LCLs and BLs. In the upper panel, surface expression of HLA-I molecules as detected by indirect immunofluorescence is shown. Mean logarithmic fluorescence intensity was determined by fluorescence-activated cell sorter (FACS) analysis; thin and thick lines indicate the isotype control and the HLA-ABC signal respectively, for each cell line. In the lower panel, expression of TAP-1 and TAP-2 in two LCLs and in two BLs, as detected by Western blot analysis, is shown. β-Actin was used as loading control. One representative experiment out of three is shown.

4.2.2 Expression and activity of proteasomes in LCL and BL

It has previously been demonstrated that BL cells express proteasomes with different subunit composition and enzymatic activity, perhaps resulting in the generation of a distinct set of MHC-I binding peptides^{66,100}.

Thus, we investigated the levels of expression of IFN- γ -regulated β subunits (LMP2, LMP7 and MECL-1) and proteasome regulators (PA28 α - β , 19S) in LCL and BL cells by Western blotting. As shown in a representative experiment (Figure 5), Jijoye and BJAB B95.8 lines expressed levels of proteasomes comparable to those found in LCLs, evidenced by the detection of similar amounts of the constitutively expressed α subunits. However, a significant down-regulation of MECL-1 and a less marked down-regulation of LMP2 and LMP7 were detected in BL lines. To investigate whether these differences in the expression of subunit composition correlated with differences in enzymatic activity, we analyzed the chymotryptic- and tryptic-like activities of proteasomes semi-purified from LCL and BL cells in enzyme kinetics assays, using Suc-LLVY-AMC and Boc-LRR-AMC as reference substrates.

Proteasomes isolated from BL cells demonstrated far lower chymotryptic-like and tryptic-like activities than proteasomes isolated from LCLs (Figure 6). This is in agreement with the pattern of expression of the catalytic subunits in LCLs, as increased expression of LMP7 and MECL1 is associated with increased chymotryptic and tryptic activities.

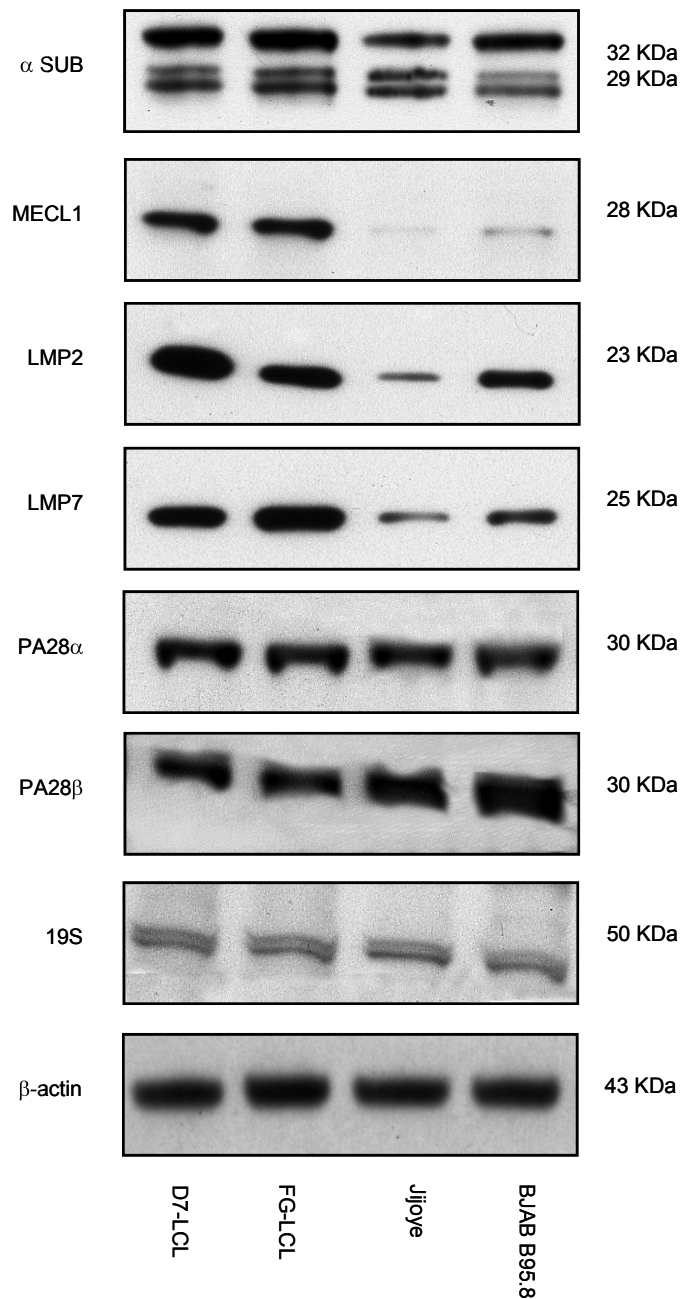


Figure 5. Expression of proteasome subunits and regulators in BL and LCL cells. Equal amounts of semipurified proteasomes were loaded onto a 12% SDS-PAGE and electroblotted onto Protran nitrocellulose membranes. The blots were probed with specific Abs, as reported in the Materials and Methods. β -Actin was used as loading control. One representative experiment out of three is shown.

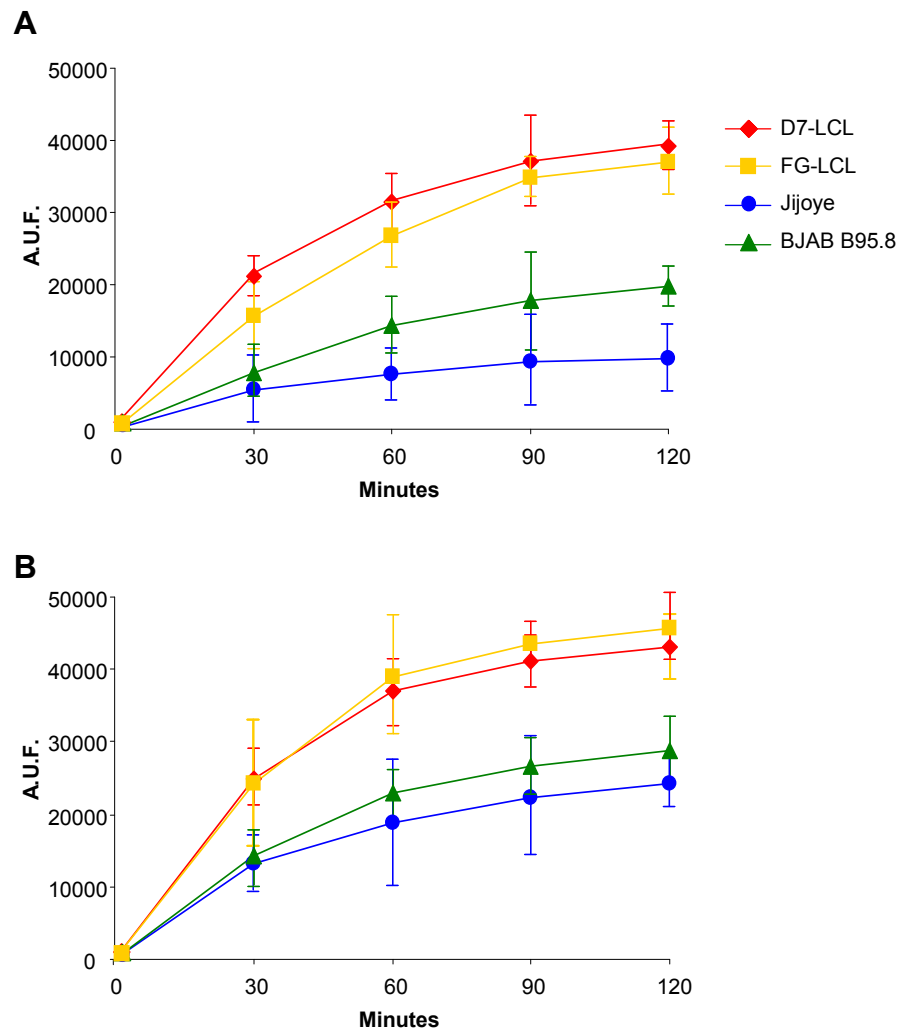


Figure 6. Proteolytic activity of proteasomes isolated from BL and LCL cells. **(A)** The trypsin-like and **(B)** chymotrypsin-like activities of proteasomes are shown respectively. Proteasome activity is expressed as arbitrary units of fluorescence (A.U.F.). Mean \pm SD of 3 independent experiments is shown.

4.3 MODULATION AND INDUCTION OF BLs RECOGNITION BY HPV-SPECIFIC CTL

4.3.1 Evaluation of the effect of the Gly-Ala repeat domain on HPV-mediated lysis in BL

The EBNA1 protein contains a GAR domain that inhibits proteasomal degradation⁸⁴. Removal of GAR increases proteasome-dependent processing, leading to better presentation of EBNA1-derived CTL epitopes^{77,95}. To assess whether the GAR was responsible for the poor presentation of the HPV epitope in BL cells, stable transfected sublines of BJAB that express either EBNA1 (BJAB E1) or a GAR-deleted EBNA1 (BJAB E1 Δ GA) were used as target cells in a standard ⁵¹Cr-release assay. Interestingly BJAB E1 Δ GA was efficiently recognized by HPV-specific CTL, confirming the inhibitory effect of the GAR domain on antigen processing in BL cells (Figure 7).

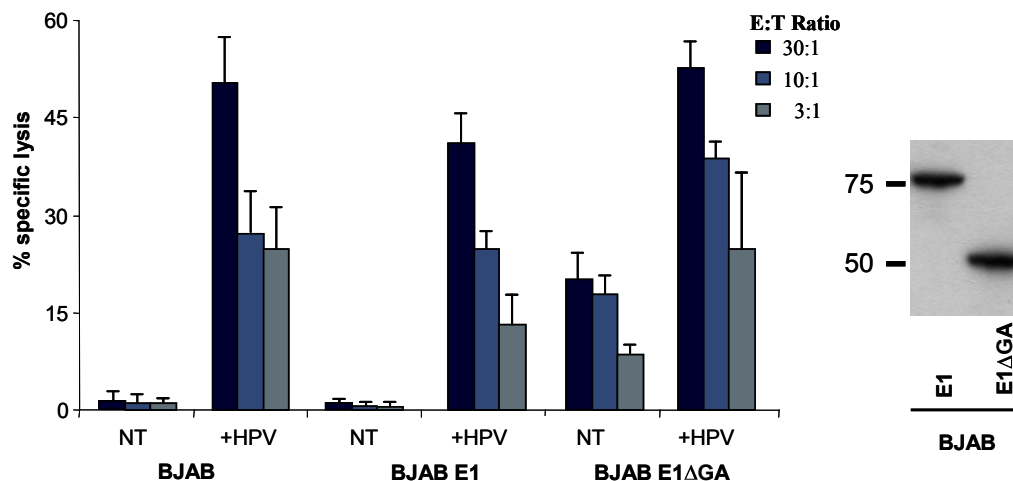


Figure 7. Role of Gly-Ala domain (GAR) on HPV epitope presentation. HPV-specific cytotoxic T-lymphocyte were tested against untreated or HPV-pulsed BJAB cells or BJAB cells stably expressing EBNA1 (BJAB E1) or the GAR-deleted form (BJAB E1 Δ GA). Results are expressed as the per cent specific lysis obtained at the indicated effector : target ratio. One representative experiment out of three is shown. In the next panel, expression of EBNA1 (E1) and GAR-deleted EBNA1 (E1 Δ GA) in transfected BJAB cells, as detected by Western blot analysis, is shown.

4.3.2 Modulation of antigen processing affects HPV epitope presentation in BL cells

Previous results suggest that one of the major differences between BL cells and LCLs is in the expression and activity of proteasomes, which may result in poor generation of the HPV epitope. It has already been shown that modulation of antigen processing and partial inhibition of proteasomes may restore the generation of certain T cell epitopes¹⁰¹⁻¹⁰³. Thus, we treated BL cells with molecules which modulate various steps of the antigen processing pathways. Specifically, Jijoye cells were treated overnight either with proteasome inhibitors (MG132, epoxomicin and PS-341), tripeptidyl peptidase II inhibitors (butabindide and AAF-CMK), a lysosomal acidification inhibitor (chloroquine), an autophagic process inducer (rapamycin) or IFN- γ , which increases proteasome and ERAP activities as well as HLA class I and TAP expression. All drugs were used at the selected concentrations which correspond to their known biological effect without effects on cell viability. As shown in Figure 8, only partial inhibition of proteasomes leads to an increased recognition of Jijoye cells by HPV-specific CTLs, while all other treatments failed to affect target cell lysis.

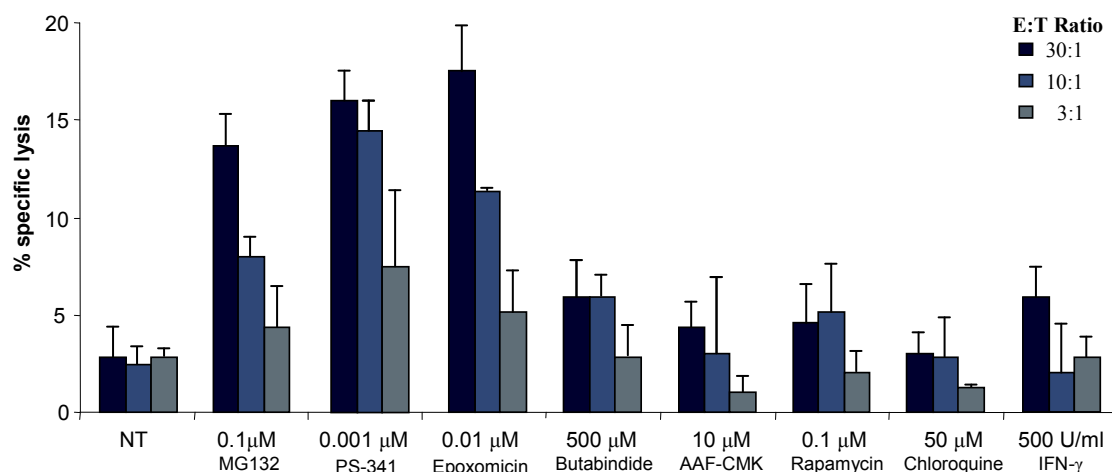


Figure 8. Effect on HPV-epitope presentation in BLs by modulation of different steps of the antigen processing pathways. HPV-specific CTL cultures were tested against Jijoye cells treated overnight or not with the indicated molecules. Results are expressed as the percent specific lysis obtained at the indicated effector : target ratio. Mean \pm SD of 3 independent experiments is shown.

Similar results were obtained with BJAB B95.8 cells, while -B53 and -B35 negative BL cells, used as a negative control in all assays, were unaffected by these treatments (not shown). These results suggest that proteasomes from BL cells, although less efficient in degrading reference substrates than proteasomes from LCLs, destroy the HPV epitope, which can, however, be generated and presented after partial inhibition of the proteasomes.

4.3.3 *In vitro* generation of HPV epitope by proteasomes isolated from BLs

To evaluate whether proteasomes from BL cells are able to generate the HPV epitope, we analyzed the *in vitro* degradation of an HPV peptide precursor featuring 5 amino acids at the C terminus (HPV + 5). Proteasomes were semi-purified from Jijoye cells treated or not with epoxomicin under the same conditions inducing HPV-specific lysis. Subsequently, the *in vitro* HPV precursor degradation was evaluated at different time points by HPLC analysis. As shown in Figure 9, the HPV precursor was degraded in a time-dependent fashion. Proteasomes isolated from Jijoye cells and treated with epoxomicin were still capable of degrading the HPV precursor, albeit to lesser extent. Interestingly, the appearance of a single peptide was evident during the HPV + 5 degradation. As this peptide eluted from the HPLC column with the same retention time as the HPV peptide, it was identified as the HPV epitope, a hypothesis confirmed by mass spectroscopy (data not shown). The generation of the HPV epitope by proteasomes isolated from untreated Jijoye cells was maximal after 1 h and subsequently decreased in a time-dependent fashion suggesting a further degradation to products which were undetectable under our conditions. In contrast, proteasomes isolated from Jijoye cells treated with epoxomicin still generated the HPV epitope, which was not further degraded since its presence could be still detected after 48 h. These *in*

in vitro findings suggest that BL cells treated with proteasomes inhibitors do not degrade the HPV epitope resulting in its presentation by class I molecules.

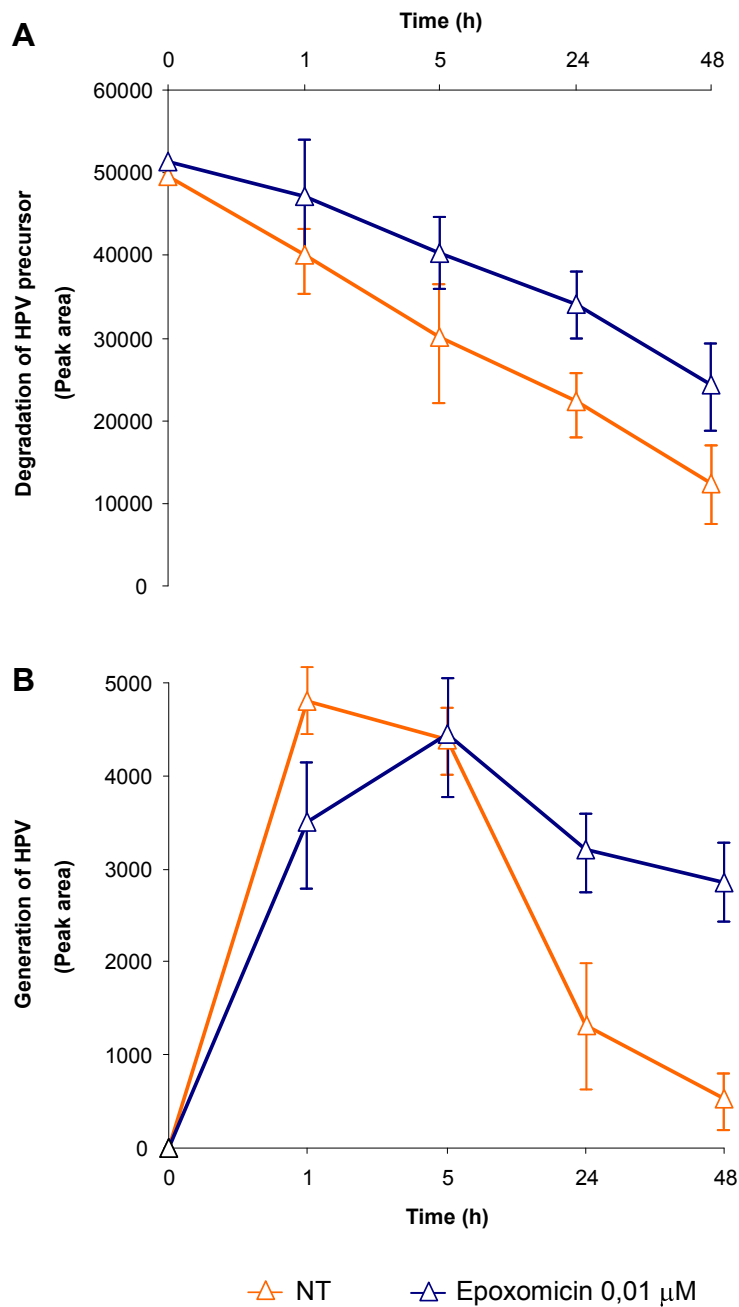


Figure 9. *In vitro* generation of the HPV epitope by proteasomes isolated from BL cells. **(A)** The HPV + 5 peptide (HPV precursor) was incubated with proteasomes purified from Jijoye previously treated with 0,01 μM epoxomicin or untreated (NT). HPV precursor degradation was monitored at different time points, and its degradation was evaluated by HPLC analysis. Data are expressed as peak area of HPV precursor. **(B)** HPV generation at different time points relating to the degradation of HPV precursor in Jijoye cells treated with 0,01 μM epoxomicin or untreated (NT). Data are expressed as peak area of HPV, as evaluated by HPLC analysis. One representative experiment out of three is shown. Mean ± SD of 3 independent experiments is shown.

5 DISCUSSION

As a result of its ubiquitous expression in EBV-associated malignancies, EBNA1 has long been considered an ideal target for immunotherapeutic approaches¹⁰⁴. The first part of this study was aimed at exploring new potential epitopes presented by HLA-A2 and HLA-A24 molecules. An epitope prediction algorithm was used to identify four potential epitopes that were then tested for their capacity to reactivate T-cell responses in PBLs from healthy EBV-positive donors. The LQT peptide corresponding to amino acids 566–574 of EBNA1 induced HLA-A2-restricted CTL responses in three out of 14 HLA-A2-positive donors tested. It should be noted that the minimal epitope was not the one predicted by the algorithm although the latter contains the correct anchor residues for binding to HLA-A2 molecules¹⁰⁵. This is in line with the observation that some CTL epitopes do not contain conventional anchor residues and binding to the presenting allele is instead dependent on secondary anchors. The reactivation of LQT-specific CTL in only three out of 14 of the donors tested suggests that this epitope may only account for a minor component of the EBV-specific CTL response, suggesting that it is a particularly weak epitope.

Afterwards to assay the presentation, in its natural context, of a known EBNA1-derived epitope (referred as HPV, an HLA-B35/B53 presented epitope), HPV-specific CTL cultures, generated by peptide stimulation from EBV-seropositive healthy individuals, were used. These cultures were tested against LCL and EBV-positive BL cells using either cytotoxicity or IFN- γ release. In the case of EBNA1-specific T cell responses, failure to lyse EBNA1-expressing target cells has frequently been observed,^{95,106} although low levels of lysis have been reported in some studies^{79,80}. In contrast, specific recognition of EBNA1-derived epitopes has

in many cases been revealed by the induction of IFN- γ release, which is considered a more sensitive method for detecting target cell recognition. By this approach, we confirmed that the presence of HPV-specific T cell responses is in the same range as that seen for the immunodominant HLA-B35-restricted YPL epitope derived from EBNA3^{80,107}. This finding, together with the identification of other EBNA1-derived epitopes restricted by several class I alleles⁷⁶⁻⁸⁰, further highlights the importance of EBNA1 as a target of EBV-positive malignancies, and makes evaluation of the recognition of EBV-infected cells and EBV-associated malignancies by EBNA1-specific CTLs crucial.

Hence, we set out to demonstrate that LCLs are recognized and killed by HPV-specific CTL cultures, indicating that the GAR domain affords the protein antigen only partial protection from CD8+ T cell recognition. Therefore our results support the idea that EBNA1-specific T cell responses are primed *in vivo* by a direct interaction between the CD8 T cell repertoire and naturally infected B cells in which endogenously expressed EBNA1 is targeted intracellularly by the proteasome, despite the presence of the GAR domain^{77,79,80}.

In contrast to what observed in LCL, we show that BL cells were not recognized by HPV-specific CTLs, thereby suggesting that the GAR domain affords the EBNA1 antigen protection from CTL-mediated lysis in this type of cells. Since it has previously been demonstrated that the stability of EBNA1 although varying in different cell lines, does not correspond to the level of generation of EBNA1-derived CTL epitopes⁷⁹, lack of presentation of the HPV epitope in BL cells should not be due to a GAR stabilization effect of EBNA1. Instead, it should be ascribable to the particular antigen processing machinery present in BL cells, which differs from that found in LCLs. Furthermore, deletion of the GAR domain has also been demonstrated to provoke no major effect on EBNA1 protection from degradation, suggesting that the GAR domain has other, as yet unidentified, effects¹⁰⁸.

One of the major differences between BL cells and LCL is the proteasome^{66,98-99}. Indeed, using the same cells assayed in cytotoxicity, BL cells were found to present proteasomes with a different subunit composition, correlating with a much lower chymotryptic and tryptic-like activities with respect to LCLs. This may result in their poor capacity to generate the HPV epitope due the presence of the GAR domain, whose deletion restores the capacity of BL cells to present the HPV epitope⁷⁸. Indeed, we demonstrated that BJAB cells expressing a GAR-deleted EBNA1, are recognized by HPV-specific CTLs further confirming that low expression of HLA class I molecules and TAPs may only partially affect the presentation of the HPV epitope which is not generated and presented in BJAB expressing wild-type EBNA1⁷⁸. Intriguingly, we found that BLs treatment with proteasome inhibitors partially restores the capacity of BL cells to present the EBNA1 epitope, thereby suggesting that proteasomes from BL cells, although less active against prototype substrate peptides, which only partially indicate the *in vivo* proteasomal activities, degrade the HPV epitope during the processing of EBNA1. It remains to be elucidated whether other EBNA1-derived CTL epitopes may be more efficiently generated and presented after partial inhibition of proteasomes or whether this effect is restricted to the HPV epitope. Therefore, the question is whether the GAR domain can specifically alter EBNA1 processing by the proteasome in BL cells. Interestingly, it has been demonstrated that the effect of the GAR domain may either prevent or promote proteasomal degradation, depending on its location in the protein¹⁰⁸. It is tempting to speculate that this effect may also be influenced by the type of proteasome, since it has been also shown that GAR affects the unfolding/recognition of protein substrates by proteasomes¹⁰⁸. Although the role of GAR on the generation of EBNA1-derived CTL epitopes still remains to be elucidated and requires further investigation, in our experimental setting, it is clear that this domain affects the generation of the

HPV epitope in BL cells but not in LCLs demonstrating that GAR effects are cell-dependent.

In conclusion, our study together with previous reports strongly support the idea that EBNA1-specific CTLs might be exploited therapeutically to target EBV+ malignancies in combination with chemotherapy and/or protocols designed to restore antigen-presenting capacity in the tumor. In this context, it has been recently demonstrated that tubacin, a molecule which inhibits histone deacetylase 6, demonstrates a fairly selective capacity to induce apoptosis in BL cells, but not in LCLs¹⁰⁹. Furthermore, the combination of tubacin with a proteasome inhibitor induced efficient killing of BL cells¹⁰⁹, which are known to be resistant to proteasome inhibitor-induced apoptosis^{66,110}. These findings, together with those reported in this study, suggest that the use of proteasome inhibitors, alone or in combination with other drugs such as tubacin, may represent a strategy for the treatment of EBNA1 carrying tumors, since proteasome inhibitors, in addition to their effect as pro-apoptotic drugs may also increase the immunogenicity of EBNA1, thereby resulting in the efficient elimination of EBNA1-positive malignancies.

REFERENCES

- 1 Altomare, L. *et al.* Levitation and movement of human tumor cells using a printed circuit board device based on software-controlled dielectrophoresis. *Biotechnol Bioeng* **82**, 474-479 (2003).
- 2 Bianchi, N., Zuccato, C., Lampronti, I., Borgatti, M. & Gambari, R. Fetal hemoglobin inducers from the natural world: a novel approach for identification of drugs for the treatment of beta-thalassemia and sickle-cell anemia. *eCAM* **6**, 141-151 (2009).
- 3 Borgatti, M. *et al.* Dielectrophoresis-based 'Lab-on-a-chip' devices for programmable binding of microspheres to target cells. *Int J Oncol* **27**, 1559-1566 (2005).
- 4 Borgatti, M. *et al.* Separation of white blood cells from erythrocytes on a dielectrophoresis (DEP) based 'Lab-on-a-chip' device. *Int J Mol Med* **15**, 913-920 (2005).
- 5 Borgatti, M., Bianchi, N., Mancini, I., Feriotto, G. & Gambari, R. New trends in non-invasive prenatal diagnosis: applications of dielectrophoresis-based Lab-on-a-chip platforms to the identification and manipulation of rare cells. *Int J Mol Med* **21**, 3-12 (2008).
- 6 Borgatti, M. *et al.* Dielectrophoresis based lab-on-a-chip platforms for the identification and manipulation of rare cells and microspheres: implications for non-invasive prenatal diagnosis. *Minerva Biotechnol* **19**, 43-50 (2007).
- 7 Borgatti, M. *et al.* Antibody-antigen interactions in dielectrophoresis buffers for cell manipulation on dielectrophoresis-based lab-on-a-chip devices. *Minerva Biotechnol* **19**, 71-74 (2007).
- 8 Fabbri, E. *et al.* Levitation and movement of tripalmitin-based cationic lipospheres on a dielectrophoresis-based lab-on-a-chip device. *J Appl Polym Sci* **109**, 3484-3491 (2008).
- 9 Gambari, R. *et al.* Applications to cancer research of "lab-on-a-chip" devices based on dielectrophoresis (DEP). *Technol Cancer Res Treat* **2**, 31-40 (2003).
- 10 Medoro, G., Guerrieri, R., Manaresi, N., Nastruzzi, C. & Gambari, R. Lab on a chip for live-cell manipulation. *IEEE Des Test Comput* **24**, 26-36 (2007).
- 11 Schuetze, J., Ilgen, H. & Farner, W. R. An integrated micro cooling system for electronic circuits. *IEEE Trans Ind Electron* **48**, 281-285 (2001).
- 12 Wego, A., Richter, S. & Pagel, L. Fluidic microsystems based on printed circuit board technology. *J Micromech Microeng* **11**, 528-531 (2001).
- 13 Nguyen, N. T. & Huang, X. Miniature valveless pumps based on printed circuit board technique. *Sens Actuators A* **88**, 104-111 (2001).
- 14 Jung, E. *et al.* Lamination and laser structuring for a microwell array. *Microsystem Technologies* **14**, 931-936 (2008).
- 15 Gong, M. & Kim, C. J. Two dimensional digital microfluidic system by multilayer printed circuit board. *J Microelectromech Syst* **17**, 257-264 (2008).

- 16 Petrou, P. S., Moser, I. & Jobst, G. BioMEMS device with integrated microdialysis probe and biosensor array. *Biosens Bioelectron* **17**, 859–865 (2002).
- 17 lafelice, B. *et al.* in *MicroTAS*. 563-565.
- 18 Aschenbrenner, R., Ostmann, A., Beutler, U., Simon, J. & Reichl, H. Electroless nickel/copper plating as a new bump metallization. *IEEE Transactions on components, packaging and manufacturing technology, Part B: Advanced packaging* **18**, 334–338 (1995).
- 19 Gazzola, D., lafelice, B., Jung, E., Franchi, E. & Guerrieri, R. An integrated electronic meniscus sensor for measurement of evaporative flow. *Sens Actuators A* **146**, 194–200 (2008).
- 20 Jung, E. *et al.* in *Design, test, integration and packaging of MEM/MOEMS*. 184–188.
- 21 Yager, P. *et al.* Microfluidic diagnostic technologies for global public health. *Nature* **442**, 412-418 (2006).
- 22 Floriano, P. N. *et al.* A grazing incidence surface X-ray absorption fine structure (GIXAFS) study of alkanethiols adsorbed on Au, Ag, and Cu. *Chem Phys Lett* **321**, 175-181 (2000).
- 23 Bain, C. D. *et al.* Formation of monolayer films by the spontaneous assembly of organic thiols from solution onto gold. *J Am Chem Soc* **111**, 321-335 (1989).
- 24 Colavita PE, D. M., Molliet A, Evans U, Reddic J, Zhou J, Chen D, Miney PG, Myrick ML. . Effects of metal coating on self-assembled monolayers on gold. 1. Copper on dodecanethiol and octadecanethiol. *Langmuir* **18**, 8503-8509 (2002).
- 25 Braun, T. *et al.* in *Electronics Packaging Technology*. 9th edn 406-410.
- 26 Rickinson, A. B. & Moss, D. J. Human cytotoxic T lymphocyte responses to Epstein-Barr virus infection *Annu Rev Immunol* **15**, 405-431 (1997).
- 27 Lampronti, I. *et al.* Accumulation of gamma-globin mRNA in human erythroid cells treated with angelicin. *Eur J Haematol* **71**, 189-195 (2003).
- 28 Fibach, E., Bianchi, N., Borgatti, M., Prus, E. & Gambari, R. Mithramycin induces fetal hemoglobin production in normal and thalassemic human erythroid precursor cells. *Blood* **102** 1276-1281 (2003).
- 29 Gambari, R. *et al.* Human leukemia K-562 cells: induction of erythroid differentiation by 5-azacytidine *Cell Differ* **14**, 87-97 (1984).
- 30 Accetta, A. *et al.* New uracil dimers showing erythroid differentiation inducing activities. *J Med Chem* **52**, 87-94 (2009).
- 31 Micheletti, F. *et al.* Selective amino acid substitutions of a subdominant Epstein-Barr virus LMP2-derived epitope increase HLA / peptide complex stability and immunogenicity: implications for immunotherapy of Epstein-Barr virus-associated malignancies. *Eur J Immunol* **29**, 2579-2589 (1999).
- 32 De Jager, W., te Velthuis, H., Prakken, B. J. & Kuis W, R. G. Simultaneous detection of 15 human cytokines in a single sample of stimulated peripheral blood mononuclear cells. *Clin Diagn Lab Immunol* **10**, 133-139 (2003).
- 33 Kerr, J. R., Cunniffe, V. S., Kelleher, P., Coats, A. J. & Matthey, D. L. Circulating cytokines and chemokines in acute symptomatic parvovirus B19 infection: negative association between levels of pro-inflammatory cytokines

- and development of B19-associated arthritis. *J Med Virol* **74**, 147-155 (2004).
- 34 Fibach, E. *et al.* Effects of rapamycin on accumulation of alpha-, beta- and gamma-globin mRNAs in erythroid precursor cells from beta-thalassaemia patients. *Eur J Haematol* **77** 437-441 (2006).
- 35 Bocchi, M. *et al.* Dielectrophoretic trapping in microwells for manipulation of single cells and small aggregates of particles. *Biosens Bioelectron* **24**, 1177-1183 (2009).
- 36 Loeher, T., Manassis, D., Ostmann, A. & Reichl, H. in *European Microelectronics and Packaging conference & exhibition*. 16th edn 630-634.
- 37 Liu, L., Huang, Y. D., Zhang, Z. Q., Jiang, Z. X. & Wu, L. N. Ultrasonic treatment of aramid fiber surface and its effect on the interface of aramid/epoxy composites. *Appl Surf Sci* **254**, 2594-2599 (2008).
- 38 Song, S. N., Tan, H. H. & Ong, P. L. in *Electronics Packaging Technology* 7th edn 848-852.
- 39 McDonald, J. C. & Whitesides, G. M. Poly(dimethylsiloxane) as a material for fabricating microfluidic devices. *Acc Chem Res* **35**, 491-499 (2002).
- 40 Hui, A. Y. N., Wang, G., Lin, B. & Chan, W. T. Microwave plasma treatment of polymer surface for irreversible sealing of microfluidic devices. *Lab Chip* **5**, 1173-1177 (2005).
- 41 Shull, K. R. *et al.* Adhesive transfer of thin viscoelastic films. *Langmuir* **21**, 178-186 (2005).
- 42 Gabriele, S., Versaevel, M., Preira, P. & Théodoly, O. A simple microfluidic method to select, isolate, and manipulate single-cells in mechanical and biochemical assays. *Lab Chip* **10**, 1459-1467 (2010).
- 43 Park, K., Suk, H. J., Akin, D. & Bashir, R. Dielectrophoresis-based cell manipulation using electrodes on a reusable printed circuit board. *Lab Chip* **9**, 2224-2229 (2009).
- 44 Fuchs, A. B. *et al.* Electronic sorting and recovery of single live cells from microlitre sized samples. *Lab Chip* **6**, 121-126 (2006).
- 45 Altomare, L. *et al.* Levitation and movement of human tumor cells using a printed circuit board device based on software-controlled dielectrophoresis. *Biotechnol Bioeng* **82**, 474-479 (2003).
- 46 Gambari, R. *et al.* Applications to cancer research of "Lab-on-a-chip" devices based on dielectrophoresis (DEP). *Technol Cancer Res Treat* **2**, 31-40 (2003).
- 47 Baraldi, P. G. *et al.* Synthesis and antitumor activity of new benzoheterocyclic derivatives of distamycin A. *J Med Chem* **43**, 2675-2684 (2000).
- 48 Abbas, A., Lichtman, A. & Pober, J. *Immunologia cellulare e molecolare*. (Nuova Libreria, 2002).
- 49 Myung, J., Kim, K. & Crews, C. The ubiquitin proteasome pathway and proteasome inhibitors. *Med Res Rev* **21**, 245-273 (2001).
- 50 Princiotta, M. *et al.* Quantitating protein synthesis, degradation, and endogenous antigen processing. *Immunity* **18**, 343-354 (2003).
- 51 Rock, K. & Goldberg, A. L. Degradation of cell proteins and the generation of MHC class I-presented peptides. *Immunology* **17**, 739-779 (1999).

- 52 Beninga, J., Rock, K. L. & Goldberg, A. L. Interferon-gamma can stimulate post-proteasomal trimming of the N terminus of an antigenic peptide by inducing leucine aminopeptidase. *J Biol Chem* **273**, 18734-18742 (1998).
- 53 Kloetzel, P. M. Generation of major histocompatibility complex class I antigens: functional interplay between proteasomes and TPPII. *Nat Immunol* **5**, 661-669 (2004).
- 54 Engelhard, V. H. Structure of peptides associated with MHC class I molecules. *Curr Opin Immunol* **6**, 13 (1994).
- 55 Elliott, T., Smith, M., Driscoll, P. & McMichael, A. Peptide selection by class I molecules of the major histocompatibility complex. *Curr Biol* **3**, 854 (1993).
- 56 Engelhard, V. H. Structure of peptides associated with class I and class II MHC molecules. *Annu Rev Immunol* **12**, 181 (1994).
- 57 Silver, M. L., Guo, H. C., Strominger, J. L. & Wiley, D. Atomic structure of a human MHC molecule presenting an influenza virus peptide. *Nature* **360**, 367 (1992).
- 58 Madden, D. R., Garboczi, D. N. & Wiley, D. C. The antigenic identity of peptide/MHC complexes: a comparison of the conformations of five viral peptides presented by HLA-A2. *Cell* **75**, 693 (1993).
- 59 Rohren, E. M., Pease, L. R., Ploegh, H. L. & Schumacher, T. N. M. Polymorphisms in pockets of major histocompatibility complex class I molecules influence peptide preference. *J Exp Med* **77**, 1713 (1993).
- 60 Van Bleek, G. M. & Nathenson, S. G. The structure of the antigen-binding groove of major histocompatibility complex class I molecules determines specific selection of self-peptides. *Proc Natl Acad Sci USA* **88**, 11032-11036 (1991).
- 61 Kelly, A. *et al.* Assembly and function of the two ABC transporter proteins encoded in the human major histocompatibility complex. *Nature* **355**, 641-644 (1992).
- 62 Hewitt, E. W. The MHC class I antigen presentation pathway: strategies for viral immune evasion. *Immunology* **110**, 163-169 (2003).
- 63 Ploegh, H. L. Viral strategies of immune evasion. *Science* **280**, 248-253 (1998).
- 64 Yewdell, J. W. & Hill, A. B. Viral interference with antigen presentation. *Nature* **3** 1019-1025 (2002).
- 65 Chen, H. L. *et al.* Structural and functional analysis of beta2 microglobulin abnormalities in human lung and breast cancer. *Int J Cancer* **67**, 756-763 (1996).
- 66 Gavioli, R., Frisan, T., Vertuani, S., Bornkamm, G. W. & Masucci, M. G. c-myc overexpression activates alternative pathways for intracellular proteolysis in lymphoma cells. *Nat Cell Biol* **3**, 283-288 (2001).
- 67 Preta, G. *et al.* Inhibition of serine-peptidase activity enhances the generation of a survivin-derived HLA-A2-presented CTL epitope in colon-carcinoma cells. *Scand J Immunol* **68**, 579-588 (2008).
- 68 Pope, J. H. Establishment of cell lines from peripheral leukocytes in infectious mononucleosis. *Nature* **216**, 810-811 (1967).
- 69 Khanna, R. & Burrows, S. R. Role of cytotoxic T lymphocytes in Epstein-Barr virus-associated diseases. *Annu Rev Microbiol* **54**, 19-48 (2000).

- 70 Pamer, E. & Cresswell, P. Mechanisms of MHC class I-restricted antigen processing. *Annu Rev Immunol* **16**, 323-358 (1998).
- 71 Gavioli, R. *et al.* Recognition of the Epstein-Barr virus-encoded nuclear antigens EBNA-4 and EBNA-6 by HLA A11 restricted cytotoxic T lymphocytes: Implications for the down-regulation of HLA A11 in Burkitt's lymphoma. *Proc Natl Acad Sci USA* **89**, 5862-5866 (1992).
- 72 Gavioli, R. *et al.* Multiple HLA A11-restricted cytotoxic T-lymphocyte epitopes of different immunogenicities in the Epstein-Barr virus-encoded nuclear antigen 4. *J Virol* **67**, 1572-1578 (1993).
- 73 Micheletti, F. *et al.* Selective amino acid substitutions of a subdominant Epstein-Barr virus LMP2-derived epitope increase HLA / peptide complex stability and immunogenicity: implications for immunotherapy of Epstein-Barr virus-associated malignancies. *Eur J Immunol* **29**, 2579-2589 (1999).
- 74 Murray, R. J. *et al.* Identification of target antigens for the human cytotoxic T cell response to Epstein-Barr virus (EBV): implications for the immune control of EBV-positive malignancies. *J Exp Med* **176**, 157-168 (1992).
- 75 Khanna, R. *et al.* Localization of Epstein-Barr virus cytotoxic T cell epitopes using recombinant vaccinia: implications for vaccine development. *J Exp Med* **176**, 169-176 (1992).
- 76 Blake, N. *et al.* Human CD8+T cell responses to EBV EBNA1:HLA class I presentation of the Gly-Ala containing protein requires exogenous processing. *Immunity* **7**, 791-802 (1997).
- 77 Lee, S. P. *et al.* CD8 T cell recognition of endogenously expressed Epstein-Barr virus nuclear antigen 1. *J Exp Med* **199**, 1409-1420 (2004).
- 78 Marescotti, D. *et al.* Characterization of an human leukocyte antigen A2-restricted Epstein-Barr virus nuclear antigen-1-derived cytotoxic T-lymphocyte epitope. *Immunology* **129**, 386-395 (2010).
- 79 Tellam, J. *et al.* Endogenous presentation of CD8 T cell epitopes from Epstein-Barr Virus-Encoded Nuclear Antigen 1. *J Exp Med* **199** 1421-1431 (2004).
- 80 Voo, K. S. *et al.* Evidence for the presentation of major histocompatibility complex class I-restricted Epstein-Barr Virus Nuclear Antigen 1 peptides to CD8 T lymphocytes. *J Exp Med* **199**, 459-470 (2004).
- 81 Yin, Y., Manoury, B. & Fahraeus, R. Self-inhibition of synthesis and antigen presentation by Epstein-Barr Virus-Encoded EBNA1. *Science* **301**, 1371-1374 (2003).
- 82 Apcher, S. *et al.* mRNA translation regulation by the Gly-Ala repeat of Epstein-Barr virus nuclear antigen 1. *J Virol* **83**, 1289-1298 (2009).
- 83 Levitskaya, J. *et al.* Inhibition of antigen processing by internal repeat region of Epstein Barr Virus Nuclear Antigen-1. *Nature* **375**, 685-688 (1995).
- 84 Levitskaya, J., Sharipo, A., Leonchiks, A., Ciechanover, A. & Masucci, M. Inhibition of ubiquitin/proteasome-dependent protein degradation by the Gly-Ala repeat domain of the Epstein Barr Virus Nuclear Antigen-1. *Proc Natl Acad Sci USA* **94**, 12616-12621 (1997).
- 85 Merlo, A. *et al.* Virus-specific cytotoxic CD4+ T cells for the treatment of EBV-related tumors. *J Immunol* **184**, 5895-5902 (2010).

- 86 Heslop, H. E. *et al.* Long-term outcome of EBV-specific T-cell infusions to prevent or treat EBV-related lymphoproliferative disease in transplant recipients. *Blood* **115**, 925-935 (2010).
- 87 Polack, A. *et al.* c-myc activation renders proliferation of Epstein-Barr virus (EBV)-transformed cells independent of EBV nuclear antigen 2 and latent membrane protein 1. *Proc Natl Acad Sci USA* **93**, 10411-10416 (1996).
- 88 Wilson, J. B., Bell, J. L. & Levine, A. J. Expression of Epstein-Barr virus nuclear antigen-1 induces B cell neoplasia in transgenic mice. *EMBO J* **15**, 3117-3126 (1996).
- 89 Kang, M. S., Hung, S. C. & Kieff, E. Epstein-Barr virus nuclear antigen 1 activates transcription from episomal but not integrated DNA and does not alter lymphocyte growth. *Proc Natl Acad Sci USA* **98**, 15233-15238 (2001).
- 90 Gavioli, R. *et al.* HIV-1 tat protein modulates the generation of cytotoxic T cell epitopes by modifying proteasome composition and enzymatic activity. *J Immunol* **173**, 3838-3843 (2004).
- 91 Gavioli, R. *et al.* High structural side chain specificity required at the second position of immunogenic peptides to obtain stable MHC/peptide complexes. *FEBS Letters* **421**, 95-99 (1998).
- 92 Parker, K. C., Bednarek, M. A. & Coligan, J. E. Scheme for ranking potential HLA-A2 binding peptides based on independent binding of individual peptide side-chains. *J Immunol* **152**, 163-175 (1994).
- 93 Micheletti, F. *et al.* The lifespan of MHC class I/complexes determines the efficiency of cytotoxic T lymphocyte responses. *Immunology* **96**, 411-415 (1999).
- 94 Chen, W., Khilko, S., Fecondo, J., Margulies, D. H. & McCluskey, J. Determinant selection of major histocompatibility complex class I-restricted antigenic peptides is explained by class I-peptide affinity and is strongly influenced by nondominant anchor residues. *J Exp Med* **180**, 1471-1483 (1994).
- 95 Blake, N., Haigh, T., Shaka'a, G., Croom-Carter, D. & Rickinson, A. The importance of exogenous antigen in priming the human CD8+ T cell response: lesson from the EBV nuclear antigen EBNA1. *J Immunol* **165**, 7078-7087 (2000).
- 96 Masucci, M. G. *et al.* Down-regulation of class I HLA antigens and of the Epstein-Barr virus encoded latent membrane protein in Burkitt's lymphoma lines. *Proc Natl Acad Sci USA* **84**, 4567-4571 (1987).
- 97 Masucci, M. G. *et al.* Allele specific down-regulation of MHC class I antigens in Burkitt's lymphoma lines. *Cellular Immunology* **120**, 396-400 (1989).
- 98 Frisan, T. *et al.* Defective presentation of MHC class I-restricted cytotoxic T-cell epitopes in Burkitt's lymphoma cells. *Int J Cancer* **68**, 251-258 (1996).
- 99 Rowe, M. *et al.* Restoration of endogenous antigen processing in Burkitt's lymphoma cells by Epstein-Barr virus latent membrane protein-1: coordinate up-regulation of peptide transporters and HLA-class I antigen expression. *Eur J Immunol* **25**, 1374-1384 (1995).
- 100 Frisan, T., Levitsky, V., Polack, A. & Masucci, M. G. Phenotype-dependent differences in proteasome subunit composition and cleavage specificity in B cell lines. *J Immunol* **160**, 3281-3289 (1998).

- 101 Vinitzky, A. *et al.* The generation of MHC class I-associated peptides is only partially inhibited by proteasome inhibitors: involvement of nonproteasomal cytosolic proteases in antigen processing? *J Immunol* **159**, 554-564 (1997).
- 102 Luckey, C. J. *et al.* Proteasomes can either generate or destroy MHC class I epitopes: Evidence for nonproteasomal epitope generation in the cytosol. *J Immunol* **161**, 112-121 (1998).
- 103 Valmori, D. *et al.* Modulation of proteasomal activity required for the generation of a cytotoxic T lymphocyte-defined peptide derived from the tumor antigen MAGE-3. *J Exp Med* **189**, 895-905 (1999).
- 104 Khanna, R., Moss, D. J. & Burrows, S. R. Vaccine strategies against Epstein-Barr virus-associated diseases: lessons from studies on cytotoxic T-cell-mediated immune regulation. *Immunol Rev* **170**, 49-64 (1999).
- 105 Rammensee, H. G., Friede, T. & Stevanoviic, S. MHC ligands and peptide motifs: first listing. *Immunogenetics* **41**, 178-228 (1995).
- 106 Shi, Y. & Lutz, C. T. Interferon-gamma control of EBV-transformed B cells: a role for CD8+ T cells that poorly kill EBV-infected cells. *Viral Immunol* **15**, 213-225 (2002).
- 107 Young, L. S. & Rickinson, A. B. Epstein-Barr virus:40years on. *Nature Reviews* **4**, 757-768 (2004).
- 108 Daskalogianni, C. *et al.* Gly-Ala repeats induce position- and substrate-specific regulation of 26 S proteasome-dependent partial processing. *J Biol Chem* **283**, 30090-30100 (2008).
- 109 Kawada, J., Zou, P., Mazitschek, R., Bradner, J. E. & Cohen, J. I. Tubacin kills Epstein-Barr virus (EBV)-Burkitt lymphoma cells by inducing reactive oxygen species and EBV lymphoblastoid cells by inducing apoptosis. *J Biol Chem* **284**, 17102-17109 (2009).
- 110 Zou, P., Kawada, J., Pesnicak, L. & Cohen, J. I. Bortezomib induces apoptosis of Epstein-Barr virus (EBV)-transformed B cells and prolongs survival of mice inoculated with EBV-transformed B cells. *J Virol* **81**, 10029-10036 (2007).

ABBREVIATIONS

Abs	Antibodies
Al	Aluminium
APC	Antigen Presenting Cell
AraC	Arabinoside C
ATP	Adenosine Triphosphate
AUF	Arbitrary Units of Fluorescence
Au over Ni	Gold over Nickel
Au over Ni + ODT	Gold over Nickel + Octadecanethiol
Au over Pd	Gold over Palladium
Au over Pd + ODT	Gold over Palladium + Octadecanethiol
β2m	β2-microglobulin
BLs	Burkitt's lymphoma
BOT	Bottom
Certonal FC-732T	Certonal FC-732 tempered
COCHISE	Cell-On-CHIp bioSEnsor
Cpm	Counts per minute
CTL	Cytotoxic T Lymphocytes
Cu	Copper
Cu + ODT	Copper + Octadecanethiol
DAF	Die attach film
DEP	Dielectrophoresis
DEPC	Diethylpyrocarbonate
DI water	Deionized water
DMSO	Dimethyl sulfoxide
DTT	Dithiothreitol
E:T	Effector:Target
E1	EBNA1
EAs	Early antigens
EBNA	EBV nuclear antigen
EBV	Epstein Barr Virus
ER	Endogenous Reticulum
ERAP	Endoplasmic-reticulum aminopeptidase
FBS	Fetal bovine serum
GAr	Glycine-Alanine repeat domain
HD	Hodgkin disease
HLA	Human Leucocyte Antigen
HPLC	High-performance liquid chromatography
IFN	Interferon

Ig	Immunoglobulin
IM	Infectious Mononucleosis
kDa	Kilo Dalton
KHz	Chilohertz
LCL	Lymphoblastoid cell line
LMP1 and 2	Latent Membrain Protein 1 and 2
LMP2 and 7	Low molecular weight protein 2 and 7
LOC	Lab-on-a-Chip
LOC K562	K562 manipulated in Lab-on-a-chip
MECL1	Multicatalytic endopeptidase like 1
MEMS	Microelectromechanical systems devices
MHC	Major Histocompatibility Complex
MHz	Megahertz
μTAS	Micro Total Analysis Systems
MID	Middle
NK	Natural Killer
NPC	Nasopharyngeal Carcinoma NPC
ODT	Octadecanethiol
PA28	Proteasome Activator 28
PBL	Peripheral Blood Lymphocyte
PCB	Printed Circuit Board
Pd	Palladium
Pd + ODT	Palladium + Octadecanethiol
PDMS	Poly(dimethylsiloxane)
PF after lam	Polyurethane foil after lamination
PF before lam	Polyurethane foil before lamination
PHA	Phytohaemagglutinin
PI	Polyimide
PP	Polyurethane powder
Py	Pyralux
RCC	Resin Coated Copper
SAMs	Self-assembled Monolayers
SD	Standard Deviation
SDS	Sodium Dodecyl Sulfate
SFU	Spot-Forming Units
TAP	Transporter associated with antigen processing
TPPII	Tripetidil peptidase II

PUBLICATIONS

- **Destro F.**, Sforza F., Sicurella M., Marescotti D., Gallerani E., Baldisserotto A., Marastoni M., Gavioli R. Proteasome inhibitors induce the presentation of an EBNA1-derived CTL epitope in Burkitt's lymphoma cells. *Immunology*. *In press*.
- **Destro F.**, Borgatti M., Iafelice B., Gavioli R., Braun T., Bauer J., Böttcher L., Jung E., Bocchi M., Guerrieri R., Gambari R. Effects of biomaterials for Lab-on-a-chip production on cell growth and expression of differentiated functions of leukemic cell lines. *J Mater Sci Mater Med*. 2010;21:2653-64.
- Marescotti D., **Destro F.**, Baldisserotto A., Marastoni M., Coppotelli G., Masucci M., Gavioli R. 2009. Characterization of an human leucocyte antigen A2-restricted Epstein-Barr virus nuclear antigen-1-derived cytotoxic T-lymphocyte epitope. *Immunology*. 2010;129:386-95.
- Mazzuferi M., Bovolenta R., Bocchi B., Braun T., Bauer J., Jung E., Iafelice B., Guerrieri R., **Destro F.**, Borgatti M., Bianchi N., Limonato M., Gambari R. The biocompatibility of materials used in printed circuit board technologies with respect to primary neuronal and K562 cells. *Biomaterials*. 2010;31:1045-54.
- Baldisserotto A., **Destro F.**, Vertuani G., Marastoni M., Gavioli R., Tomatis R. 2009. N-Terminal-prolonged vinyl ester-based peptides as selective proteasome beta1 subunit inhibitors. *Bioorg Med Chem*. 2009;17:5535-40.
- Baldisserotto A., Ferretti V., **Destro F.**, Franceschini C., Marastoni M., Gavioli R., Tomatis R. Alpha,beta-unsaturated N-acylpyrrole peptidyl derivatives: new proteasome inhibitors. *J Med Chem*. 2010;53:6511-5.
- Bazzaro M., Anchoori R.K., Mudiam M.K.R., Issaenko O., Kumar S., Karanam B., Lin Z., Vogel R.I., Gavioli R., **Destro F.**, Ferretti V., Roden R.B.S., Khan S.R. α,β -Unsaturated carbonyl system of chalcone-based derivatives is responsible for broad inhibition of proteasomal activity and preferential killing of Human Papilloma Virus (HPV) positive cervical cancer cells. *J Med Chem*. 2011;54:449–56.
- Salvatori F., Breveglieri G., Zuccato C., Finotti A., Bianchi N., Borgatti M., Feriotto G., **Destro F.**, Canella A., Brognara E., Lampronti I., Breda L., Rivella S., Gambari R. Production of beta-globin and adult hemoglobin following G418 treatment of erythroid precursor cells from homozygous beta(0)39 thalassemia patients. *Am J Hematol*. 2009;84:720-8.
- Salvatori F., Cantale V., Breveglieri G., Zuccato C., Finotti A., Bianchi N., Canella A., Pinotti M., Borgatti M., Feriotto G., **Destro F.**, Breda L., Rivella S., Gambari R. Development of K562 cell clones expressing β -globin mRNA carrying the $\beta^{\circ}39$ thalassemia mutation for the screening of correctors of stop codon mutations. *Biotechnol Appl Biochem*. 2009;54:41-52.
- Cellini S., Fortini C., Gallerani E., **Destro F.**, Brocca Cofano E., Caputo A. and Gavioli R. Identification of new HIV-1 Gag-specific cytotoxic T lymphocyte responses in BALB/c mice. *Virology J*. 2008;5:81.

- Jung E., Menessis D., Neumann A., Boettcher L., Braun T., Bauer J., Reichel H., Iafelice B., **Destro F.**, Gambari R. Lamination and laser structuring for a DEP microwell array. *Microsyst Technol.* 2008;14:931-936.
- Jung E., Menessis D., Neumann A., Boettcher L., Braun T., Bauer J., Reichel H., Iafelice B., **Destro F.**, Gambari R. Lamination and laser structuring for a DEP microwell array. *Proceedings of DTIP. Stresa, April 2007*;184-188.
- Iafelice B., **Destro F.**, Manassis D., Gazzola D., Jung E., Boettcher L., Reichel H., Gambari R. Aluminum printed circuit board technology for biomedical micro-devices. *Proceedings of MicroTAS. Paris, October 2007*;563-565.
- Breveglieri G., Salvatori F., Finotti A., Bertuzzi I., **Destro F.**, Falzoni S., Bianchi N., Borgatti M., Zuccato C., Feriotto G., Breda L., Rivella S., Gambari R. Cellular biosensors for the identification of fetal hemoglobin inducers. *Minerva Biotec.* 2007;19:123-132.

Effects of biomaterials for Lab-on-a-chip production on cell growth and expression of differentiated functions of leukemic cell lines

Federica Destro · Monica Borgatti · Bruno Iafelice · Riccardo Gavioli · Tanja Braun · Jörg Bauer · Lars Böttcher · Erik Jung · Massimo Bocchi · Roberto Guerrieri · Roberto Gambari

Received: 30 April 2010 / Accepted: 30 June 2010 / Published online: 13 July 2010
© Springer Science+Business Media, LLC 2010

Abstract The rapid increase of the applications for Lab-on-a-chip devices has attracted the interest of researchers and engineers on standard process of the electronics industry for low production costs and large scale development, necessary for disposable applications. The printed circuit board technology could be used for this purpose, in particular for the wide range of materials available. In this paper, assays on biocompatibility of materials used for Lab-on-a-chip fabrication has been carried out using two tumor cell lines growing in suspension, the human chronic myelogenous leukemia K562 cell line, able to undergo erythroid differentiation when cultured with chemical inducers, and the lymphoblastoid cell line (LCL), extensively used for screening of cytotoxic T-lymphocytes (CTLs). We have demonstrated that some materials strongly inhibit cell proliferation of both the two cell lines

to an extent higher than 70–75%, but only after a prolonged exposure of 3–6 days (Copper, Gold over Nickel, Aramid fiber filled epoxy uncured, b-stage epoxy die attach film, Tesa 4985 adhesive tape, Pyralux uncured, Copper + 1-octadecanethiol). However, when experiments were performed with short incubation time (1 h), only Aramid fiber filled epoxy uncured was cytotoxic. Variation of the results concerning the other materials was appreciable when the experiments performed on two cell lines were compared together. Furthermore, the effects of the materials on erythroid differentiation and CTL-mediated LCL lysis confirmed, in most of the cases, the data obtained in cytotoxic and antiproliferative tests.

Abbreviations

PCB	Printed circuit board
CTLs	Cytotoxic T-lymphocytes
LCL	Lymphoblastoid cell line
ITRS	International technology roadmap for semiconductors
RCC	Resin coated copper
DAF	Die attach film
PDMS	Poly(dimethylsiloxane)
SAMS	Self-assembled monolayers
ODT	Octadecanethiol
PF before lam	Polyurethane film before lamination
PF after lam	Polyurethane film after lamination
PP	Polyurethane powder
Certonal FC-732T	Certonal FC-732 tempered
EBV	Epstein-Barr Virus
FBS	Fetal bovine serum
EBNA-3	EBV nuclear antigen 3
HLA-A2	Human leukocyte antigen A2
E:T	Effector:target
Cpm	Counts per minute

Federica Destro and Monica Borgatti have contributed equally to this study.

Electronic supplementary material The online version of this article (doi:10.1007/s10856-010-4125-2) contains supplementary material, which is available to authorized users.

F. Destro · M. Borgatti · R. Gavioli · R. Gambari (✉)
BioPharmaNet, Department of Biochemistry and Molecular
Biology, University of Ferrara, Ferrara, Italy
e-mail: gam@unife.it

B. Iafelice · T. Braun · J. Bauer · L. Böttcher · E. Jung
Fraunhofer Institute for Reliability and Microintegration (IZM),
Berlin, Germany

B. Iafelice · R. Guerrieri
Advanced Research Center on Electronic Systems (ARCES),
University of Bologna, Bologna, Italy

M. Bocchi
MindSeeds Laboratories, Bologna, Italy

Characterization of an human leucocyte antigen A2-restricted Epstein–Barr virus nuclear antigen-1-derived cytotoxic T-lymphocyte epitope

Diego Marescotti,^{1,2} Federica Destro,¹ Anna Baldisserotto,³ Mauro Marastoni,³ Giuseppe Coppotelli,² Maria Masucci² and Riccardo Gavioli¹

¹Department of Biochemistry and Molecular Biology, University of Ferrara, Ferrara, Italy,

²Department of Pharmaceutical Sciences, University of Ferrara, Ferrara, Italy, and

³Department of Cell and Molecular Biology (CMB) Karolinska Institute, Stockholm, Sweden

doi:10.1111/j.1365-2567.2009.03190.x

Received 25 August 2009; revised 15

September 2009; accepted 21 September 2009.

Correspondence: R. Gavioli, Department of Biochemistry and Molecular Biology, University of Ferrara, Via L. Borsari 46, 44100 Ferrara, Italy.

Email: riccardo.gavioli@unife.it

Senior author: Riccardo Gavioli

Summary

The Epstein–Barr virus (EBV) nuclear antigen 1 (EBNA1) is regularly expressed in all proliferating virus-infected cells and is therefore an interesting target for immunotherapy. Alleles of the human leucocyte antigen (HLA) -A2 family are dominantly expressed in Caucasians so we sought to identify EBNA1-specific cytotoxic T-lymphocyte (CTL) responses restricted through this allele. We report on the characterization of the LQTHIFAEV (LQT) epitope. LQT-specific memory CTL responses were reactivated in three of 14 healthy EBV seropositive donors (21%) whereas responses to HLA-A2-restricted epitopes, two derived from LMP2 and one from EBNA3A, were detected in 93%, 71% and 42% of the donors, respectively. The LQT-specific CTL clones did not lyse EBV-carrying lymphoblastoid cell lines and Burkitt's lymphoma cell lines nor EBNA1-transfected Burkitt's lymphoma cells but specifically released interferon- γ upon stimulation with HLA-matched EBNA1-expressing cells and this response was enhanced by deletion of the Gly-Ala repeat domain that inhibits proteasomal degradation. The poor presentation of the endogenously expressed LQT epitope was not affected by inhibition of peptidases that trim antigenic peptides in the cytosol but full presentation was achieved in cells expressing a trojan antigen construct that releases the epitope directly into the endoplasmic reticulum. Hence, inefficient proteasomal processing appears to be mainly responsible for the poor presentation of this epitope.

Keywords: antigen processing; cytotoxic T lymphocyte; Epstein–Barr virus nuclear antigen 1; Epstein–Barr virus; Gly-Ala repeat

Introduction

CD8⁺ T lymphocytes play an important role in the control of viral infections by generating effectors that are able to recognize and kill infected cells.^{1,2} T-cell receptors (TCR) expressed by cytotoxic T lymphocytes (CTL) recognize virus-infected cells via interaction of the TCR with peptides derived from the processing of endogenously expressed viral proteins presented on the surface of the target cell as a complex with major histocompatibility complex (MHC) class I molecules.³ The principal enzymatic activity responsible for the generation of class I-associated peptides is that of the proteasome, a large multicatalytic protease that is essential for the degradation of intracellular proteins.⁴ Moreover, it has been demonstrated that other cytosolic and endoplasmic reticulum (ER) resident proteases act on products released by the proteasome.⁵

Although the complex network of proteases involved in antigen processing should ensure the efficient presentation of viral antigens, several viruses have evolved strategies for interfering with this pathway, allowing them to evade destruction by the immune system. One of the best examples of ubiquitin-proteasome targeting involves the Epstein–Barr virus (EBV), a γ -herpesvirus associated with several human tumours.⁶ This virus is widespread and establishes life-long persistent infections in the B lymphocytes in the vast majority of human adults. The EBV-infected B cells can proliferate *in vitro*, giving rise to lymphoblastoid cell lines (LCL) that express at least nine latency-associated viral antigens: the EBV nuclear antigens EBNA1, -2, -3A, -3B, -3C, -LP and the membrane proteins LMP1, LMP2A and LMP2B.⁷

The proliferation of these virus-infected cells is monitored *in vivo* by T lymphocytes that specifically recognize



Contents lists available at ScienceDirect

Biomaterials

journal homepage: www.elsevier.com/locate/biomaterials

The biocompatibility of materials used in printed circuit board technologies with respect to primary neuronal and K562 cells

Manuela Mazzuferi^{a,b}, Roberta Bovolenta^{a,b}, Massimo Bocchi^{c,d}, Tanja Braun^e, Joerg Bauer^e, Erik Jung^e, Bruno Iafelice^e, Roberto Guerrieri^d, Federica Destro^f, Monica Borgatti^{f,g}, Nicoletta Bianchi^f, Michele Simonato^{a,b,*}, Roberto Gambari^{f,g,**}

^a Department of Clinical and Experimental Medicine, Section of Pharmacology and Neuroscience Center, University of Ferrara, Ferrara 44100, Italy

^b National Institute of Neuroscience, Italy

^c MindSeeds Laboratories, Viale Ercolani 3, I-40138 Bologna, Italy

^d Advanced Research Center on Electronic Systems (ARCES), University of Bologna, Viale C. Pepoli 3/2, I-40123 Bologna, Italy

^e Fraunhofer Institute for Reliability and Microintegration (IZM), Germany

^f BioPharmaNet, Department of Biochemistry and Molecular Biology, University of Ferrara, Ferrara 44100, Italy

^g Biotechnology Center, University of Ferrara, Ferrara 44100, Italy

ARTICLE INFO

Article history:

Received 18 September 2009

Accepted 9 October 2009

Available online 29 October 2009

Keywords:

Biocompatibility

Lab-on-a-chip

Biodevices

Printed circuit board

Eukaryotic cells

ABSTRACT

Printed circuit board (PCB) technology can be used for producing lab-on-a-chip (LOAC) devices. PCBs are characterized by low production costs and large-scale development, both essential elements in the frame of disposable applications. LOAC platforms have been employed not only for diagnostic and/or analytical purposes, but also for identification and isolation of eukaryotic cells, including cancer and stem cells. Accordingly, the compatibility of the employed materials with the biological system under analysis is critical for the development of LOAC devices to be proposed for efficient and safe cell isolation. In this study, we analyzed the *in-vitro* compatibility of a large set of materials and surface treatments used for LOAC development and evaluation with quasi-standard PCB processes. Biocompatibility was analyzed on hippocampal primary cells (a model of attached cell cultures), in comparison with the reference K562 cell line (a model of cells growing in suspension). We demonstrate here that some of the materials under study alter survival, organization, morphology and adhesion capacity of hippocampal cells, and inhibit growth and differentiation of K562 cells. Nonetheless, a subset of the materials tested did not negatively affect these functions, thus demonstrating that PCB technology, with some limitations, is suitable for the realization of LOAC devices well compatible at least with these preparations.

© 2009 Elsevier Ltd. All rights reserved.

1. Introduction

The development of lab-on-a-chip (LOAC) devices for biomedical applications, including manipulation of single cells, is an exciting new research field requiring strict collaboration between electronic engineers and molecular/cellular biologists [1–9]. In the process of LOAC designing and manufacturing, one crucial issue is the choice of biomaterials. The development of modern

biomaterials is more critical for LOAC designed for identification and isolation of eukaryotic cells (like cancer and stem cells) than for diagnostic or analytical applications; for such applications, LOAC platforms have to guarantee isolation of biologically active cells whose growth capacity, differentiation potential and biological properties in general should not be altered by the LOAC-based manipulation. Hence, materials with good biocompatibility need to be used for these applications, even if the eukaryotic cells to be isolated and manipulated are expected to be exposed for a short length of time [10].

In the past few years, printed circuit board (PCB) technology has reached a resolution of tens of micrometers, which is enough for many microfluidics applications [10–13]. The main limitation of this approach in biomedical applications is the biocompatibility of the constituent materials. Recently the range of materials for PCB technologies has been extended. Many have already been developed for

* Corresponding author. Dipartimento di Medicina Clinica e Sperimentale, Sezione di Farmacologia, Via Fossato di Mortara, 17–19, 44100 Ferrara, Italy. Tel: +39 532 45 5211; fax: +39 532 45 5205.

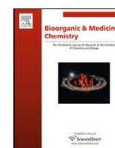
** Corresponding author. Dipartimento di Biochimica e Biologia Molecolare, Sezione di Biologia Molecolare, Via Fossato di Mortara, 74, 44100 Ferrara, Italy. Tel: +39 532 97 4443; fax: +39 532 97 4500.

E-mail addresses: michele.simonato@unife.it (R. Simonato), gam@unife.it (R. Gambari).



Contents lists available at ScienceDirect

Bioorganic & Medicinal Chemistry

journal homepage: www.elsevier.com/locate/bmc

N-Terminal-prolonged vinyl ester-based peptides as selective proteasome β 1 subunit inhibitors

Anna Baldisserotto^a, Federica Destro^b, Gianni Vertuani^a, Mauro Marastoni^{a,*}, Riccardo Gavioli^b, Roberto Tomatis^a

^a Department of Pharmaceutical Sciences and Biotechnology Center, University of Ferrara, Via Fossato di Mortara 17-19, I-44100 Ferrara, Italy

^b Department of Biochemistry and Molecular Biology, University of Ferrara, I-44100 Ferrara, Italy

ARTICLE INFO

Article history:
Received 28 April 2009
Revised 8 June 2009
Accepted 14 June 2009
Available online 18 June 2009

Keywords:
Synthesis
Pseudopeptides
Proteasome inhibition
Post-acidic activity

ABSTRACT

The synthesis and biological properties of vinyl ester peptide-based molecules bearing linear N-terminal amino acids are reported. Compounds were tested *in vitro* for their capacity to inhibit the chymotryptic-, tryptic-like, and post-acidic activities of the proteasome. Some analogues showed selective inhibition of post-acidic (PGPH) activity, which is attributed to the β 1 subunit. Interestingly, active compounds demonstrated higher inhibitory activity toward 'standard' proteasomes than toward immunoproteasomes. The inhibitory potency was found to be related to the amino acid sequence and to the length of the N-terminal residues. The new inhibitors demonstrated resistance to plasmatic proteases and a good capacity to permeate the cell membrane.

© 2009 Elsevier Ltd. All rights reserved.

1. Introduction

Proteasomes are the primary sites of protein degradation in mammalian cells. These large (2.4 MDa) multi-subunit protease complexes perform ATP-dependent degradation of poly-ubiquitinated proteins, and are responsible for the majority of the non-lysosomal proteolysis which occurs in eukaryotic cells.¹ Their central component, the barrel-shaped proteolytic 20S proteasome core particle which consists of four seven-subunit rings, is capped at one or both ends by 19S regulatory particles.^{2,3} 20S proteasomes belong to the family of N-terminal nucleophile hydrolases. They possess only three active proteolytic sites, all of which are located on the β subunits (β 1, β 2, β 5) of each of the two middle rings. Each catalytic subunit possesses a characteristic substrate specificity;⁴ the chymotrypsin-like site, ChT-L (β 5), cleaves peptide bonds after hydrophobic residues, the trypsin-like site, Th-L (β 2), after a basic residue, and the third site (β 1) after an acidic residue (PGPH activity), preferentially aspartate residues demonstrating caspase-like activity.^{5,6} The antiviral cytokine INF- γ induces transcription of the three additional β subunits (LMP2, MECL-1, and LMP7), which can replace their constitutive homologues (β 1, β 2, and β 5) in a newly assembled proteasome.^{7–10} The resulting immunoproteasomes show slightly different substrate specificities *in vitro*. In consequence, the immunoproteasome generates more peptides

than the proteasome for major histocompatibility complex (MHC) class I antigen presentation.^{11,12}

The functional integrity of proteasomes is required for a variety of cellular functions, such as metabolic adaptation, cell differentiation, cell cycle control, stress response, degradation of abnormal proteins, and generation of epitopes presented by MHC class I receptors.^{13,14} Hence deregulation of the ubiquitin-proteasome protein degradation pathway in humans is implicated in several diseases, such as neurodegenerative, autoimmune, and metabolic disorders, in addition to cancer. The idea of targeting the proteasomal pathway represents an appealing new approach for treatment of these pathologies.

Indeed, inhibition of the proteasome influences the stability of many proteins, in particular those involved in cell cycle regulation: most of the cells treated with proteasome inhibitors become sensitive to apoptosis.^{15,16} Thus, the development of new and potentially more active or selective proteasome inhibitors represents a stimulating approach for the treatment of many diseases.

In previous studies, we characterized a class of vinyl-ester-bearing proteasome inhibitors able to interact with catalytic threonine in the same way to that proposed for the well-known vinyl sulfone peptide. Moreover, these vinyl ester inhibitors showed good resistance to proteolysis and the ability to permeate the cell membrane.^{17–23} Interestingly, some of these molecules demonstrated a selective inhibitory capacity for trypsin-like activity at nanomolar concentrations, were non-toxic, did not inhibit cell proliferation and were able to modulate the generation of antigenic peptides linked by MHC class I molecules.¹⁸

* Corresponding author. Tel.: +39 532 455281; fax: +39 532 291296.
E-mail address: mru@dns.unife.it (M. Marastoni).

α,β -Unsaturated *N*-Acylpyrrole Peptidyl Derivatives: New Proteasome Inhibitors

Anna Baldisserotto,[†] Valeria Ferretti,[‡] Federica Destro,[§] Christian Franceschini,[†] Mauro Marastoni,^{*,†} Riccardo Gavioli,[§] and Roberto Tomatis[†]

[†]Department of Pharmaceutical Sciences and Biotechnology Center, [‡]Department of Chemistry and Center for Structural Diffraction, and [§]Department of Biochemistry and Molecular Biology, University of Ferrara, I-44100 Ferrara, Italy

Received January 29, 2010

Because of the encouraging results obtained using vinyl ester derivatives, we synthesized and tested a novel series of peptide-based proteasome inhibitors bearing a new pharmacophore unit at the C-terminal. *N*-Acylpyrrole moiety is a potential substrate for Michael addition by catalytic threonine. Several analogues have demonstrated a selective inhibition of the multicatalytic complex $\beta 1$ subunits, the capacity to permeate cellular membrane, and good pharmacokinetics properties.

Introduction

The 26S proteasome, a multicatalytic and multisubunit threonine protease complex (2.4 MDa), is implicated in many biological processes, including the generation of antigenic peptides presented by major histocompatibility complex class I (MHC I) molecules and degradation of most cytosolic proteins in mammalian cells.^{1–6} The 26S proteasome consists of a central 20S core containing three different active sites ($\beta 1$, $\beta 2$, and $\beta 5$) and two 19S regulatory complexes. On the basis of the preferential cleavage of short fluorogenic peptidic substrates, the various activities of the proteasome have been assigned to individual subunits and classified as “chymotrypsin-like” ($\beta 5$), “tryptic-like” ($\beta 2$), and “peptidyl-glutamyl peptide hydrolyzing”, PGPH² ($\beta 1$).^{7,8}

As previously mentioned, proteasome plays an essential role in protein turnover in living cells, and deregulation of the ubiquitin–proteasome pathway in humans causes several diseases, such as cancer and neurodegenerative, autoimmune, and metabolic disorders. Furthermore, proteasome inhibition has a negative influence on the stability of many proteins, especially those involved in cell cycle regulation. Indeed, most cells become sensitive to apoptosis after treatment with proteasome inhibitors.^{9,10} Interestingly, tumor cells are usually more sensitive to proteasome inhibition than their normal counterparts. Indeed, healthy cells display cell-cycle arrest when treated with proteasome inhibitors but, unlike tumor cells, are not as susceptible to apoptosis.^{11,12} Thus, selective inhibitors of catalytic proteasome subunits are appealing targets for drug development.¹³

Many inhibitors of the ubiquitin–proteasome pathway that are able to interact with the 20S catalytic core of the multicatalytic complex and that can readily enter cells and selectively inhibit this degradation pathway are currently available. These

synthetic inhibitors possess a homogeneous structural profile; they are generally peptide-based compounds with a C-terminal pharmacophore function required for primary interaction with catalytic threonine on the enzyme. The peptide component seems to be important for determining specificity for the three catalytic sites by secondary interaction with the enzymatic pockets. Essentially, most of these inhibitors act on the chymotrypsin-like activity of the proteasome, although they do undergo partial inhibition. Recently, research has begun to address the development of molecules with specific activity for the proteasome subunits, and already considerable progress has been made, particularly by Crews et al. who, by varying the sequence at P2–P4 in epoxomicin, were able to generate specific inhibitors of the chymotrypsin-like and postacidic activities, although the physiological consequences of $\beta 1$ -subunit inhibition still remain to be clarified.^{14,15} Likewise, new aldehyde compounds have shown an interesting selectivity for the trypsin-like activity, as have vinyl sulfone analogues, although the foremost proteasome inhibitor to date (bortezomib, Velcade), approved by the U.S. Food and Drug Administration as a prescription drug for the treatment of multiple myeloma, is selective for the chymotrypsin-like activity with a partial action on the $\beta 1$ site.^{16,17}

We recently reported the design and synthesis of small peptide molecules with selective inhibitory activity toward the three catalytic sites and good pharmacokinetic properties. In our early studies, we have identified new oligopeptide inhibitors with different C-terminal pharmacophore units: amide analogues, compounds with arecholine derivatives, and in particular, a class of compounds bearing a C-terminal vinyl ester selective and specific for the $\beta 2$ activity of the proteasome. The pharmacophoric vinyl ester group is able to interact with the catalytic Thr in the same way as the well-known vinyl sulfone analogues.¹⁸ The best of these derivatives inhibit the $\beta 2$ subunit in the nanomolar range, are nontoxic, do not affect cell proliferation, and are capable of modulating the generation of antigenic peptides linked by MHC class I molecules. N-Terminal elongation has also been performed on vinyl ester prototypes, and in another series we have cyclized the linear peptide portion: both the N-terminal elongated peptides and the cyclic analogues have been shown to selectively inhibit the $\beta 1$ subunit.

*To whom correspondence should be addressed. Phone: +39-532-291281. Fax: +39-532-291296. E-mail: mru@unife.it.

[†]Abbreviations: Boc, *tert*-butoxycarbonyl; ChT-L, chymotrypsin-like; Fmoc, fluorenylmethoxycarbonyl; HATU, *O*-(7-azabenzotriazolyl)tetramethyluronium hexafluorophosphate; HOBt, *N*-hydroxybenzotriazole; NMM, *N*-methylmorpholine; PGPH, peptidylglutamyl peptide hydrolyzing; TFA, trifluoroacetic acid; T-L, trypsin-like; WSC, water-soluble carbodiimide (1-ethyl-3-(3'-dimethylaminopropyl)carbodiimide); Z, benzyl-oxycarbonyl-*N*-hydroxysuccinimide; VAP, vinylacylpyrrole.

α,β -Unsaturated Carbonyl System of Chalcone-Based Derivatives Is Responsible for Broad Inhibition of Proteasomal Activity and Preferential Killing of Human Papilloma Virus (HPV) Positive Cervical Cancer Cells

Martina Bazzaro,^{*,†,◇} Ravi K. Anchoon,^{‡,§,×} Mohana Krishna R. Mudiham,^{§,×} Olga Issaenko,[†] Srinivas Kumar,[§] Balasubramanyam Karanam,[‡] Zhenhua Lin,^{‡,•} Rachel Isaksson Vogel,[∞] Riccardo Gavioli,[‡] Federica Destro,[‡] Valeria Ferretti,[#] Richard B. S. Roden,^{‡,§,†,◇} and Saeed R. Khan^{*,§,◇}

[†]Masonic Cancer Center and Department of Obstetrics, Gynecology and Women's Health, University of Minnesota Twin Cities, Minneapolis, Minnesota 55455, United States, [‡]Department of Pathology, [§]Department of Oncology, and [¶]Department of Gynecology and Obstetrics, The Johns Hopkins University, Baltimore, Maryland 21231, United States, [∞]Department of Biochemistry and Molecular Biology, University of Ferrara, Ferrara, Italy, [#]Department of Chemistry and Center for Structural Diffractometry, University of Ferrara, I-44100, Ferrara, Italy, and [×]Masonic Cancer Center Biostatistics and Bioinformatics Core, University of Minnesota Twin Cities, Minneapolis, Minnesota 55455, United States. [◇]M.B., R.B.S.R., and S.R.K. contributed equally to this work. ^{*}R.K.A. and M.K.R.M. contributed equally to this work. [•]Current address: Department of Pathology, Yanbian University College of Medicine and Key Laboratory of Organism Functional Factors of the Changbai Mountain, Ministry of Education, Yanji-City, Jilin-Province, P. R. China.

Received May 14, 2010

Proteasome inhibitors have potential for the treatment of cervical cancer. We describe the synthesis and biological characterization of a new series of 1,3-diphenylpropen-1-one (chalcone) based derivatives lacking the boronic acid moieties of the previously reported chalcone-based proteasome inhibitor 3,5-bis(4-boronic acid benzylidene)-1-methylpiperidin-4-one and bearing a variety of amino acid substitutions on the amino group of the 4-piperidone. Our lead compound **2** (RA-1) inhibits proteasomal activity and has improved dose-dependent antiproliferative and proapoptotic properties in cervical cancer cells containing human papillomavirus. Further, it induces synergistic killing of cervical cancer cell lines when tested in combination with an FDA approved proteasome inhibitor. Exploration of the potential mechanism of proteasomal inhibition by our lead compound using *in silico* docking studies suggests that the carbonyl group of its oxopiperidine moiety is susceptible to nucleophilic attack by the γ -hydroxythreonine side chain within the catalytic sites of the proteasome.

Introduction

The 26S proteasome is composed of two 19S regulatory subunits (termed "caps") and one 20S catalytic subunit (referred to as the "proteolytic core").^{1,2} The targeting of a protein for degradation by the proteasome occurs via its enzymic conjugation to the small protein ubiquitin. Chains of ubiquitin are recognized by the proteasome caps to facilitate the entrance of the targeted protein into the proteolytic chamber wherein the actual degradation occurs. The 20S proteasome comprises four stacked rings: two α - (outer) and two β - (inner) rings. Each β -ring is composed of seven subunits containing three catalytic sites: the $\beta 1$ subunit is associated with a peptidylglutamyl peptide hydrolyzing-like (PGPH-like) activity; the $\beta 2$ subunit is associated with the trypsin-like activity (T-like); the $\beta 5$ subunit is associated with the chymotrypsin-like activity (CT-like). All three proteolytic activities utilize the γ -hydroxyl group of an N-terminal threonine residue within each catalytic site for nucleophilic attack of the α -amine proton donor/acceptor within the targeted protein.³

*To whom correspondence should be addressed. For M.B.: (address) Masonic Cancer Center, Room 490, 420 Delaware Street SE, Minneapolis, Minnesota 55455; (phone) 612-6252889; (fax) 612-626-0665; (e-mail) mbazzaro@umn.edu. For S.R.K.: (address) DPQR/CDER/FDA, Room 1012, New Hampshire Avenue, Silver Spring, Maryland; (phone) 301-796-0051; (fax) 703-796-9816; (e-mail) saeed.khan2@fda.hhs.gov.

© 2010 American Chemical Society

The polypeptide targets of the proteasome include proteins involved in cell cycle progression, survival, and inflammation, and while the ubiquitin-dependent proteasomal degradation is crucial for both normal and malignant cells, the higher demand for metabolic/catabolic activity associated with the malignant phenotype renders the ubiquitin–proteasome pathway a suitable tool for cancer treatment.^{4,5}

Inhibition of the catalytic activities of the proteasome can be achieved by compounds that covalently bind the N-terminal threonine residue in the catalytic sites of the β -subunits (this includes bortezomib⁶ (PS-341), salinosporamide A⁷ (NPI-0052), and carfilzomib⁸) or by compounds that bind to the catalytic sites of the β -subunits in a noncovalent fashion^{9,10} like in the case of TMC-95A,^{11,12} ritonavir,¹³ and lipopeptides.¹⁴

Undoubtedly, members of both classes have been shown to have potential as antineoplastic agents with bortezomib, a covalent slowly reversible proteasome inhibitor,¹⁵ to be the first FDA approved for the treatment of multiple myeloma and mantle cell lymphoma.¹⁵

Proteasome inhibitors may be particularly efficacious for certain cancers types with critical pathways that are dependent upon proteolytic degradation. Human papillomavirus (HPV⁷)

^a Abbreviations: AcOH, acetic acid; THF, tetrahydrofuran; DCM, dichloromethane; NMM, *N*-methylmorpholine; HPV, human papilloma virus; DMEM, Dulbecco's modified Eagle medium; SFM, serum free medium.

Published on Web 12/27/2010

pubs.acs.org/jmc

Production of β -globin and adult hemoglobin following G418 treatment of erythroid precursor cells from homozygous β^0 39 thalassemia patients

Francesca Salvatori,¹ Giulia Breveglieri,¹ Cristina Zuccato,² Alessia Finotti,² Nicoletta Bianchi,² Monica Borgatti,² Giordana Feriotta,² Federica Destro,¹ Alessandro Canella,¹ Eleonora Brognara,² Ilaria Lampronti,² Laura Breda,³ Stefano Rivella,³ and Roberto Gambari^{1,2*}

In several types of thalassemia (including β^0 39-thalassemia), stop codon mutations lead to premature translation termination and to mRNA destabilization through nonsense-mediated decay. Drugs (for instance aminoglycosides) can be designed to suppress premature termination, inducing a ribosomal readthrough. These findings have introduced new hopes for the development of a pharmacologic approach to the cure of this disease. However, the effects of aminoglycosides on globin mRNA carrying β -thalassemia stop mutations have not yet been investigated. In this study, we have used a lentiviral construct containing the β^0 39-thalassemia globin gene under control of the β -globin promoter and a LCR cassette. We demonstrated by fluorescence-activated cell sorting (FACS) analysis the production of β -globin by K562 cell clones expressing the β^0 39-thalassemia globin gene and treated with G418. More importantly, after FACS and high-performance liquid chromatography (HPLC) analyses, erythroid precursor cells from β^0 39-thalassemia patients were demonstrated to be able to produce β -globin and adult hemoglobin after treatment with G418. This study strongly suggests that ribosomal readthrough should be considered a strategy for developing experimental strategies for the treatment of β^0 -thalassemia caused by stop codon mutations. *Am. J. Hematol.* 84:720–728, 2009. © 2009 Wiley-Liss, Inc.

Introduction

Nonsense mutations, giving rise to UAA, UGA, and UAG premature translation termination codons (PTTCs) within the coding region of mRNAs, account for ~10–30% of all described gene lesions causing human inherited diseases [1–5]. As recently reviewed by Mort et al. [6], pathological nonsense mutations resulting in TGA (38.5%), TAG (40.4%), and TAA (21.1%) occur in different proportions to naturally occurring stop codons. Of the 23 different nucleotide substitutions that cause nonsense mutations, the most frequent are CGA → TGA (21%; resulting from methylation-mediated deamination) and CAG → TAG (19%) [6].

There are numerous examples of inherited diseases caused by nonsense mutations, such as cystic fibrosis [7,8], lysosomal storage disorders [9], Duchenne muscular dystrophy [10,11], and thalassemia [12,13]. There are also noninherited diseases associated to de novo formation of stop codons. For instance, in cancers many tumor suppressor genes exhibit a disproportionate number of somatic nonsense mutations [14], many of which were found to occur recurrently in the hypermutable CpG dinucleotide, as expected [14].

The major molecular consequences of stop mutations are the promotion of premature translational termination and the nonsense-mediated RNA decay (NMD) [15–18]. These two features are strictly associated. NMD, in fact, recognizes and degrades transcripts harboring PTTCs, thereby preventing the production of truncated and faulty proteins. NMD is considered as a very important pathway in an mRNA surveillance system that typically degrades transcripts containing PTTCs to prevent unnecessary processing of RNA precursors and unnecessary translation of aberrant transcripts [15–18]. Failure to eliminate these mRNAs with PTTCs may result in the synthesis of abnormal proteins that can be toxic to cells through dominant-negative or gain-of-function effects.

As far as thalassemia syndromes, in the β^0 39-thalassemia, the CAG (Gln) codon is mutated to an UAG stop codon [12,13], leading to premature translation termination and to mRNA destabilization through NMD [19,20]. The β^0 39-thalassemia mutation is very frequent in Italy (about 70% of the total β -thalassemia mutations) [21] and, in general, in the whole Mediterranean area. Other examples of stop mutation of the β -globin mRNA occur at position 15, 37, 59, and 127 of the mRNA sequence [22–27].

In the last few years, it has been demonstrated that drugs can be designed and produced to suppress premature termination, inducing a ribosomal readthrough of premature, but not normal termination codons [28–30]. The molecular basis of this phenomenon is related to the sequence "context" surrounding normal termination codons, which makes the normal termination codons refractory to

¹BioPharmaNet, Department of Biochemistry and Molecular Biology, Ferrara University, Ferrara, Italy; ²Laboratory for the Development of Pharmacological and Pharmacogenomic Therapy of Thalassemia, Biotechnology Center, Ferrara University, Ferrara, Italy; ³Department of Pediatric and Hematology-Oncology, Weill Medical College of Cornell University, New York, New York

Contract grant sponsor: Telethon; Contract grant number: GGP07257; Contract grant sponsors: Fondazione CARIPARO (Cassa di Risparmio di Padova e Rovigo), AIRC, Cofin-2005, STAMINA Project (University of Ferrara), UE ITHANET Project (eInfrastructure for the Thalassemia Research Network), Regione Emilia-Romagna (Spinner Project), Associazione Veneta per la Lotta alla Talassemia (AVLT), Rovigo.

Conflict of interest: Nothing to report.

*Correspondence to: Roberto Gambari, Department of Biochemistry and Molecular Biology, University of Ferrara, Via Fossato di Mortara n.74, Ferrara 44100, Italy. E-mail: gam@unife.it

Received for publication 10 April 2009; Revised 20 August 2009; Accepted 20 August 2009

Am. J. Hematol. 84:720–728, 2009.

Published online 25 August 2009 in Wiley InterScience (www.interscience.wiley.com). DOI: 10.1002/ajh.21539

© 2009 Wiley-Liss, Inc.

American Journal of Hematology

720

http://www3.interscience.wiley.com/cgi-bin/jh/35105

Development of K562 cell clones expressing β -globin mRNA carrying the β^{039} thalassaemia mutation for the screening of correctors of stop-codon mutations

Francesca Salvatori*, Vera Cantale*, Giulia Breveglieri*, Cristina Zuccato†, Alessia Finotti†, Nicoletta Bianchi†, Monica Borgatti†, Giordana Feriotta†, Federica Destro†, Alessandro Canella†, Laura Breda†, Stefano Rivella‡ and Roberto Gambari*†

*BioPharmaNet, Department of Biochemistry and Molecular Biology, Ferrara University, Via Fossato di Mortara 74, 44100 Ferrara, Italy, †Laboratory for the Development of Pharmacological and Pharmacogenomic Therapy of Thalassaemia, Biotechnology Center, Ferrara University, Via Fossato di Mortara 64/b, 44100 Ferrara, Italy, and ‡Department of Pediatric Hematology–Oncology, Children's Cancer and Blood Foundation Laboratories, Weill Medical College of Cornell University, New York, NY 10021, U.S.A.

Nonsense mutations, giving rise to UAA, UGA and UAG stop codons within the coding region of mRNAs, promote premature translational termination and are the leading cause of approx. 30% of inherited diseases, including cystic fibrosis, Duchenne muscular dystrophy and thalassaemia. For instance, in β^{039} -thalassaemia the CAG (glutamine) codon is mutated to the UAG stop codon, leading to premature translation termination and to mRNA destabilization through the well-described NMD (nonsense-mediated mRNA decay). In order to develop an approach facilitating translation and, therefore, protection from NMD, aminoglycoside antibiotics have been tested on mRNAs carrying premature stop codons. These drugs decrease the accuracy in the codon–anticodon base-pairing, inducing a ribosomal read-through of the premature termination codons. Interestingly, recent papers have described drugs designed and produced for suppressing premature translational termination, inducing a ribosomal read-through of premature but not normal termination codons. These findings have introduced new hopes for the development of a pharmacological approach to the therapy of β^{039} -thalassaemia. In this context, we started the development of a cellular model of the β^{039} -thalassaemia mutation that could be used for the screening of a high number of aminoglycosides and analogous molecules. To this aim, we produced a lentiviral construct containing the β^{039} -thalassaemia globin gene under a minimal LCR (locus control region) control and used this construct for the transduction of K562 cells, subsequently subcloned, with the purpose to obtain several K562 clones with different integration copies of the construct. These clones were then treated with Geneticin (also known as G418) and other aminoglycosides and the production of β -globin was analysed by FACS analysis. The results

obtained suggest that this experimental system is suitable for the characterization of correction of the β^{039} -globin mutation causing β -thalassaemia.

Introduction

Nonsense mutations, giving rise to UAA, UGA and UAG stop codons within the coding region of mRNAs, promote premature translational termination [1–4] and are the leading cause of up to 30% of inherited diseases [2,4], including cystic fibrosis [5], Duchenne muscular dystrophy [6] and thalassaemia [7–12]. For instance, in β^{039} -thalassaemia the CAG (glutamine) codon of the β -globin mRNA is mutated to the UAG stop codon [7,8], leading to premature translation termination and to mRNA destabilization through the well-described NMD (nonsense-mediated mRNA decay) [3,4]. Other examples of stop mutations of the β -globin mRNA occur at positions 15 [9], 37 [10,11] and 127 [12] of the mRNA sequence.

In order to develop an approach facilitating translation and, therefore, protection from NMD, aminoglycoside antibiotics have been tested on mRNAs carrying premature stop codons. These drugs bind the decoding centre of the ribosome and decrease the accuracy in the codon–anticodon base-pairing, inducing a ribosomal read-through of premature termination codons [13,14]. Despite their

Key words: aminoglycoside antibiotics, K562 cell, locus control region, nonsense mutation, thalassaemia.

Abbreviations used: C, threshold cycle value; FAM, 6-carboxyfluorescein; FBS, fetal bovine serum; GAPDH, glyceraldehyde-3-phosphate dehydrogenase; GFP, green fluorescent protein; LB, Luna–Bertani; LCR, locus control region; LTR, long terminal repeat; MOI, multiplicity of infection; NMD, nonsense-mediated mRNA decay; PE, phycoerythrin; PGK, phosphoglycerate kinase; RT–PCR, reverse transcription–PCR; SV40, simian virus 40; TAMRA, 6-carboxytetramethylrhodamine; wt, wild-type.

† To whom correspondence should be addressed (email gam@unife.it).

Short report

Open Access

Identification of new HIV-1 Gag-specific cytotoxic T lymphocyte responses in BALB/c mice

Silvia Cellini¹, Cinzia Fortini¹, Eleonora Gallerani¹, Federica Destro¹, Egidio Brocca Cofano², Antonella Caputo² and Riccardo Gavioli^{*1}

Address: ¹Department of Biochemistry and Molecular Biology, Via L. Borsari 46, University of Ferrara, 44100, Ferrara, Italy and ²Department of Histology, Microbiology and Medical Biotechnologies, Via A. Gabelli 63, University of Padova, 35121, Padova, Italy

Email: Silvia Cellini - silvia.cellini@unife.it; Cinzia Fortini - cinziafortini@libero.it; Eleonora Gallerani - gllnr@unife.it; Federica Destro - fedex.des@libero.it; Egidio Brocca Cofano - broccace@mail.nih.gov; Antonella Caputo - antonella.caputo@unipd.it; Riccardo Gavioli* - r.gavioli@unife.it

* Corresponding author

Published: 14 July 2008

Received: 27 May 2008

Virology Journal 2008, **5**:81 doi:10.1186/1743-422X-5-81

Accepted: 14 July 2008

This article is available from: <http://www.virologyj.com/content/5/1/81>

© 2008 Cellini et al; licensee BioMed Central Ltd.

This is an Open Access article distributed under the terms of the Creative Commons Attribution License (<http://creativecommons.org/licenses/by/2.0>), which permits unrestricted use, distribution, and reproduction in any medium, provided the original work is properly cited.

Abstract

Background: As HIV-specific cytotoxic T cells play a key role during acute and chronic HIV-1 infection in humans, the ability of potential anti-HIV vaccines to elicit strong, broad T cell responses is likely to be crucial. The HIV-1 Gag antigen is widely considered a relevant antigen for the development of an anti-HIV vaccine since it is one of the most conserved viral proteins and is also known to induce T cell responses. In the majority of studies reporting Gag-specific cellular immune responses induced by Gag-based vaccines, only a small number of Gag T cell epitopes were tested in preclinical mouse models, thus giving an incomplete picture of the numerous possible cellular immune responses against this antigen. As is, this partial knowledge of epitope-specific T cell responses directed to Gag will unavoidably result in a limited preclinical evaluation of Gag-based vaccines.

Results: In this study we identified new Gag CD8⁺ T cell epitopes in BALB/c mice vaccinated with the HIV-1 Gag antigen alone or in combination with the HIV-1 Tat protein, which was recently shown to broaden T cell responses directed to Gag. Specifically, we found that CTL responses to Gag may be directed to nine different CTL epitopes, and four of these were mapped as minimal CTL epitopes.

Conclusion: These newly identified CTL epitopes should be considered in the preclinical evaluation of T cell responses induced by Gag-based vaccines in mice.

Background

Cellular immune responses are a critical part of the host defence against viruses, with cytotoxic T lymphocytes (CTLs) playing a key role in recognizing and eliminating infected cells. CTLs identify their targets as 8–10 amino acid long peptides which are derived from the intracellular degradation of viral antigens and presented in associa-

tion with major histocompatibility complex class I (MHC-I) molecules at the surface of infected cells [1-3].

Several studies have indicated that HIV-specific T cell responses play a key role in limiting the progression of acute and chronic infection in humans [4,5], and that long-term non-progressors have consistently higher levels

Lamination and laser structuring for a microwell array

Erik Jung · Dion Manassis · Alexander Neumann ·
 Lars Böttcher · Tanja Braun · Jörg Bauer · Herbert Reichl ·
 Bruno Iafelice · Federica Destro · Roberto Gambari

Received: 19 June 2007 / Accepted: 25 November 2007 / Published online: 11 December 2007
 © Springer-Verlag 2007

Abstract Microtechnology becomes a versatile tool for biological and biomedical applications. Microwells have been established long but remained non-intelligent up to now. Merging new fabrication techniques and handling concepts with microelectronics enables to realize intelligent microwells suitable for future improved cancer treatment. The described technology depicts the basis for the fabrication of electronically enhanced microwell. Thin aluminium sheets are structured by laser micro machining and laminated successively to obtain registration tolerances of the respective layers of $<5 \mu\text{m}$. The microwells lasermachined into the laminate are with 50–350 μm diameter, allowing to contain individual cells within the microwell as well as provide access holes for the layer-to-layer contacting. A permeable membrane attached to the bottom of the microwell plate is used for fluid handling. The individual process steps are described and results on the microstructuring as well as on biocompatibility of the materials are given.

1 Introduction

Cell handling for cell-to-cell interaction detection is currently done in configurations mimicking patch clamp

E. Jung (✉) · D. Manassis · A. Neumann · L. Böttcher ·
 T. Braun · J. Bauer · H. Reichl
 Fraunhofer IZM, Berlin, Germany
 e-mail: erju@izm.fhg.de

B. Iafelice
 University of Bologna, Bologna, Italy

F. Destro · R. Gambari
 University of Ferrara, Ferrara, Italy

techniques, allowing precise control of the cell position (Van Duijn 1998). Some techniques employed here are

- Glass pipette (std. patch clamp protocol) (Neher 1974).
- Laser based tweezers (Bishop et al. 2003).
- Electrostatic planar cells (Sigworth and Klemic 2002).
- SiO_2 structured Micromanipulators (Lehnert et al. 2002).

Using either of these techniques, the cell manipulation and detection of cell behaviour under certain influences (e.g. cell–cell interaction) are separate tasks done with separate equipment.

Also, none of the techniques fully employs the power of merging modern microelectronic control, planar fabrication techniques and circuit fabrication.

The described approach implements these techniques and makes use of

- Biocompatible materials selection.*
- Lamination technique for mass manufacturable layer stacks.*
- Laser structuring for small hole (i.e. a geometric confinement) and large area (i.e. control circuitry routing).*

As well as

- Surface modification.*
- Tailored metal/dielectric layers for a dielectrophoretic control in 3D of cell position.*
- Cell nutrition through a selectively permeable membrane,*
- and cell-dispensing into the microwell.

The aspects marked with an asterisk are described in the paper in detail.

DTIP

of MEMS & MOEMS Stresa, Italy, 24-27 April 2007

LAMINATION AND LASER STRUCTURING FOR A DEP MICROWELL ARRAY

*E. Jung, D. Manassis, A. Neumann, Lars Böttcher, T. Braun,
J. Bauer, H. Reichl, Fraunhofer IZM, Germany
B. Iafelice, University of Bologna, Italy
Federica Destro, Roberto Gambari, University of Ferrara, Italy*

ABSTRACT

Microtechnology becomes a versatile tool for biological and biomedical applications. Microwells have been established long but remained non-intelligent up to now. Merging new fabrication techniques and handling concepts with microelectronics enables to realize intelligent microwells suitable for future improved cancer treatment.

The described technology depicts the basis for the fabrication of electronically enhanced microwell. Thin aluminium sheets are structured by laser micro machining and laminated successively to obtain registration tolerances of the respective layers of $<5\mu\text{m}$.

The microwells lasermachined into the laminate are with $50\dots350\mu\text{m}$ diameter, allowing to contain individual cells within the microwell as well as provide access holes for the layer-to-layer contacting

A permeable membrane attached to the bottom of the microwell plate is used for fluid handling.

The individual process steps are described and results on the microstructuring as well as on biocompatibility of the materials are given.

1. INTRODUCTION

Cell handling for cell-to-cell interaction detection is currently done in configurations mimicking patch clamp techniques, allowing precise control of the cell position ^{1/}. Some techniques employed here are

- Glass pipette (std. patch clamp protocol) ^{2/}
- Laser based tweezers ^{3/}
- Electrostatic planar cells ^{4/}
- SiO₂ structured Micromanipulators ^{5/}

Using either of these techniques, the cell manipulation and detection of cell behaviour under certain influences (e.g. cell-cell interaction) are separate tasks done with separate equipment.

Also, none of the techniques fully employs the power of merging modern microelectronic control, planar fabrication techniques and circuit fabrication.

The described approach implements these techniques and makes use of

- Biocompatible materials selection *
- Lamination technique for mass manufacturable layer stacks *
- Laser structuring for small hole (i.e. a geometric confinement) and large area (i.e. control circuitry routing) *

As well as

- Surface modification *
- Tailored metal/dielectric layers for a dielectrophoretic control in 3D of cellposition *
- Cell nutrition through a selectively permeable membrane *
- and Cell-Dispensing into the microwell

The aspects marked with an asterix are described in the paper in detail.

Part of the structure that is used for determining the cell-cell interaction is depicted in /Figure 1/

ALUMINIUM PRINTED CIRCUIT BOARD TECHNOLOGY FOR BIOMEDICAL MICRO-DEVICES

B. Iafelice^{1,2}, F. Destro³, D. Manassis¹, D. Gazzola², E. Jung¹, M. Borgatti³,
T. Braun¹, J. Bauer¹, R. Gavioli³, R. Gambari³, A. Ostmann¹, R. Guerrieri²

¹Berlin Center of Advanced Packaging (BeCAP) –

Fraunhofer IZM & Technical University Berlin, GERMANY

²Advanced Research Center on Electronic Systems (ARCES) – University of Bologna, ITALY

³Department of Biochemistry and Molecular Biology, Ferrara University, ITALY

Keywords: Printed circuit board, Biomedical microdevice, Microfluidics, Aluminium, Lab on a Chip

Motivation – We present an innovative Printed Circuit Board (PCB) technology for biomedical microdevices. The fabrication process combines biocompatible tested materials and pure metal layers to build micro systems that mix active/passive electronics with microfluidics. Its peculiarity with respect to existing technologies is that it uses standard PCB processes, thereby preserving its characteristics as low production cost and large scale development, necessary for disposable applications.

State of art – Several technologies for microfluidic device fabrication and packaging have been proposed to integrate sensing capabilities and electrical interfaces into a single device [1]. All of these approaches require complex steps or expensive facilities, and mostly are useful for prototyping only. Otherwise the demand for low priced disposable has steadily increased due to the large developments in the area of devices miniaturization. However it is extremely expensive to transform one of these technologies in large scale production. In the last years, PCB technology reached resolutions of tens of micrometers which are enough for many microfluidics applications. As example in [2-4] micro channels and viaducts are used to integrate liquid in quasi-standard FR4-PCBs.

Biological validation – We studied *in-vitro* the long-short time biocompatibility of a set of materials used in standard and quasi-standard PCB processes (e.g. flex circuits). Biocompatibility has been carried out using a lymphoblastoid cell-line (LCL) [5] to determine possible antiproliferative effects. Furthermore, being this cell line extensively used for screening of cytotoxic T-lymphocytes (CTLs) [6], we were able to determine the effects of the materials on a specific biological function, i.e. the CTL-mediated lysis of target cells. The materials-under-test were embedded in standard multiwell plates as shown in Figure 1.

Table 1 summarizes the toxicity induced by the tested materials after long-short time. These materials have also been studied with different surface treatments modifying the hydrophilicity/hydrophobicity.

Technology – The key point of this work is to develop an extended PCB technology with the same facilities used in industrial Copper-PCB processes. Our technology allows to laminate different metal foils (Copper, Aluminium, Platinum, Gold) with several dielectric materials (Polyimide, Polyurethane, Pyralux) – see Figure 2. Wet etching, laser ablation and mechanical drilling are used to structure the electrical circuit and the microfluidics with a resolution up to ten micrometers and layer thicknesses from few micrometers to millimeters. The compatibility with standard metal covering as nickel, gold and palladium was preserved. Furthermore, surface treatments with Teflon, Certonal, thiols, and Parilene allow designing hydrophilicity/hydrophobicity in the PCB-developed microfluidics networks.

In particular Aluminium is a very interesting metal because of its low price, biocompatibility, wide range of foil thicknesses and good electrical conductivity. Additionally few nanometers of its oxide self-passivate the Aluminium surface making it stable in wet environments. The thin oxide-layer can be overcome in electrical measurements by increasing the signal frequency. The technology ability is demonstrated by developing an electronic meniscus sensor (Figure 3) [7]. The sensor can be integrated in microstructures and replicated as many times as required by its parallelism. This microsystem is a unique PCB-stack created in a unique process within microfluidic elements and electronics.

Word Count: 500

Cellular biosensors for the identification of fetal hemoglobin inducers

G. BREVEGLIERI², F. SALVATORI¹, A. FINOTTI², I. BERTUZZI², F. DESTRO², S. FALZONI³, N. BIANCHI¹, M. BORGATTI¹, C. ZUCCATO¹, G. FERIOTTO¹, L. BREDA⁴, S. RIVELLA⁴, R. GAMBARI^{1,2}

The development of cellular systems for the screening of molecules able to induce the production of fetal or adult hemoglobin in erythroid cells isolated from β -thalassemia patients is very important for the identification of molecules of interest for pharmacological therapy of thalassemia. This article reports the development of a cellular system for the identification of inducers of fetal hemoglobin preferentially acting on the human γ -globin gene promoter. To achieve this aim, green and red fluorescence protein genes were cloned under the control of γ -globin and β -globin promoters, respectively. The developed K562 clones were tested for the increase of fluorescence after treatment with sodium butyrate and hydroxyurea, two well-known inducers of fetal hemoglobin.

KEY WORDS: Fetal hemoglobin - beta-thalassemia - Histone deacetylases - Hydroxyurea - Green fluorescent proteins.

Pharmacologically mediated stimulation of human β -globin gene expression and increase of fetal haemoglobin (HbF) levels is considered a potential therapeutic modality in hematological disorders, including β -thalassemia and sickle cell anemia.¹

Based on this assumption, several HbF inducers have been recently studied, including hydroxyurea,¹ histone deacetylase-inhibitors,² mithramycin,³ rapamycin,⁴ tallimustine,⁵ cisplatin analogs,⁶ For instance,

Acknowledgments.—R.G. is granted by Fondazione Cariparo (Cassa di Risparmio di Padova e Rovigo), AIRC, Cofin-2005, by STAMINA Project (University of Ferrara), by UE ITHANET Project (Infrastructure for the Thalassaemia Research Network) and by Telethon (contract GGP07257). This research is also supported by Regione Emilia-Romagna (Spinner Project) and by Associazione Veneta per la Lotta alla Talassemia (AVLT), Rovigo.

Address reprint requests to: R. Gambari, ER-GenTech, Section of Molecular Biology, Department of Biochemistry and Molecular Biology, University of Ferrara, Ferrara, Italy. E-mail: gam@unife.it

¹Laboratory for the Development of Pharmacological and Pharmacogenomic Therapy of Thalassemia Biotechnology Centre, Ferrara, Italy

²ER-GenTech, Department of Biochemistry and Molecular Biology University of Ferrara, Ferrara, Italy

³Department of Experimental and Diagnostic Medicine Section of General Pathology University of Ferrara, Ferrara, Italy

⁴Weill Medical College of Cornell University, New York, NY, USA

angelicin,⁷ an angular psoralen found in several medicinal plant extracts, was found to induce erythroid differentiation of the human leukemic K562 cell line and increased HbF production in primary human erythroid precursor cells. With respect to the screening of HbF inducers, high-throughput approaches are highly needed. To this aim, the use of K562 cells is commonly considered for a first screening. However, the employment of this system gives few indications on the mechanism of action of the inducer molecules.

Accordingly, several groups described the use of reporter genes under the transcriptional control of the γ -globin gene promoter, in order to identify HbF inducers acting on the transcription efficiency of the γ -globin gene. For instance, Skarpidi *et al.*⁸ developed a rapid and efficient method for detecting HbF inducers, based on a recombinant DNA construct in which the coding sequences of two different luciferase reporter genes, firefly and renilla, are substituted for those of human γ -globin and β -globin genes, respectively. The activity of these genes can be distinguished

ACKNOWLEDGEMENTS

In first place, I would like to thank my main supervisor Prof. Roberto Gambari and my co-supervisor Prof. Riccardo Gavioli, for teaching me and supporting me all these years. Thanks to give me the opportunity to work in your labs and to improve my capacities and knowledge.

I would like also express my sincere gratitude and thanks to all members of the two lab groups (1st and 3rd floor) for their support and friendship. Without your help this thesis would not have been accomplished. In particular I would like to thank all the present and past colleagues of Gavioli's group for the goods time spent together inside out the lab! A special thanks to Monica and Laura, for sharing with me the COCHISE project and for their essential help.

My friends from Albacity: for the happy moments together since we were children and for always being here for me.

My brother Alessandro: simply for being my brother and for support me nevertheless now you are 250km far away. I know I can always count on you!

My boyfriend Marco: for all the special moments we have had together, for your understanding and for your endless patience.

Finally, last but not least, I would like to thank the two persons who made all this possible: my mother Maria and My father Luciano. Thanks for your true love and unconditional support, without your help I could not be here!!!

This work was supported by grants from: the EU CoChiSe Project, AIRC, Fondazione Cassa di Risparmio di Padova e Rovigo (CARIPARO), University of Ferrara and Fondazione Cassa di Risparmio di Ferrara.